

การแยกถักนินจากชีวมวลโดยใช้ตัวเร่งปฏิกิริยาวิวิธพันธุ์ชนิดกรด



นางสาวอิสรา มงคลพิชญรักษ์

จุฬาลงกรณ์มหาวิทยาลัย

CHULALONGKORN UNIVERSITY

บทคัดย่อและแฟ้มข้อมูลฉบับเต็มของวิทยานิพนธ์ตั้งแต่ปีการศึกษา 2554 ที่ให้บริการในคลังปัญญาจุฬาฯ (CUIR)  
เป็นแฟ้มข้อมูลของนิสิตเจ้าของวิทยานิพนธ์ ที่ส่งผ่านทางบัณฑิตวิทยาลัย

The abstract and full text of theses from the academic year 2011 in Chulalongkorn University Intellectual Repository (CUIR)  
are the thesis authors' files submitted through the University Graduate School.

วิทยานิพนธ์นี้เป็นส่วนหนึ่งของการศึกษาตามหลักสูตรปริญญาวิทยาศาสตรมหาบัณฑิต

สาขาวิชาปิโตรเคมีและวิทยาศาสตร์พอลิเมอร์

คณะวิทยาศาสตร์ จุฬาลงกรณ์มหาวิทยาลัย

ปีการศึกษา 2558

ลิขสิทธิ์ของจุฬาลงกรณ์มหาวิทยาลัย

SEPARATION OF LIGNIN FROM BIOMASS USING ACIDIC HETEROGENEOUS CATALYSTS

Miss Isara Mongkolpichayarak



A Thesis Submitted in Partial Fulfillment of the Requirements  
for the Degree of Master of Science Program in Petrochemistry and Polymer Science

Faculty of Science

Chulalongkorn University

Academic Year 2015

Copyright of Chulalongkorn University

Thesis Title	SEPARATION OF LIGNIN FROM BIOMASS USING ACIDIC HETEROGENEOUS CATALYSTS
By	Miss Isara Mongkolpichayarak
Field of Study	Petrochemistry and Polymer Science
Thesis Advisor	Duangamol Tungasmita, Ph.D.
Thesis Co-Advisor	Assistant Professor Sehanat Prasongsuk, Ph.D.

---

Accepted by the Faculty of Science, Chulalongkorn University in Partial  
Fulfillment of the Requirements for the Master's Degree

.....Dean of the Faculty of Science  
(Associate Professor Polkit Sangvanich, Ph.D.)

THESIS COMMITTEE

.....Chairman  
(Professor Pattarapan Prasassarakich, Ph.D.)

.....Thesis Advisor  
(Duangamol Tungasmita, Ph.D.)

.....Thesis Co-Advisor  
(Assistant Professor Sehanat Prasongsuk, Ph.D.)

.....Examiner  
(Associate Professor Nuanphun Chantarasiri, Ph.D.)

.....External Examiner  
(Papapida Pornsuriyasak, Ph.D.)

อิศรา มงคลพิชญรักษ์ : การแยกลิกนินจากชีวมวลโดยใช้ตัวเร่งปฏิกิริยาวิวิธพันธุ์ชนิดกรด (SEPARATION OF LIGNIN FROM BIOMASS USING ACIDIC HETEROGENEOUS CATALYSTS) อ.ที่ปรึกษาวิทยานิพนธ์หลัก: ดร. ดวงกมล ตุงคะสมิต, อ.ที่ปรึกษาวิทยานิพนธ์ร่วม: ผศ. ดร. สีหนาท ประสงค์สุข, 128 หน้า.

งานวิจัยนี้ศึกษาการแยกลิกนินจากชีวมวลด้วยตัวเร่งปฏิกิริยาวิวิธพันธุ์ชนิดกรด โดยศึกษาตัวแปรที่มีผลต่อ ร้อยละผลผลิตของลิกนิน โดยตัวแปรที่ทำการศึกษาได้แก่ ชนิดของตัวเร่งปฏิกิริยา อุณหภูมิ เวลา และอัตราส่วนเอทานอลต่อน้ำ พบว่าการแยกลิกนินด้วยภาวะที่เหมาะสมคือ ตัวเร่งปฏิกิริยาแอมเบอร์ลิสต์-15 อัตราส่วนเอทานอลต่อน้ำเท่ากับ 80:20 โดยปริมาตร ที่อุณหภูมิ 200 องศาเซลเซียส เป็นเวลา 30 นาที ในเครื่องปฏิกรณ์ความดัน โดยลิกนินที่แยกได้จากไมยราบยักษ์ที่ผ่านการปรับสภาพด้วย 1% โดยน้ำหนักของกรดซัลฟิวริก ให้ร้อยละผลผลิตเป็น 16.83 ลิกนินที่แยกได้จากซังข้าวโพดให้ร้อยละผลผลิตเป็น 11.60 เมื่อนำลิกนินที่แยกได้จากไมยราบยักษ์ที่ผ่านการปรับสภาพด้วย 1% โดยน้ำหนักของกรดซัลฟิวริก และซังข้าวโพด มาผ่านการทำให้บริสุทธิ์ด้วยวิธี Klason lignin พบว่าให้ร้อยละเป็น 95.77 และ 72.49 ตามลำดับ จากนั้นตรวจสอบโครงสร้างของลิกนินที่แยกได้ และ Klason lignin จากตัวอย่างทั้งสองด้วยเทคนิคฟูเรียร์ทรานส์ฟอร์มอินฟราเรดสเปกโตรสโคปี (FTIR) เทคนิคโปรตอน-นิวเคลียร์ แมกเนติกเรโซแนนซ์ สเปกโตรสโคปี ( $^1\text{H}$  NMR) เทคนิคคาร์บอน-นิวเคลียร์แมกเนติกเรโซแนนซ์ สเปกโตรสโคปี ( $^{13}\text{C}$  NMR) เครื่องวิเคราะห์องค์ประกอบของธาตุ (C, H, O, N Analyzer) ตรวจสอบลักษณะพื้นผิวด้วยกล้องจุลทรรศน์อิเล็กตรอนแบบส่องกราด และทดสอบการทนต่อการสลายตัวทางความร้อนด้วยเทคนิคเทอร์โมแกรวิเมตริกอะนาไลซิส (TGA) จากการไพโรไลซิสลิกนิน และ Klason lignin จากไมยราบยักษ์ และซังข้าวโพด ด้วยตัวเร่งปฏิกิริยา ZSM-5 ที่อุณหภูมิ 300 องศาเซลเซียส เป็นเวลา 30 นาที พบว่าให้ความเลือกจำเพาะต่อผลิตภัณฑ์ 1,2,4-trimethoxybenzene (14.5-15.4%) และ catechol (26.6-30.3%) ตามลำดับ

สาขาวิชา ปีโตรเคมีและวิทยาศาสตร์พอลิเมอร์ ลายมือชื่อนิสิต .....

ปีการศึกษา 2558

ลายมือชื่อ อ.ที่ปรึกษาหลัก .....

ลายมือชื่อ อ.ที่ปรึกษาร่วม .....

# # 5672149723 : MAJOR PETROCHEMISTRY AND POLYMER SCIENCE

KEYWORDS: LIGNIN / HETEROGENEOUS CATALYSTS

ISARA MONGKOLPICHAYARAK: SEPARATION OF LIGNIN FROM BIOMASS USING ACIDIC HETEROGENEOUS CATALYSTS. ADVISOR: DUANGAMOL TUNGASMITA, Ph.D., CO-ADVISOR: ASST. PROF. SEHANAT PRASONGSUK, Ph.D., 128 pp.

This research studied the separation of lignin with heterogeneous catalysts. The effects of parameters for lignin separation such as types of catalysts, reaction temperature, time and ethanol to deionized water ratio were investigated. The result showed that lignin separation was achieved by using Amberlyst-15 at 200 °C for 30 min with EtOH:water (80:20 v/v) in pressure Parr reactor equipment. The result illustrated that the isolated lignin from giant sensitive plant by pretreatment with 1 wt% of H<sub>2</sub>SO<sub>4</sub> pretreatment and from corncob were 16.83% and 11.60%, respectively. Then, the isolated lignin from both plants were purified with Klason method that showed lignin purity as 95.77% and 72.49%, respectively. The structure of isolated lignin and Klason lignin from both two samples were confirmed by Fourier transform infrared spectroscopy (FTIR), proton-1 Nuclear Magnetic Resonance Spectroscopy (<sup>1</sup>H NMR), carbon-13 Nuclear Magnetic Resonance Spectroscopy (<sup>13</sup>C NMR) and C, H, O, N analyzer. In addition, the morphological structure and thermal degradation were characterized by scanning electron microscope (SEM) and thermogravimetric analysis (TGA). The isolated lignin, Klason lignin from giant sensitive plant and corncob were pyrolyzed with ZSM-5 at 300 °C for 30 min. The results illustrated the high product selectivity of 1,2,4-trimethoxybenzene (14.5-15.4%) and catechol (26.6-30.3%), respectively.

Field of Study: Petrochemistry and  
Polymer Science

Academic Year: 2015

Student's Signature .....

Advisor's Signature .....

Co-Advisor's Signature .....

## ACKNOWLEDGEMENTS

Firstly, I would like to grateful my advisor, Dr. Duangamol Tungasmita and my co-advisor, Assist. Prof. Dr. Sehanat Prasongsuk, for valuable advice, guidance in this research and resolve advice of my thesis problem. Their helpful is benefit for me too much.

I would like to give my gratitude to Prof. Dr. Pattarapan Prasassarakich as the chairman, Assoc. Prof. Dr. Nuanphun Chantarasiri and Dr. Papapida Pornsuriyasak who have been members of thesis committee, for all of their kindness and useful advice in this research.

I am grateful to Department of Petrochemistry and Polymer Science, Faculty of Science, Chulalongkorn University for providing the accommodation in laboratories and instruments. I would like to thank the Department of Botany, Faculty of Science, Chulalongkorn University for supporting as raw biomass. I would like to thank the 90th anniversary of Chulalongkorn University (Ratchadaphiseksomphot Endowment Fund) for research grants. In addition, Thailand Japan Technology Transfer Project a loan supported by Japan Banks for International Cooperation (TJTTP-JBIC) for instrument support. I would like to many thanks the members of Materials Chemistry and Catalysis Research Unit and my friend for their assistance throughout the research.

Finally, I would like to express my deepest gratitude to my family for their love, support, understanding and encouragement throughout graduate study.

## CONTENTS

	Page
THAI ABSTRACT .....	iv
ENGLISH ABSTRACT .....	v
ACKNOWLEDGEMENTS .....	vi
CONTENTS .....	vii
LIST OF TABLES .....	xiv
LIST OF FIGURES .....	xvi
LIST OF SCHEMES .....	xx
LIST OF ABBREVIATIONS .....	xxi
CHAPTER I INTRODUCTION .....	1
1.1 Background.....	1
1.2 Literature reviews .....	2
1.2.1 Hardwood pretreatment.....	2
1.2.2 Lignin separation from biomass.....	3
1.2.3 Lignin transformation to fine chemicals.....	5
1.3 Objectives.....	5
1.4 Scope of this work.....	6
CHAPTER II THEORY .....	7
2.1 Biomass .....	7
2.1.1 Definition .....	7
2.2 Composition and structure of biomass .....	7
2.2.1 Cellulose .....	8
2.2.2 Hemicellulose .....	9

2.2.3 Lignin.....	9
2.2.3.1 General properties of lignin .....	9
2.2.3.2 Type of lignin .....	10
2.2.3.3 Application of lignin.....	13
2.3 Type of biomass pretreatment .....	13
2.3.1 Physical pretreatment .....	14
2.3.1.1 Mechanical comminution.....	14
2.3.2 Chemical pretreatment.....	14
2.3.2.1 Acid hydrolysis.....	14
2.3.2.1.1 Dilute acid pretreatment.....	14
2.3.2.1.2 Concentrated acid pretreatment .....	15
2.3.2.2 Alkaline Pretreatment .....	15
2.3.3 Biological pretreatment.....	16
2.4 Method for separated lignin from biomass .....	16
2.4.1 Organosolv process.....	16
2.4.2 Ionic liquid pretreatment .....	16
2.4.3 Oxidative process with hydrogen peroxide (H <sub>2</sub> O <sub>2</sub> ).....	17
2.4.4 Ozonolysis pretreatment .....	17
2.5 Mechanism of lignin separation from biomass .....	17
2.5.1 $\alpha$ -Ether cleavage of the lignin in wood .....	17
2.5.2 $\beta$ -O-4 bond cleavage of the lignin in wood.....	18
2.6 Catalysts.....	21
2.6.1 Type of catalyst.....	21



	Page
2.6.2 Type of porous material .....	22
2.6.2.1 Microporous material .....	23
2.6.2.1.1 Zeolite structure .....	23
2.6.2.1.2 ZSM-5 .....	25
2.6.2.1.3 Zeolite- $\beta$ .....	26
2.6.2.2 Mesoporous material .....	27
2.6.2.2.1 SBA-15 .....	27
2.6.2.2.1.1 Structure and properties of SBA-15 .....	27
2.6.2.2.1.2 Synthesis of SBA-15 and formation mechanism .....	27
2.6.2.2.2 Modification of SBA-15 .....	28
2.6.2.2.2.1 Al-SBA-15 .....	28
2.6.2.3 Resin catalyst .....	29
2.6.2.3.1 Amberlyst-15 .....	29
2.7 Characterization of SBA-15.....	29
2.7.1 X-ray Powder Diffraction (XRD) .....	29
2.7.2 Nitrogen adsorption-desorption .....	30
2.7.3 Aluminium-27 Nuclear Magnetic Resonance ( $^{27}\text{Al-NMR}$ ) .....	31
2.7.4 Inductively Coupled Plasma-Mass Spectroscopy (ICP-MS) .....	32
2.8 Characterization of lignin.....	33
2.8.1 Fourier transform infrared spectroscopy (FTIR) .....	33
2.8.2 Scanning electron microscope (SEM) .....	34
2.8.3 Proton Nuclear Magnetic Resonance Spectroscopy ( $^1\text{H NMR}$ ) .....	35

	Page
2.8.4 Proton Nuclear Magnetic Resonance Spectroscopy ( $^{13}\text{C}$ NMR).....	36
2.8.5 Thermogravimetric analysis (TGA).....	37
2.8.6 Elemental analysis (C, H, O and N).....	37
CHAPTER III EXPERIMENTS.....	39
3.1 Chemicals, Gases and Materials.....	39
3.2 Instruments and Apparatus .....	41
3.2.1 Oven .....	41
3.2.2 Furnace.....	41
3.2.3 X-ray powder diffraction (XRD) .....	42
3.2.4 Surface area analysis.....	42
3.2.5 Aluminium-27 Nuclear Magnetic Resonance ( $^{27}\text{Al}$ -NMR) .....	42
3.2.6 Inductively Coupled Plasma-Mass Spectroscopy (ICP-MS).....	42
3.2.7 PARR reactor .....	42
3.2.8 Fourier transform infrared spectroscopy (FTIR).....	43
3.2.9 Nuclear Magnetic Resonance Spectroscopy ( $^1\text{H}$ and $^{13}\text{C}$ NMR ).....	43
3.2.10 Scanning electron microscope (SEM) .....	43
3.2.11 Thermogravimetric analysis (TGA).....	43
3.2.12 Elemental analyzer (C, H, O and N).....	43
3.2.13 Centrifuge.....	43
3.2.14 Gas chromatograph-mass spectrometer (GC-MS).....	44
3.3 Determine component of giant sensitive plant .....	44
3.3.1 Neutral detergent fiber (NDF) method.....	44
3.3.2 Acid detergent fiber (ADF) method.....	45

	Page
3.3.3 Permanganate detergent (PML) method .....	46
3.3.4 Analysis of cellulose with calcination .....	47
3.4 Biomass pretreatment .....	47
3.4.1 Hardwood.....	47
3.4.2 Agricultural residue .....	47
3.5 Synthesis of SBA-15.....	47
3.5.1 Synthesis of Al-SBA-15.....	48
3.6 Acid-base titration.....	49
3.7 Lignin separation from biomass.....	50
3.8 Parameters affecting biomass pretreatment.....	51
3.8.1 Acid pretreatment of giant sensitive plant .....	51
3.8.1.1 Effect of amount of $H_2SO_4$ .....	51
3.8.1.2 Effect of temperature.....	52
3.8.2 Parameters affecting lignin separation .....	52
3.8.2.1 Effect of EtOH/ $H_2O$ ratio .....	52
3.8.2.2 Effect of reaction temperature.....	52
3.8.2.3 Effect of reaction time .....	52
3.8.2.4 Effect of catalyst type.....	52
3.9 Determine pure isolated lignin with Klason method .....	52
3.10 Lignin transformation to fine chemicals with optimal condition.....	53
CHAPTER IV RESULTS AND DISCUSSIONS.....	54
4.1 The component of biomass .....	54
4.2 Giant sensitive pretreatment with dilute acid .....	54

4.3 Characterization of catalysts .....	57
4.3.1 Pure SBA-15 and Al-SBA-15 .....	57
4.3.1.1 X-ray powder diffraction (XRD).....	57
4.3.1.2 Nitrogen adsorption-desorption .....	58
4.3.2 <sup>27</sup> Al-MAS-NMR spectra of Al-SBA-15.....	60
4.3.3 Elemental analysis of Al-SBA-15.....	60
4.3.5 Acid-base titration .....	62
4.4 Lignin separation from hardwood and agricultural residue .....	63
4.5 Lignin Separation from pretreated giant sensitive plant .....	63
4.5.1 Effect of solvent ratio.....	63
4.5.2 Effect of reaction temperature.....	64
4.5.3 Effect of reaction time.....	65
4.5.4 Effect of catalyst.....	66
4.6 Lignin separation from corncob.....	67
4.7 Characterization of isolated lignin.....	67
4.7.1 Fourier transform infrared spectroscopy (FTIR).....	67
4.7.1.1 Isolated lignin from giant sensitive plant .....	67
4.7.1.2 Isolated lignin from corncob.....	69
4.7.2 Proton-1 Nuclear Magnetic Resonance Spectroscopy ( <sup>1</sup> H NMR).....	71
4.7.3 Carbon-13 Nuclear Magnetic Resonance Spectroscopy ( <sup>13</sup> C NMR) .....	73
4.7.4 Scanning electron microscope (SEM) .....	77
4.7.5 Thermogravimetric analysis (TGA) .....	80
4.7.5.1 Raw giant sensitive plant and corncob.....	80

4.7.5.2 Isolated crude lignin and Klason lignin from pretreated giant sensitive plant.....	82
4.7.5.3 Isolated crude lignin and Klason lignin from corncob .....	84
4.7.6 Elemental analysis (C, H, O and N).....	86
4.8 Lignin transformation to fine chemicals with optimal condition.....	87
4.8.1 Gas chromatograph-mass spectrometer (GC-MS).....	87
4.8.1.1 Commercial lignin and Klason commercial lignin .....	87
4.8.1.2 Isolated crude lignin and Klason lignin from pretreated giant sensitive plant.....	90
4.8.1.3 Isolated crude lignin and Klason lignin from corncob .....	93
4.9 Catechol selectivity from lignin pyrolysis.....	96
CHAPTER V CONCLUSION.....	98
REFERENCES .....	100
APPENDIX.....	109
VITA.....	128

## LIST OF TABLES

Table	Page
2.1 Structure and chemical composition of biomass. ....	8
2.2 Lignin compositions of different plants.....	11
2.3 Propotions of linkages in lignin. ....	12
2.4 Difference of homogeneous and heterogenous catalysts [51]. ....	22
2.5 IUPAC category of porous materials [52]. ....	23
2.6 Comparison of ZSM-5 and Zeolite- $\beta$ . ....	26
2.7 Properties of SBA-15[60]. ....	27
4.1 The component of biomass.....	54
4.2 Effect of time on giant sensitive plant pretreatment without dilute acid.....	55
4.3 Effect of various concentration of dilute acid on giant sensitive plant pretreatment at 100 °C for 8 .....	56
4.4 Properties of pure SBA-15 and Al-SBA-15.....	59
4.5 Si/Al mole ratio of Al-SBA-15.....	61
4.6 Properties of Amberlyst-15, ZSM-5 and Zeolite- $\beta$ .....	62
4.7 Acid amount of catalysts.....	62
4.8 Lignin separation from hardwood and agricultural residue.....	63
4.9 Effect of solvent ratio on isolated lignin from pretreated giant sensitive plant and corncob.....	64
4.10 Effect of temperature on isolated lignin from pretreated giant sensitive plant and corncob.....	65
4.11 Effect of time on isolated lignin from pretreated giant sensitive plant and corncob.....	65

4.12	Effect of various catalysts on isolated lignin from pretreated giant sensitive plant and corncob.....	66
4.13	The comparison of isolated lignin from pretreated giant sensitive plant and corncob.....	67
4.14	Elemental analysis.....	86
4.15	Compound identified by GC-MS in catalytic pyrolysis of commercial lignin.....	87
4.16	Compound identified by GC-MS in catalytic pyrolysis of Klason commercial lignin.....	88
4.17	Compound identified by GC-MS in catalytic pyrolysis of isolated crude lignin from pretreated giant sensitive plant.....	90
4.18	Compound identified by GC-MS in catalytic pyrolysis of Klason lignin from pretreated giant sensitive plant.....	91
4.19	Compound identified by GC-MS in catalytic pyrolysis of isolated crude lignin from corncob.....	93
4.20	Compound identified by GC-MS in catalytic pyrolysis of Klason lignin from corncob.....	94

## LIST OF FIGURES

Figure	Page
1.1 Pretreated biomass with dilute acid [10]. .....	2
1.2 Degradation mechanism of $\beta$ -O-4 linkages during organosolv process. ....	4
2.1 Chemical structure of cellulose [22].....	8
2.2 Main components of hemicellulose [22]. ....	9
2.3 Schematic representation of the location and structure of lignin in biomass [28].....	10
2.4 Three main phenylpropane units of lignin [29]. ....	11
2.5 The type of linkages as formed in lignin structure [29]. ....	12
2.6 Application of lignin as renewable resource from biomass [30]. ....	13
2.7 Effects of various pretreatment processes on structure of biomass [31]. ....	14
2.8 Side chain rearrangement in hot water [48]. ....	18
2.9 Mechanism of the $\beta$ -O-4 bond cleavage [49].....	20
2.10 The relationship between activation energy ( $E_a$ ) and enthalpy ( $\Delta H$ ) of the reaction with and without a catalyst [50]. ....	21
2.11 Binding of building units (PBU and SBU) in three-dimensional zeolite- clinoptilolite structure [54]. ....	23
2.12 Secondary Building Units (SBUs) in zeolites [55]. ....	24
2.13 The structure of zeolite. ....	25
2.14 (a) Skeletal diagram of the (100) face of ZSM-5 and (b) Channel structure of ZSM-5 [57]. ....	25
2.15 The structure of zeolite- $\beta$ [58]. ....	26
2.16 Hexagonal structure of SBA-15 [59]. ....	27



2.17	The pore evolution upon thermal treatment, depending on pre-treatment and aging [61].	28
2.18	Synthesis of Al-SBA-15 using basic probe inducing to form the bridging hydroxyl group.	29
2.19	The structure of Amberyst-15 unit [62].	29
2.20	Diffraction of X-ray by regular planes of sample [64].	30
2.21	The IUPAC type of adsorption isotherm [66].	31
2.22	The processes of ICP-MS [68].	33
2.23	The main processes of FTIR [69].	33
2.24	The main processes of SEM [70].	34
2.25	An example of $^1\text{H}$ NMR spectrum of a poplar mill-wood lignin using DMSO as solvent [71].	36
2.26	$^{13}\text{C}$ NMR spectrum of a milled wood lignin isolated from a hardwood <i>Buddleja davidii</i> [71].	37
3.1	The temperature program for the calcination of SBA-15 catalyst.	41
4.1	%Yield of isolated crude lignin from giant sensitive plant pretreatment without dilute acid solution at $100^\circ\text{C}$ for 1-8 h.	56
4.2	%Yield of isolated crude lignin from giant sensitive plant pretreatment with 0.25-2% $\text{H}_2\text{SO}_4$ at $100^\circ\text{C}$ for 8 h.	57
4.3	XRD patterns of (a) pure SBA-15 and (b) Al-SBA-15.	58
4.4	Nitrogen adsorption-desorption isotherms of (a) pure SBA-15 and (b) Al-SBA-15.	59
4.5	$^{27}\text{Al}$ -MAS-NMR spectra of Al-SBA-15.	60
4.6	FTIR spectra of (a) raw giant sensitive plant, (b) pretreated giant sensitive plant with 1% $\text{H}_2\text{SO}_4$ at $100^\circ\text{C}$ for 8 h, (c) isolated crude lignin, (d) Klason lignin and (e) residue. Separation condition: 3.0 g of pretreated giant	

	sensitive plant, 0.63 g of Amberlyst-15, C <sub>2</sub> H <sub>5</sub> OH:H <sub>2</sub> O = 80:20 (v/v) at 200°C for 30 min.....	69
<b>4.7</b>	FTIR spectra of (a) raw corncob, (b) isolated crude lignin, (c) Klason lignin and (d) residue. Separation condition: 3.0 g of corncob, 0.63 g of Amberlyst-15, C <sub>2</sub> H <sub>5</sub> OH:H <sub>2</sub> O = 80:20 (v/v) at 200°C for 30 min. ....	70
<b>4.8</b>	<sup>1</sup> H NMR spectrums of crude lignin from commercial, pretreated giant sensitive plant and corncob.....	72
<b>4.9</b>	<sup>1</sup> H NMR spectra of Klason lignin from crude lignin of pretreated giant sensitive plant (Figure D-4) and corncob (Figure D-5).....	73
<b>4.10</b>	Guaiacyl phenolic unit (a) and syringyl unit (b).....	74
<b>4.11</b>	<sup>13</sup> C NMR spectrums of crude lignin from commercial (Figure D-6), pretreated giant sensitive plant (Figure D-7) and corncob (Figure D-8).....	75
<b>4.12</b>	<sup>13</sup> C NMR spectrums of Klason lignin from crude lignin from giant sensitive plant (Figure D-9) and corncob (Figure D-10). ....	76
<b>4.13</b>	SEM images (1,500 × magnification) of (a) raw giant sensitive plant, (b) pretreatment with 1% (w/w) H <sub>2</sub> SO <sub>4</sub> as 15:2 ratio of raw giant sensitive plant to H <sub>2</sub> SO <sub>4</sub> and (c) residue from separated lignin, (10,000 × magnification) of (d) isolated lignin and (e) Klason lignin; Separation condition: 3.0 g of pretreated giant sensitive plant, 0.63 g of Amberlyst-15, C <sub>2</sub> H <sub>5</sub> OH:H <sub>2</sub> O = 80:20 (v/v) at 200°C for 30 min.....	78
<b>4.14</b>	SEM images (1,500 × magnification) of (a) raw corncob and (b) residue from separated lignin, of (c) isolated lignin (10,000 × magnification) and (d) Klason lignin; Separation condition: 3.0 g of corncob, 0.63 g of Amberlyst-15, C <sub>2</sub> H <sub>5</sub> OH:H <sub>2</sub> O = 80:20 (v/v) at 200°C for 30 min.....	79
<b>4.15</b>	TGA and DTG curves of (a) raw giant sensitive plant and (b) corncob. ....	81
<b>4.16</b>	TGA and DTG curves of crude lignin and Klason lignin from pretreated giant sensitive plant.....	83

<b>4.17</b>	TGA and DTG curves of isolated lignin and Klason lignin from corncob.....	85
<b>4.18</b>	Total ion chromatograms of (a) commercial lignin and (b) Klason commercial lignin catalytic pyrolysis of lignin at 300°C for 30 min, ZSM-5 to lignin ratio of 0.75:1 with 10 g of DI water. Refer to Table 4.13 and Table 4.14 for the names of identified compounds. ....	89
<b>4.19</b>	Total ion chromatograms of (a) isolated crude lignin and (b) Klason lignin from pretreated giant sensitive plant catalytic pyrolysis of lignin at 300°C for 30 min, ZSM-5 to lignin ratio of 0.75:1 with 10 g of DI water. Refer to Table 4.15 and Table 4.16 for the names of identified compounds.....	92
<b>4.20</b>	Total ion chromatograms of (a) isolated crude lignin and (b) Klason lignin from corncob catalytic pyrolysis of lignin at 300°C for 30 min, ZSM-5 to lignin ratio of 0.75:1 with 10 g of DI water. Refer to Table 4.17 and Table 4.18 for the names of identified compounds. ....	95
<b>4.21</b>	%Selectivity based on peak area of products in liquid obtained by pyrolysis from lignin <sup>a</sup> and pure lignin <sup>b</sup> of corncob, commercial and pretreated giant sensitive plant.....	96

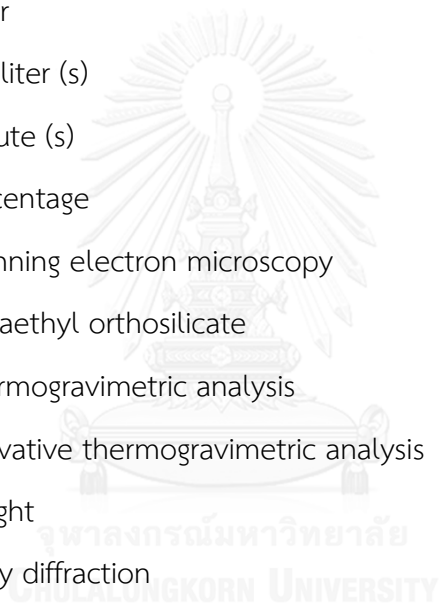
## LIST OF SCHEMES

Scheme	Page
3.1 The process of neutral detergent fiber.....	45
3.2 The process of acid detergent fiber.....	46
3.3 Diagram of SBA-15 synthesis.....	48
3.4 Diagram of Al-SBA-15 by post-synthesis method.....	49
3.5 Diagram of lignin separation.....	51



## LIST OF ABBREVIATIONS

a.u.	Arbitrary unit
BET	Brunauer-Emmett-Teller
BJH	Barret, Joyner, and Halenda
°C	Degree Celsius
GC-MS	Gas chromatograph-mass spectrometer
g	Gram (s)
hr	Hour
ml	Milliliter (s)
min	Minute (s)
%	Percentage
SEM	Scanning electron microscopy
TEOS	Tetraethyl orthosilicate
TGA	Thermogravimetric analysis
DTG	Derivative thermogravimetric analysis
wt	Weight
XRD	X-ray diffraction



# CHAPTER I

## INTRODUCTION

### 1.1 Background

Presently, petrochemical industry and polymer is quickly developed. The world encounters with petroleum sources and environmental problems such as global warming that are the world's major point. Moreover, the using of petroleum to produce many chemicals leads to carbon dioxide emission. It is believed that the one of the factors that causes global warming [1, 2]. Consequently, many countries have been focusing on renewable alternative resource to replace the non-renewable resource.

Biomass is attractive renewable alternative resource due to its low cost and abundant aromatic that can be produced to valuable chemicals such as benzene, toluene and xylene etc. Thailand is an agricultural country. As a consequence, there are of many agriculture residues [3]. That is lignocellulosic biomass that consists mainly of cellulose, hemicellulose and lignin. Especially, lignin is one of the three major polymeric components found in the cell walls of plants. Lignin's role is to act as a matrix material that binds the plant polysaccharide microfibrils and fibers. Moreover, lignin also acts other biological functions, including protect plants from biological attack and assisting in water transport by sealing plant cell walls against water leaks [4]. Thus, lignocellulosic material is necessary to pretreated in order to reduce crystallinity of structure and increase the porosity of lignocellulosic material with physical treatment (e.g. milling, grinding) in conjunction with chemical pretreatment. Generally, cellulose and hemicellulose were pretreated with dilute

acid (e.g.,  $\text{H}_2\text{SO}_4$ ,  $\text{HCl}$ ) that were digested as sugar, dissolving in solution and removed from biomass. This process showed a good result in an effective lignin solubilization [5-7]. However, using homogeneous catalysts will cause several disadvantages such as reactor corrosion, difficulty in catalytic separation and recovery from reaction mixture [8, 9]. Thus, heterogeneous catalyst (e.g. Amberlyst-15, ZSM-5, Zeolite- $\beta$ , Al-SBA-15) is one of alternative choices to solve this problem.

This work will focus on the biomass pretreatment with dilute acid. Moreover, the comparison of homogeneous and heterogeneous catalysts on lignin separation capacity was investigated. The isolated lignin is transformed to fine chemical under an optimum condition.

## 1.2 Literature reviews

This research will be distributed into 3 parts, there are biomass pretreatment, lignin separation and lignin transformation to fine chemicals under optimal condition.

### 1.2.1 Hardwood pretreatment

In this title will be explicated about the hardwood pretreatment with physical pretreatment in combination with chemical pretreatment that removed hemicellulose, reduced cellulose crystallinity and increased the porosity of hardwood as shown in Figure 1.1.

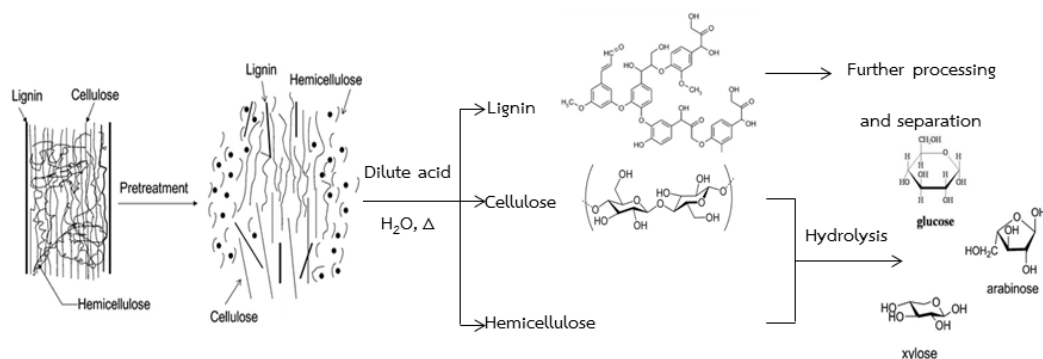


Figure 1.1 Pretreated biomass with dilute acid [10].

In 2013, Nantapipat *et al.* [11] compared the pretreatment of corncob with sulfuric acid and phosphoric acid at 120 °C for 5 min with 15: 1 liquid to solid ratio. Before pretreatment, corncobs were milled and sieved as particle size (<1.6 mm). The result was presented that 2 %w/w of sulfuric acid have effectively pretreated corncob more than phosphoric acid. Seeing that, sulfuric acid gave the highest total monomeric sugar (35.72 g/L) more than phosphoric acid (34.09 g/L) which were digested as sugar, dissolving in solution. Moreover, the structure of corncob was pretreated with sulfuric acid that reduced crystallinity with crystallinity index as 39.9.

The above research showed that pretreatment of biomass with dilute acid under optimum condition gave to the product as a reducing sugar. This product was dissolved in solution. It is the interesting choice to be used in the pretreatment of biomass to increase efficiency in the process of separation of lignin as show in the following researches.

### 1.2.2 Lignin separation from biomass

In 2009, Hang *et al.* [12] separated lignin from *miscanthus* with organosolv lignin process, using 1.2 %w/w of sulfuric acid as catalyst, EtOH/H<sub>2</sub>O = 0.65 at 190 °C for 60 min in a 1.0 L pressure Parr reactor equipment. The results showed that *miscanthus* lignin consists of *p*-hydroxyl phenol (H), guaiacyl (G) and syringyl (S) as monomer unit of the lignin structure. Each of monomer unit composes of 4%, 52% and 44% respectively. The obtained lignin was cleavage the most  $\beta$ -O-4 linkages and ester bond that was the major mechanism of lignin breakdown.

In 2010, Sannigrahi *et al.* [13] separated lignin from Loblolly pine with organosolv process, using 1.1 %w/w of sulfuric acid as catalyst, EtOH/H<sub>2</sub>O = 65% at 170 °C for 60 min in a pressure Parr reactor equipment. The results illustrated that this condition gave the isolation of 27% Klason lignin. In addition, the acid-catalyzed cleavage of  $\beta$ -O-4 linkages and ester bond were the major mechanisms of lignin cleavage. After that the isolated lignin was more condensed as phenol and carboxylic acid and lower aliphatic carbon. The result from <sup>31</sup>P NMR analysis found that the major hydroxyl groups in lignin structure were aliphatic, phenol and *p*-



hydroxyl-phenyl with 7.3, 2.7 and 2.0 mmol/g of lignin, respectively. The concentration of the different hydroxyl groups was calculated on the basis of internal standard (cyclohexanol) and the integrated peak areas.

In 2010, Hallac *et al.* isolated lignin from *Buddleja davidii* with organosolv process, using 1.5 %w/w of sulfuric acid as catalyst, EtOH/H<sub>2</sub>O = 65% at 195 °C for 60 min in a pressure Parr reactor equipment. The results reveal that this condition gave the isolation of 64% lignin from the starting material. The result of structural analysis of *Buddleja davidii* using quantitative <sup>31</sup>P NMR was shown that the major hydroxyl groups in lignin structure were aliphatic, guaiacyl, phenolic and carboxylic with 1.86, 1.66, 1.07 and 0.15 mmol/g of lignin, respectively. Furthermore, the degradation mechanism of lignin was cleavage through  $\beta$ -O-4 linkages as shown in Figure 1.2.

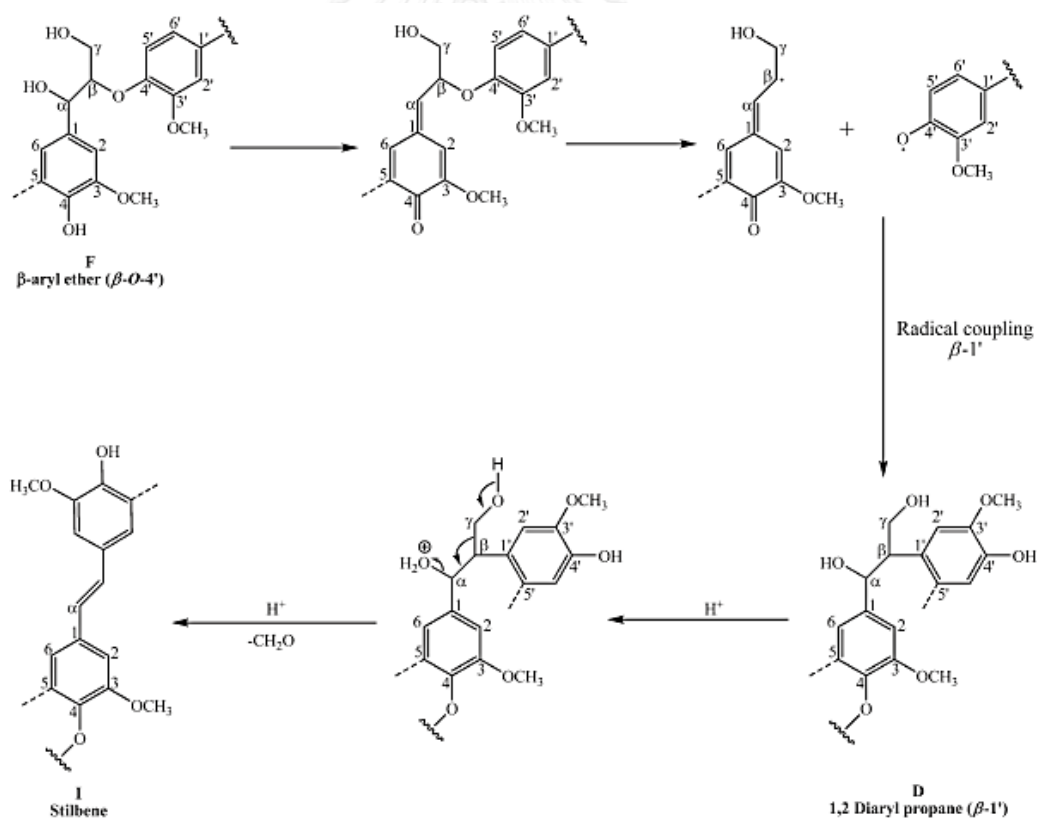


**Figure 1.2** Degradation mechanism of  $\beta$ -O-4 linkages during organosolv process.

### 1.2.3 Lignin transformation to fine chemicals

Lignin is source of abundant aromatic in natural polymer that was expected to play an important role as raw material for intermediates and products in chemical industry. The different products from lignin transformation depend on various operating parameter such as type of catalyst, temperature, time and kinds of reaction that are pyrolysis, catalytic hydrogenation, oxidation or hydrocracking.

In 2012, Li *et al.* [14] studied fast pyrolysis of Kraft lignin with HZSM-5. The result showed that the reduced  $\text{SiO}_2/\text{Al}_2\text{O}_3$  ratio of HZSM-5 can produce a type of product such as aromatic groups (benzene, toluene and xylene). On the other hand, the increased  $\text{SiO}_2/\text{Al}_2\text{O}_3$  ratio of HZSM-5 can produce a type of product such as phenol group and oxygenate compounds (vanillin, 2-methoxy-4-vinylphenol and benzene, 1,2-dimethoxy). From experiment illustrated that the increased alumina brought to catalyst as high acid and selectivity to product in aromatic groups more than phenol and oxygenate compounds.

In 2012, Ye *et al.* [15] produced 4-ethylphenol and 4-ethylguaiacol with 3.1% and 1.3% base on weight of raw lignin, respectively via mild hydrogenolysis using catalyst as 5% of Ru supported on carbon, 65 %v/v ethanol at  $375^\circ\text{C}$  for 90 min in a pressure Parr reactor equipment that was the optimum condition for hydrogenolysis reaction.

### 1.3 Objectives

1. To find the optimum condition for biomass pretreatment.
2. To compare efficiency of heterogeneous and homogeneous catalysts in lignin separation.
3. To transform lignin into fine chemicals under an optimal condition.

#### 1.4 Scope of this work

The scope of this study is distributed to 3 parts such as biomass pretreatment, lignin separation and lignin transformation to fine chemicals under optimal condition. Consequently, this research investigated the compare efficiency of heterogeneous (Amberlyst-15, ZSM-15, Zeolite- $\beta$  and Al-SBA-15) and homogeneous (e.g.  $\text{H}_2\text{SO}_4$ ,  $\text{HNO}_3$  and  $\text{HCl}$ ) catalysts in lignin separation from biomass through optimum pretreatment. After that the isolated lignin is purified with Klason lignin method. Finally, this pure lignin is transformed into fine chemicals under optimal condition.



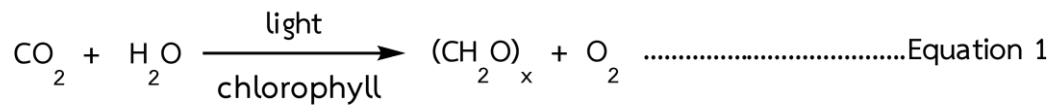
## CHAPTER II

### THEORY

#### 2.1 Biomass

##### 2.1.1 Definition

The biomass refers to organic matter which mainly consists of carbon atom, hydrogen atom and oxygen atom. The sources of the elementals receive the photosynthesis process that is showed in Equation 1. The resource of organic compound is agricultural crops, agricultural waste/residue, wood and forestry residue and waste streams [16].



#### 2.2 Composition and structure of biomass

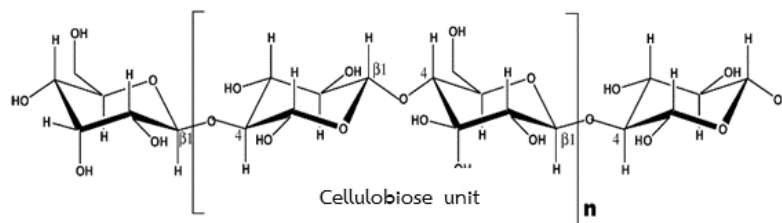
The main structure of general biomass compose of three polymer include cellulose, hemicellulose and lignin. These polymers have different main structures which depend on the type of biomass. They are can be found in cell wall. Table 2.1 shows summaries of main chemical composition of studied biomass.

**Table 2.1** Structure and chemical composition of biomass.

Biomass	Composition (wt%)				
	Cellulose	Hemicellulose	Lignin	Ash	Others
Rice straw [17]	33.4	28.2	7.4	12.8	18.2
Bagasse [18]	50.4	28.5	14.9	42.0	4.2
Corn cob [19]	52.9	32.1	13.1	1.2	0.7
Giant sensitive plant [20]	36.87	15.51	20.68	0.58	26.35

### 2.2.1 Cellulose

Cellulose is a crystalline structure and high-molecular-weight linear polymer of  $\beta$ -(1,4)-glucopyranose units linked together as shown in Figure 2.1. The main repeating unit of the cellulose polymer consists of two glucose anhydride units which are called a cellulobiose unit. The molecular formula of cellulose is  $(C_6H_{12}O_6)_n$  [21, 22].

**Figure 2.1** Chemical structure of cellulose [22].

Cellulose is insoluble in normal aqueous solutions. However, it is soluble in more exotic solvents, such as aqueous *N*-methylmorpholine-*N*-oxide (NMNO), some ionic liquids CdO/ethylenediamine (cadoxen), LiCl/*N,N*-dimethylacetamide, and near supercritical water [23, 24].

## 2.2.2 Hemicellulose

Hemicellulose is a mixture of various polymerized monosaccharides such as glucose, mannose, galactose, xylose, arabinose, 4-O-methyl glucuronic acid and galacturoic acid residues as shown in Figure 2.2. Hemicelluloses exhibit lower molecular weights than cellulose. Cellulose has only glucose in its structure, whereas hemicellulose has a heteropolysaccharide. The molecular formula of cellulose is  $(C_6H_{12}O_6)_n$ . The thermal decomposition of hemicellulose occurs at lower temperatures than crystalline cellulose due to the degree of polymerization is 50 to 200 [25].

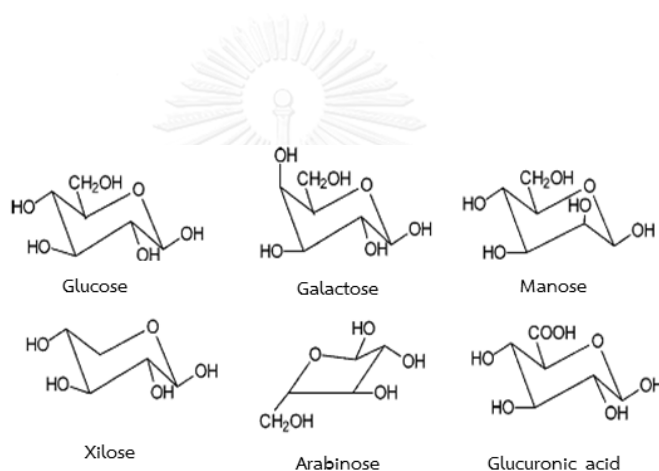


Figure 2.2 Main components of hemicellulose [22].

## 2.2.3 Lignin

### 2.2.3.1 General properties of lignin

Lignin is a naturally occurring aromatic cross-linked polymer with molecular weight more than 10,000 Daltons (Da). Lignin is an amorphous cross-linked resin with no exact structure and a non-carbohydrate component. Lignin is found largely in the cell walls with lignin acting as a linker between cellulose and hemicellulose as shown in Figure 2.3. It is the main binder for the agglomeration of fibrous cellulosic components. It can resistance the rapid microbial or fungal

destruction of the cellulosic fibers. In addition, lignin is more difficult to dehydrate than cellulose or hemicellulose due to its hydrophobicity [26, 27].

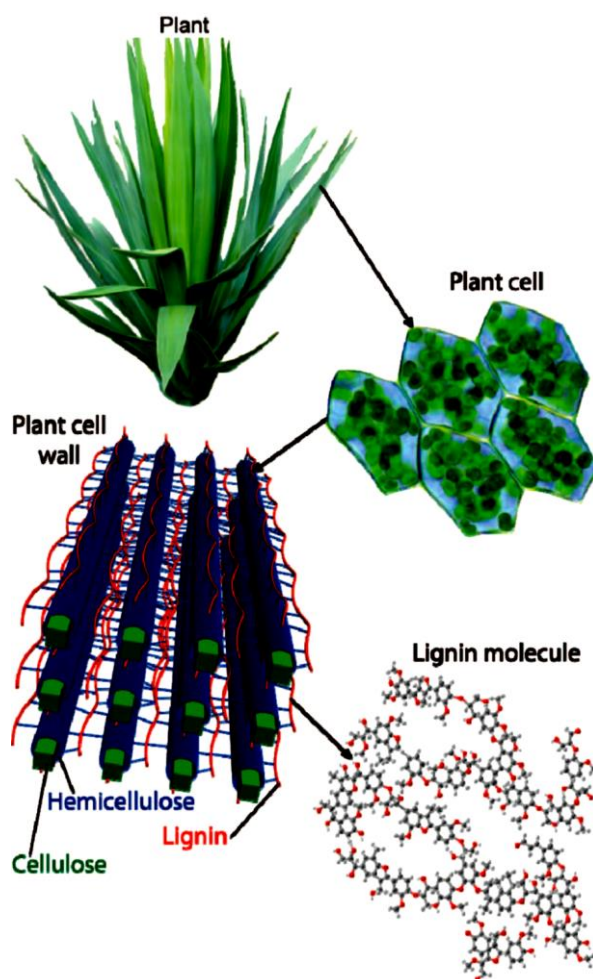


**Figure 2.3** Schematic representation of the location and structure of lignin in biomass [28].

### 2.2.3.2 Type of lignin

Lignin is polyphenolic substance that consists of an irregular array of variously bonded “hydroxy” and “methoxy” as substituted phenylpropane unit. There are three main phenylpropane units of lignin such as *p*-coumaryl alcohol, coniferyl alcohol and sinapyl alcohol as shown in Figure 2.4.

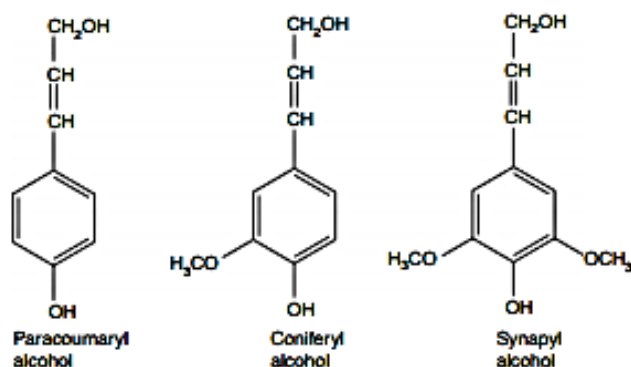


Figure 2.4 Three main phenylpropane units of lignin [29].

The composition of each lignin differs with the type of plant as shown in Table 2.2. Softwood lignin is found in pine trees which mainly compose of coniferyl alcohol and only a trace amount of sinapyl alcohol as their repeating units [28]. However, hardwood lignin is found in tropical and subtropical trees such as oak and teak which contain both coniferyl and sinapyl alcohols. It is also identified that neither hardwood nor softwood lignin contains significant proportion of *p*-coumaryl alcohol which can be found in grass lignin. The common linkages formed during lignin are the  $\beta$ -O-4 ether linkages. The other types of ether and C-C linkages can be found in lignin structure such as  $\alpha$ -O-4,  $\beta$ - $\beta$ ,  $\beta$ -5,  $\beta$ -1, 4-O-5 and 5-5 as shown in Table 2.3 and Figure 2.5.

Table 2.2 Lignin compositions of different plants.

Biomass	Composition (%wt)		
	<i>p</i> -Coumaryl alcohol	Coniferyl alcohol	Sinapyl alcohol
Softwood	<5	<95	Trace amount
Hardwood	0-8	25-50	46-75
Grasses	5-33	33-80	20-54



Table 2.3 Proportions of linkages in lignin.

Linkage type	Dimer structure	Percent of total linkage (%)
$\beta$ -O-4	Phenylpropane $\beta$ -aryl ether	45-85
5-5	Biphenyl and Dibenzodioxocin	4-25
$\beta$ -5	Phenylcomaran	9-12
$\beta$ -1	1,2- Diaryl propane	7-10
$\alpha$ -O-4	Phenylpropane $\alpha$ -aryl ether	6-8
4-O-5	Diaryl ether	4-8
$\beta$ - $\beta$	$\beta$ - $\beta$ -linked structure	3

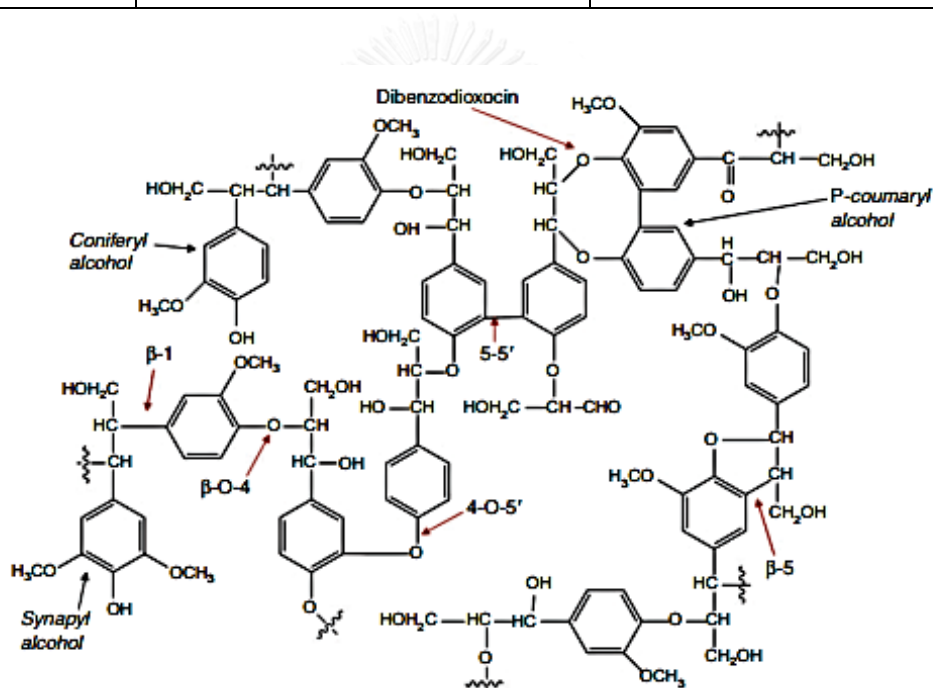


Figure 2.5 The type of linkages as formed in lignin structure [29].

### 2.2.3.3 Application of lignin

Lignin is the most abundant resource of aromatic compound which can be produced many chemical reagents such as phenolic acids, catecols, vanillin, BTX (benzene, toluene and xylene) and fuels. In addition, lignin can be generated as an adhesive that is replaced from derived from oil. The application of lignin can be summarised as shown in Figure 2.6.

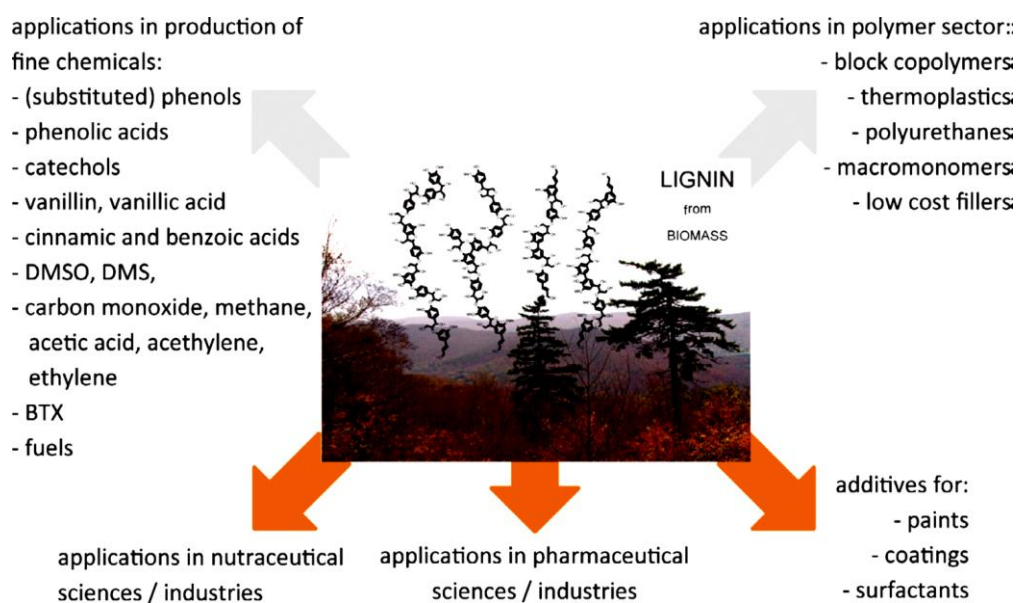
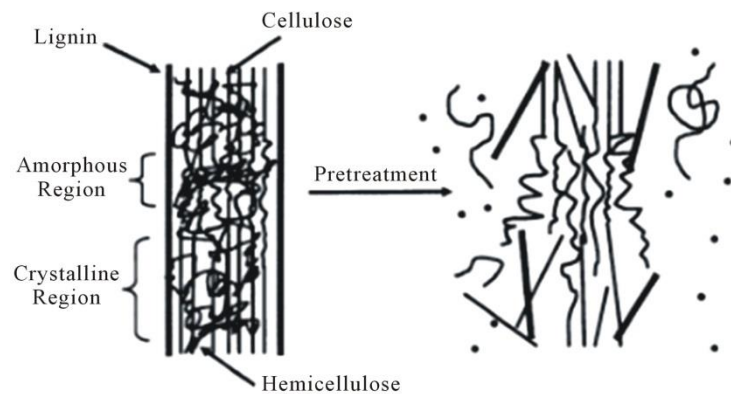


Figure 2.6 Application of lignin as renewable resource from biomass [30].

## 2.3 Type of biomass pretreatment

The goal of biomass pretreatment is to reduce the crystallinity of cellulose, increase the porosity of biomass and efficiency in lignin separation as shown in Figure 2.7.



**Figure 2.7** Effects of various pretreatment processes on structure of biomass [31].

### 2.3.1 Physical pretreatment

#### 2.3.1.1 Mechanical comminution

The mechanical comminution of biomass is chipping, grinding or milling which are used to reduce cellulose crystallinity. The particle size of biomass is 10-30 mm after chipping and 0.2-2 mm after milling or grinding. The vibratory ball milling is found to be more effective than ordinary ball mill. The energy equipment of mechanical comminution of biomass depends on both biomass characteristics and the final particle size required. Hardwood uses more energy than agricultural residues [32].

### 2.3.2 Chemical pretreatment

#### 2.3.2.1 Acid hydrolysis

Dried biomass is milled as particle size required which are submerged in acidic solution under specific temperatures for a period of time. Generally, sulfuric acid ( $H_2SO_4$ ) and phosphoric acid ( $H_3PO_4$ ) are largely used because they are relatively cheap and efficient in hydrolyzing biomass. Hydrochloric acid (HCl) and nitric acid ( $HNO_3$ ) are more volatile and easier to recover better than  $H_2SO_4$ . On the other hand, both acids are more expensive compared to sulfuric acid.

##### 2.3.2.1.1 Dilute acid pretreatment

This is method of biomass pretreatment has obtained extensive research. Generally, the dilute acid (0.2-2.5 %w/w) at high

temperature (120-210 °C) and different pressures are used to succeed reaction. A variation of the process involves two stages of pretreatment: the first stage, most hemicelluloses in the biomass are solubilized in the presence of a more dilute acid, while the second stage concerns with the using of a higher acid concentration to hydrolyze the cellulose to glucose.

Advantages of dilute acid pretreatment is high reaction rates and significantly improved hemicellulose and cellulose hydrolysis by varying the hardness of the pretreatment, but the feedstock subjected to dilute acid pretreatment may be a little harder to ferment due to the existing of fermentation inhibitors [33].

#### **2.3.2.1.2 Concentrated acid pretreatment**

This pretreatment variation uses concentrated sulfuric (65-86 %w/w), hydrochloric (41 %w/w), or phosphoric (85 %w/w) acids to crushed biomass at low temperature (30-60 °C) and pressures. The process consists of diluted with deionized water for saccharification to take place at intermediate temperatures (70-120 °C), isolated into solid and liquid fractions and followed by washing and neutralization of the solid substrates. This process uses low temperature. Nonetheless, the concentrated acid pretreatment includes corrosion of apparatus and neutralization waste when acid can't be recovered [34, 35].

#### **2.3.2.2 Alkaline Pretreatment**

The pretreatment utilizes aqueous bases such as sodium, potassium, and ammonia [36, 37] at specific temperatures and pressures to degrade ester and glycosidic side chains of biomass. This pretreatment leads to lignin structure destruction, cellulose swelling, and low crystallization. Alkaline pretreatment extracts hemicelluloses in biomass and produces organic acids which lower the pH. For example, application of KOH pretreatment on rye straw gave lower sugar yields than dilute acid. Nonetheless, It was found to give high fermentation efficiency [38].

### 2.3.3 Biological pretreatment

Biological pretreatment is usually used with the action of fungi able to produce enzymes which can successfully disrupt lignin, hemicellulose and polyphenols. On the other hand, biological pretreatment is more expensive than other pretreatments. This pretreatment is too slow for industry due to used time as 10-14 days. The mechanism of biological pretreatment by fungi is complicatedly understood and can be distinguished into two main categories such as oxidative and hydrolytic [39].

## 2.4 Method for separated lignin from biomass

### 2.4.1 Organosolv process

The organosolv process relates to adding of aqueous organic solvent mixture with inorganic acid catalyst such as  $H_2SO_4$  and HCl [40, 41] that is used to break the internal lignin and hemicellulose bonds. Generally,  $H_2SO_4$  is used extensively as a catalyst because of its strong reactivity. However, it is toxic and corrosive equipment. The solvents generally use in the process are methanol, ethanol, acetone, ethylene glycol, triethylene glycol and tetrahydrofurfuryl alcohol. The pretreated biomass residues are isolated by filtration. The principle advantage of the organosolv process is that it is typically of higher purity than lignin received from other methods.

### 2.4.2 Ionic liquid pretreatment

Ionic liquids are new kind of solvents as low melting points, ( $<100^\circ C$ ), high polarities, high thermal stability and few vapor pressures [42]. Most ionic liquids used in lignin separation are 1-Ethyl-3-methylimidazolium acetate ([Emim][CH<sub>3</sub>COO]) [43], 1-butyl-3-methylimidazolium acesulfamate ([BMIM]Ace) [44], and 1-(4-sulfobutyl)-3-methyl imidazolium hydrosulfate ([C<sub>4</sub>H<sub>8</sub>SO<sub>3</sub>Hmim]HSO<sub>4</sub>) [45]. Ionic liquids are high selective solubilization of biomass components, but they are not economic feasibility for industry use.

### 2.4.3 Oxidative process with hydrogen peroxide (H<sub>2</sub>O<sub>2</sub>)

Hydrogen peroxide is the most generally oxidizing agent. The previous studies have shown that about 50% of the lignin and most of hemicellulose were dissolved by 2% H<sub>2</sub>O<sub>2</sub> at 30 °C for 8 h. Studies show that hydrolysis of hydrogen peroxide bring about the generation of hydroxyl radicals that degrade lignin and produce low molecular weight products. Besides, the pretreatment with hydrogen peroxide is considered as a very strong treatment which leads to lignin isolation and high yields of reducing sugars. The main disadvantages of hydrogen peroxide are the high cost and demand of reactions vessels which can resist as condition [46].

### 2.4.4 Ozonolysis pretreatment

The biomass is treated with ozone that causes degradation of lignin by breaking aromatic ring structures while hemicellulose and cellulose are not disrupted. This pretreatment is more effective for lignin separation. On the other hand, ozonolysis pretreatment is the high cost that it isn't appropriate as using for large-scale applications [36]

## 2.5 Mechanism of lignin separation from biomass

Generally, the easily hydrolysable  $\alpha$ -ether linkages are the most readily broken whereas  $\beta$ -ether bonds are broken under the conditions of many process. The  $\beta$ -ether cleavage is likely to be more significant in this process that is more strongly acidic. More over Acidic organosolv process is encouraged by the hydrolysis of ether linkages between lignin and carbohydrate.

### 2.5.1 $\alpha$ -Ether cleavage of the lignin in wood

The lignin cleavage reaction that occurs under mildly acidic conditions is the breaking of  $\alpha$ -ether bond. This reaction requires the presence of a quinonemethide intermediate. Similar to  $\beta$ -ether bonds linkages,  $\alpha$ -aryl ethers are promptly hydrolyzed [47]. Cleavage of  $\alpha$ -ether and  $\beta$ -ether structures which are responsible for the formation of vanillin and vanillic acid can occur under acidic

condition. The mechanism for this reaction has not been clarified, but it is believed to be the result of oxidative reaction.

Side chain rearrangement can occur in hot water (100°C) and acid catalyzed solvolytic reaction to form  $\beta$ -5 dilignol and dihydroconiferyl alcohol [54] from  $\beta$ -ether cleavage. This rearrangement reaction under hot water and acidic condition as shown in Figure 2.8. These reactions result in allylic rearrangement of  $\gamma$ -hydroxy groups to the  $\alpha$ -position.

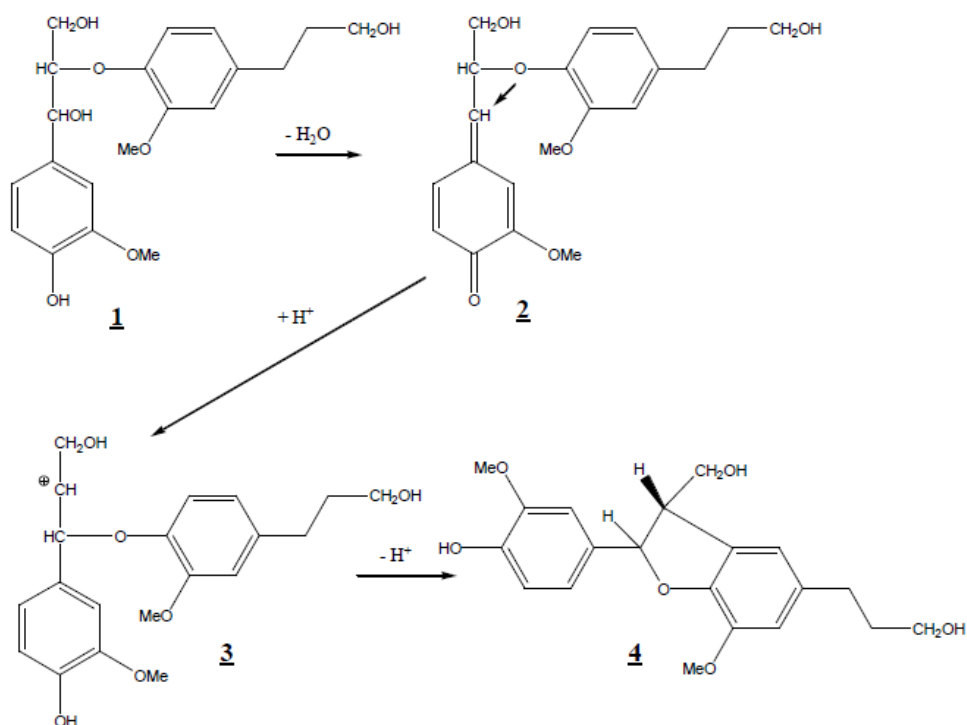


Figure 2.8 Side chain rearrangement in hot water [48].

### 2.5.2 $\beta$ -O-4 bond cleavage of the lignin in wood

The acidic system can be created by the simple reaction of water and wood at an increased temperature. The most important reaction during acidolysis of lignin is the cleavage of the  $\beta$ -O-4 bonds. Lignin units are frequently connected to each other via a  $\beta$ -O-4 bond in the  $\beta$  position. During cleavage reaction, the  $\beta$ -O-4 bond at the  $\beta$ -position of I primarily converts into a benzyl cation type intermediate II. An enol ether type of substructure III is formed (route A). The  $\beta$ -O-4 bond of III is

then hydrolyzed to yield a new phenolic lignin unit **IV** and Hibbert's ketone type substructure **V**.

Another competing route (route B), which lead to  $\beta$ -O-4 bond cleavage, has been previously described. Formaldehyde is released from the  $\gamma$ -position of **II** and another enol ether type substructure **VI** forms. The  $\beta$ -O-4 bond of **VI** is similarly hydrolyzed to yield the new phenolic unit **IV** and aldehyde **VII** as shown in Figure 2.9. This reaction is known to take place via a hemolysis of an intermediate quinone methide. The reaction can also occur under elevated temperatures [49], which makes of significance in processes such as steam hydrolysis, steam explosion *etc.*





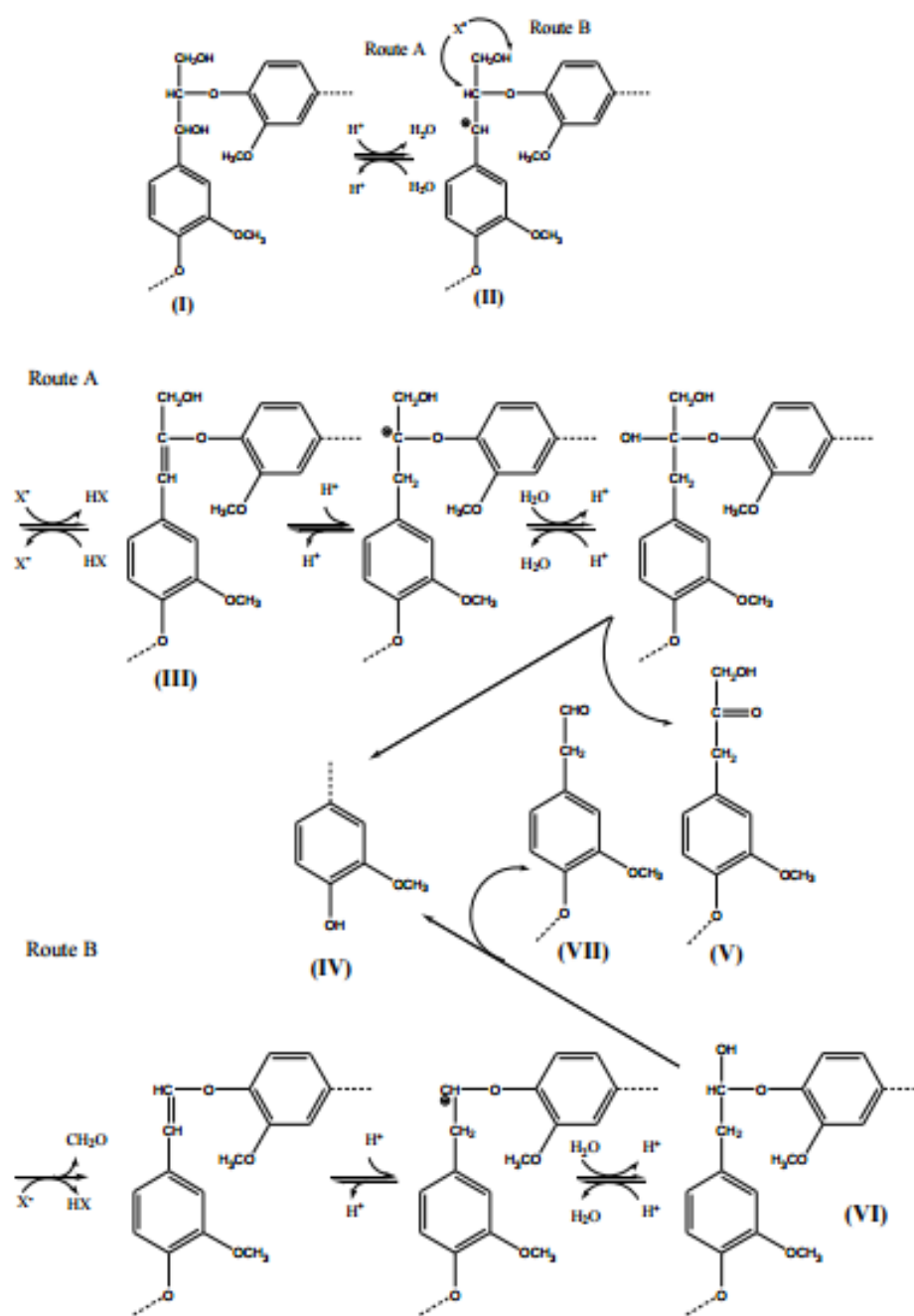
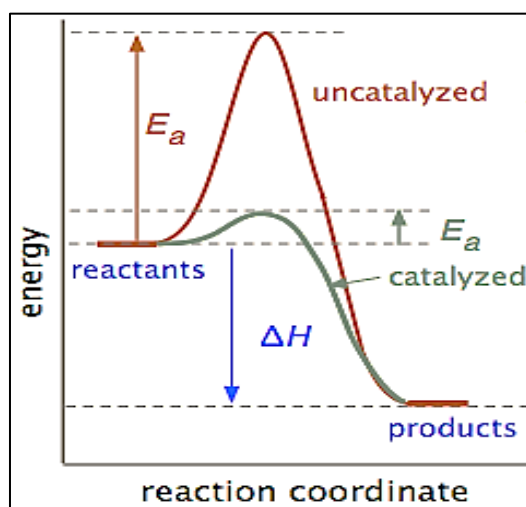


Figure 2.9 Mechanism of the  $\beta$ -O-4 bond cleavage [49].

## 2.6 Catalysts

The catalyst is substance which can decrease the activation energy ( $E_a$ ) than the corresponding uncatalyzed reaction as shown in Figure 2.10. The highest peak is referred to the transition state. Generally, the energy required to approach the transition state is high, whereas the energy to transition state reduces in catalytic reaction. Thus, the catalysts are necessary in industrial chemistry.



**Figure 2.10** The relationship between activation energy ( $E_a$ ) and enthalpy ( $\Delta H$ ) of the reaction with and without a catalyst [50].

### 2.6.1 Type of catalyst

The catalyst can be categorized into two types that are heterogeneous and homogeneous catalyst. Heterogeneous catalyst has a lower degree of dispersion than homogeneous catalyst seeing that the surface of heterogeneous catalyst is more active. Table 2.4 shows the difference of two-type catalyst.

**Table 2.4** Difference of homogeneous and heterogeneous catalysts [51].

Consideration	Homogeneous catalyst	Heterogeneous catalyst
1. Active centers	All metal atoms	Only surface atoms
2. Concentration	Low	High
3. Selectivity	High	Low
4. Diffusion problems	Practically absent	Present (mass-transfer-controlled reaction)
5. Reaction conditions	Mild (50-200 °C)	Severe (>250 °C)
6. Applicability	Limited	Wide
7. Activity loss	Irreversible reaction with product (cluster formation), poisoning	Sintering of the metal crystallites, poisoning
8. Modification possibility	High	Low
9. Thermal stability	Low	High
10. Structure/ Stoichiometry	Defined	Undefined
11. Catalyst isolation	Sometimes laborious (chemical decomposition, distillation, extraction)	Fixed-bed: unnecessary Suspension: filtration
12. Catalyst recycling	Easy	Can be very difficult
13. Cost of catalyst	High	Low

### 2.6.2 Type of porous material

The IUPAC definitions into three main types such as microporous material, mesoporous material and macroporous materials that depend on their pore size as shown in Table 2.5.

**Table 2.5** IUPAC category of porous materials [52].

Type of porous material	Pore size (Å)	Example
Microporous materials	<20	Zeolites
Mesoporous materials	20-500	SBA-15, Amberlyst-15
Macroporous materials	>500	Glasses, Ion-exchange resin

### 2.6.2.1 Microporous material

#### 2.6.2.1.1 Zeolite structure [53]

Zeolite structures consists of three dimension network of  $\text{SiO}_4$  and  $\text{AlO}_4$  tetrahedral. The tetrahedral are linked by sharing of the oxygen ions leading to the empirical formula of  $[\text{SiO}_2]$  and  $[\text{AlO}_2]^-$ . These tetrahedral refer to the primary building unit (PBU) as shown in Figure 2.11. The PBUs are assembled into the secondary building unit (SBUs). The corner of the polyhedra represents tetrahedral atoms as shown in Figure 2.12.

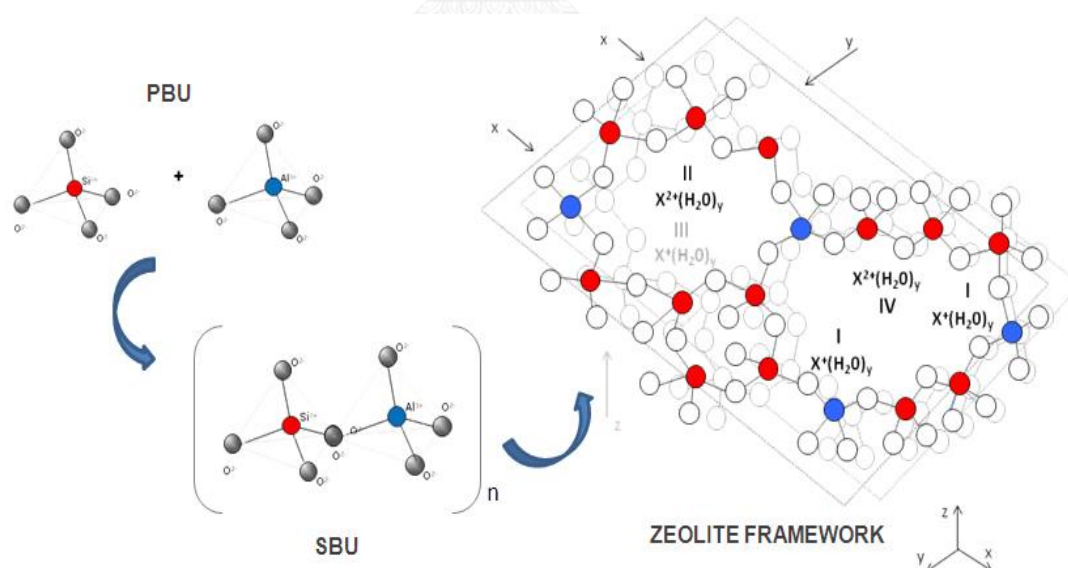


**Figure 2.11** Binding of building units (PBU and SBU) in three-dimensional zeolite-clinoptilolite structure [54].

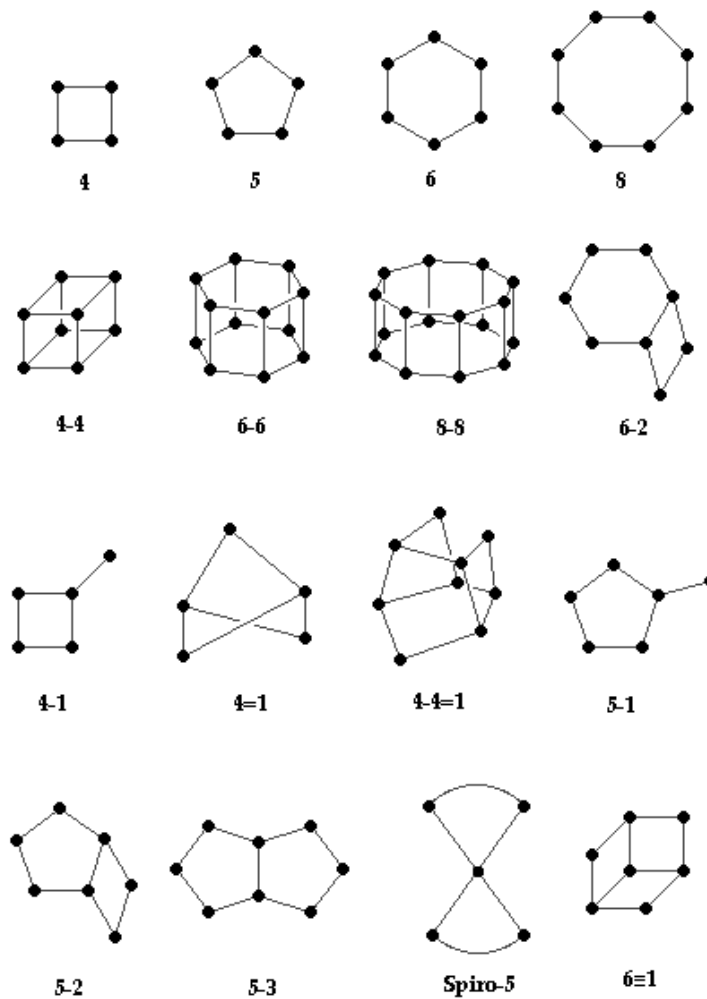
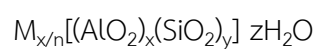


Figure 2.12 Secondary Building Units (SBUs) in zeolites [55].

As a result of the negative charge from the framework charge of zeolite is negative. So, the zeolite must be balanced by cation such as alkali or alkaline metal cations as shown in Figure 2.13. These cations can be exchanged by various types of cation. The position, size and number of cations can significantly alter the properties of zeolites. Generally, The formula for the component of zeolite is:



M: an extra framework cation for valence n, generally from the group I and II ions

x and y: the total amount of tetrahedral in the unit cell

z: the amount of water molecule located in channels and cavities inside zeolite structure

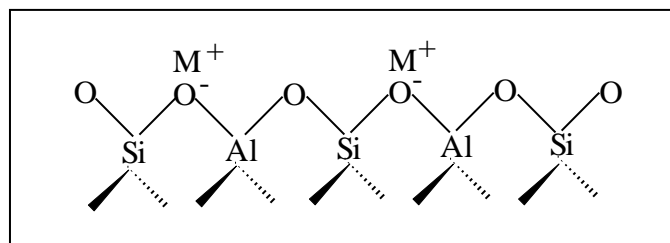


**Figure 2.13** The structure of zeolite.

#### 2.6.2.1.2 ZSM-5

ZSM-5 has a three-dimensional intersecting channel system. A straight channel of  $0.56 \times 0.54$  nm runs parallel to the a-axis and a sinusoidal channel of  $0.55 \times 0.51$  nm runs parallel to the b-axis. Molecules can also move in the direction by alternately using both channels. Although the channels are relatively small in comparison with those of the large-pore zeolites discussed previously, naphthalene molecules with a kinetic diameter of even 0.74 nm can be adsorbed into the pore system. This can be explained by the flexibility of the 10-ring apertures [56].

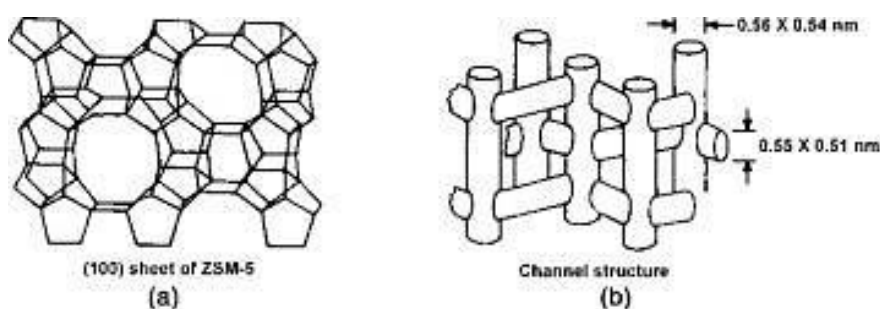


**Figure 2.14** (a) Skeletal diagram of the (100) face of ZSM-5 and (b) Channel structure of ZSM-5 [57].

### 2.6.2.1.3 Zeolite- $\beta$

Zeolite Beta is developing into a major catalyst in organic chemicals conversion, contributing to low waste technology. In comparison with other zeolites, zeolite Beta possesses unique acid properties which are related to local defects. Zeolite Beta has a three-dimensional intersecting channel system depicted in Figure 2.15. Two mutually perpendicular straight channels, each with a cross section of 0.76 0.64 nm, run in the a- and b-directions. A sinusoidal channel of 0.55 0.55 nm runs parallel to the c-direction. Zeolite Y has a three dimensional pore system, which is constructed from large supercages with diameters of 1.20 nm that are connected via apertures of 0.74 nm diameter [58].

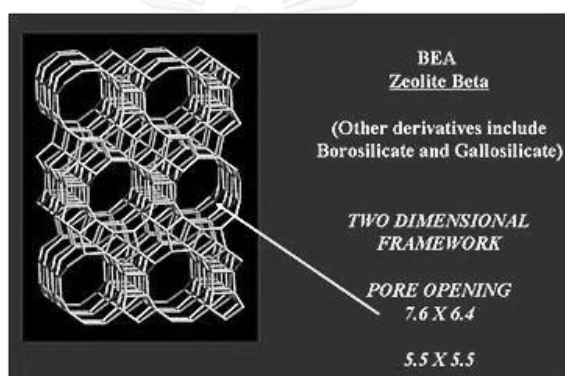


Figure 2.15 The structure of zeolite- $\beta$  [58].

Table 2.6 Comparison of ZSM-5 and Zeolite- $\beta$ .

Zeolite type	Si/Al	Pore volume (mL/g)	Crystal size ( $\mu\text{m}$ )
ZSM-5	10	0.13	0.20-100
Zeolite- $\beta$	5	0.28	0.05

## 2.6.2.2 Mesoporous material

### 2.6.2.2.1 SBA-15

#### 2.6.2.2.1.1 Structure and properties of SBA-15

The SBA-15 mesoporous material can be prepared under acidic condition that uses triblock copolymer (Pluronic 123). It is a structure directing agent. This novel material has illustrated high thermal stability owing to high pore wall thickness (31-64 Å) [59]. The SBA-15 also obtains uniform pore size and hexagonal structured channel as shown in Figure 2.15. Other properties of the SBA-15 are shown in Table 2.7.

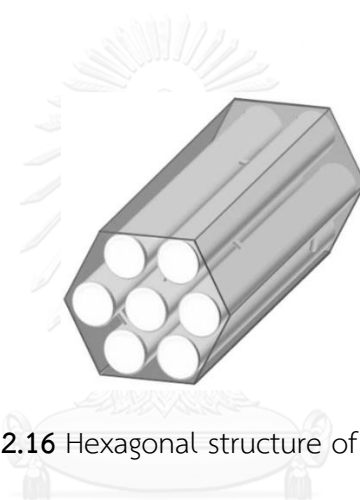


Figure 2.16 Hexagonal structure of SBA-15 [59].

Table 2.7 Properties of SBA-15 [60].

Properties	SBA-15
Pore size	46-300
Pore volume (mL/g)	0.8-1.23
Surface area (m <sup>2</sup> /g)	690-1040
Wall thickness (Å)	31-64

#### 2.6.2.2.1.2 Synthesis of SBA-15 and formation mechanism

The previous synthesis of SBA-15 reports that aging time and temperature are especially necessary factors to synthesize SBA-15. The



aging of the precursor in the mother liquors bring about an improvement on the pore size distribution as shown in Figure 2.17.

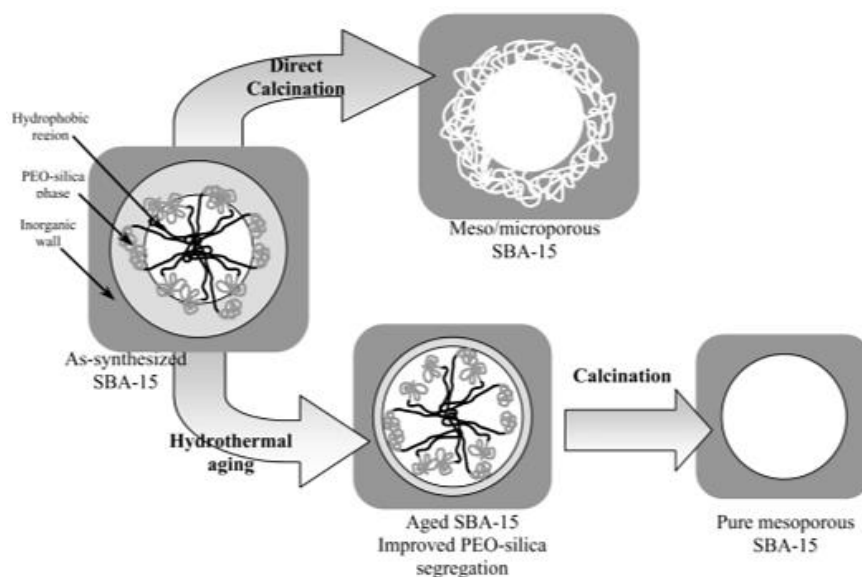


**Figure 2.17** The pore evolution upon thermal treatment, depending on pre-treatment and aging [61].

#### 2.6.2.2.2 Modification of SBA-15

##### 2.6.2.2.2.1 Al-SBA-15

Nowadays, several post synthesis method that aluminium was grafted onto the mesoporous wall with various aluminium source such as  $\text{Al}(\text{CH}_3)_3$ ,  $\text{AlCl}_3$  have been developed without the mesoporous structure seriously destroy. Figure 2.18 shows that synthesis of Al-SBA-15 use basic probe (L) (e.g. pivalonitrile, the terminal silanol groups) inducing to form the bridging hydroxyl group.

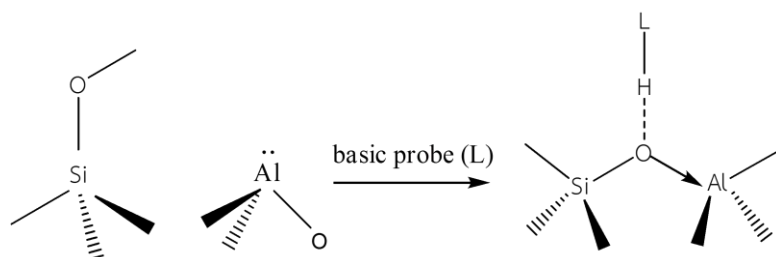


**Figure 2.18** Synthesis of Al-SBA-15 using basic probe inducing to form the bridging hydroxyl group.

### 2.6.2.3 Resin catalyst

#### 2.6.2.3.1 Amberlyst-15

Amberlyst-15 is a macro reticular polystyrene based ion exchange resin with strongly acidic sulfonic group. Thus, it serves as an excellent source of strong acid. It has been used in various acid catalyzed reactions. It is easy to measure, safe to use, and readily removed at the end of the reaction. Moreover, the advantage is that the catalyst can be regenerated and can be used several times. The structure of Amberlyst-15 unit is illustrated in Figure 2.19.

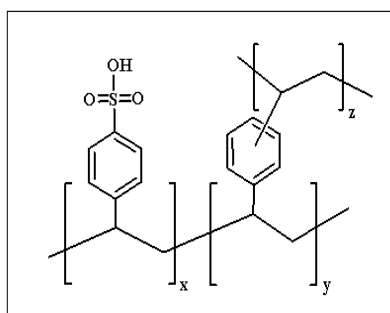


**Figure 2.19** The structure of Amberlyst-15 unit [62].

## 2.7 Characterization of SBA-15

### 2.7.1 X-ray Powder Diffraction (XRD)

X-ray powder diffraction (XRD) is a rapid analytical technique that is used to identify minerals and the crystallinity of materials. This technique can provide information including the degree of crystallinity and specifying hexagonal

mesoporous structure. In addition, it can allowed information that is the degree of hydration of sample. X-ray powder diffraction is based on constructive interference of monochromatic X-rays and a crystalline sample. These X-rays are generated by a cathode ray tube, filtered to produce monochromatic radiation, collimated to concentrate, and directed toward the sample as shown in Figure 2.20 [63]. The interaction of the incident rays with the sample produces constructive interference when conditions satisfy Bragg's law:

$$n\lambda = 2d\sin\theta$$

$n$  = the order of diffracted beam

$\lambda$  = the wavelength of X-ray source

$d$  = the distance between adjacent planes of atoms

$\theta$  = the angle between the incident beam and these planes

This law relates the wavelength of electromagnetic radiation to the diffraction angle and the lattice spacing in a crystalline sample.

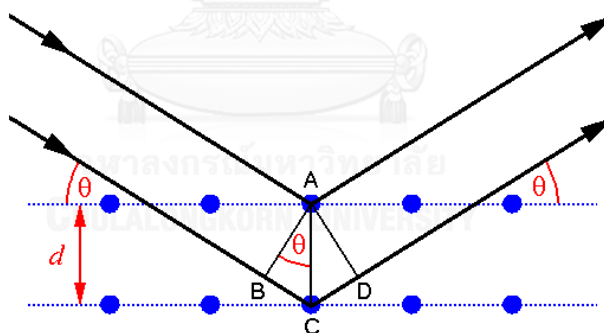


**Figure 2.20** Diffraction of X-ray by regular planes of sample [64].

### 2.7.2 Nitrogen adsorption-desorption

The nitrogen adsorption-desorption technique is used to assign the physical properties of porous material which are surface area, pore volume, pore diameter and pore size distribution. The monolayer capacity of non-porous solid that is measured by chemisorption or physisorption. The adsorption depends on gas pressure, temperature, properties of adsorptive gas as well as adsorbent solid. The

porous materials are characterized in terms of pore sizes derived from gas sorption data [65]. The IUPAC type of adsorption isotherms is demonstrated in Figure 2.21.

Type I: the isotherm of microporous materials

Type II: the non-porous materials with high external surface area

Type III: the non-porous materials with high flat surface

Type IV and V: the mesoporous materials with strong and weak interaction to nitrogen

Type VI: some materials with very strong interaction with nitrogen pretreated the multilayer adsorption

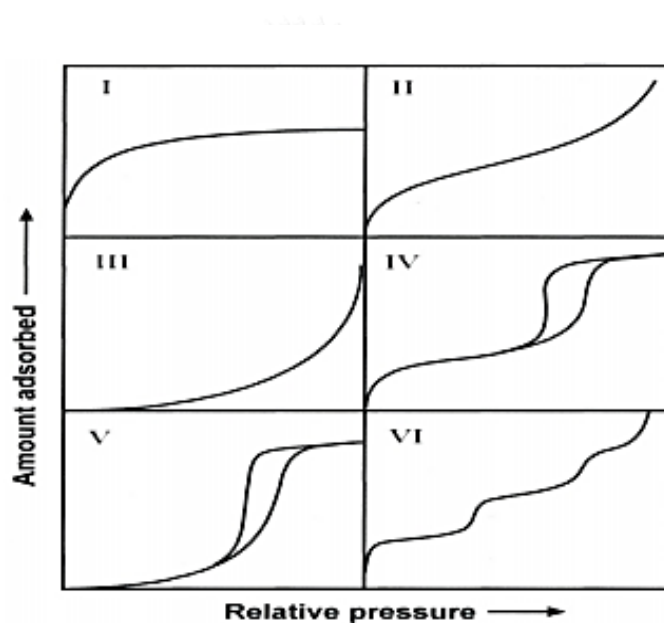


Figure 2.21 The IUPAC type of adsorption isotherm [66].

### 2.7.3 Aluminium-27 Nuclear Magnetic Resonance ( $^{27}\text{Al}$ -NMR)

$^{27}\text{Al}$ -NMR spectroscopy is used to distinguish between tetrahedrally and octahedrally jointed aluminium in the framework. The peak at about 50 ppm accords to tetrahedrally coordinated aluminium in the framework. On the contrary, the peak at 0 ppm shows that is peak of octahedrally as coordinated aluminium in the framework.

#### 2.7.4 Inductively Coupled Plasma-Mass Spectroscopy (ICP-MS)

Inductively coupled plasma mass spectrometry (ICP-MS) is a type of mass spectrometry which is able to detect metals in compound at concentrations as low as one part in  $10^{15}$  (part per quadrillion, ppq) .

The inductively coupled plasma (ICP) for spectrometry is maintained in a torch which composes of three concentric tubes, usually made of quartz. Even though, the inner tube (injector) can be sapphire if hydrofluoric acid is being used. The end of this torch is placed inside an induction coil supplied with a radio-frequency electric current. Flowing of argon gas is approached into the two outermost tubes of the torch and an electric spark that is applied for a short time to introduce free electrons into the gas stream. These electrons interact with the radio-frequency magnetic field of the induction coil and are accelerated first in one direction. When the field changes at high frequency, the accelerated electrons collide with argon atoms and sometimes a collision causes an argon atom to part with one of its electrons. The released electron is in turn accelerated by the rapidly changing magnetic field. The process continues until the rate of release of new electrons in collisions is balanced by the rate of recombination of electrons with argon ions.

For mass spectrometry, the ions from the plasma are extracted through a series of cones into a mass spectrometer. The ions are isolated on the basis of their mass-to-charge ratio and a detector receives an ion signal proportional to the concentration. The concentration of a sample can be defined through calibration with certified reference material such as single or multi-element reference standards. ICP-MS also lends itself to quantitative determinations through isotope dilution. The single point method based on an isotopically enriched standard. Other mass analyzers coupled to ICP systems include double focusing magnetic-electrostatic sector systems with both single and multiple collector. The processes of ICP-MS are demonstrated in Figure 2.22 [67].

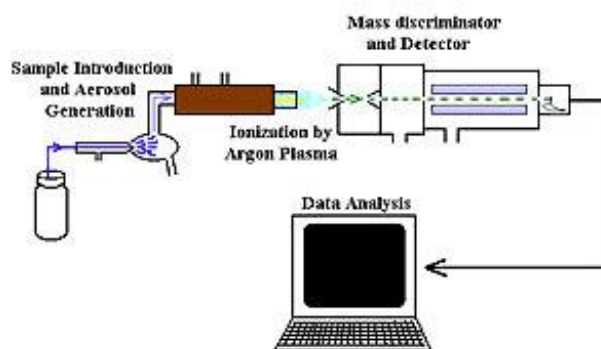


Figure 2.22 The processes of ICP-MS [68].

## 2.8 Characterization of lignin

### 2.8.1 Fourier transform infrared spectroscopy (FTIR)

FTIR is a spectroscopy technique used for studying the functional group in sample. FTIR is an intuitive way to obtain the same information. Rather than shining a monochromatic beam of light at the sample that shines a beam containing many frequencies of light at once and measures how much of that beam is absorbed by the sample. Next, the beam is modified to contain a different combination of frequencies, giving a second data point. This process is repeated many times. Afterwards, a computer takes all these data and works backwards to infer what the absorption is at each wavelength. Finally the intensity of the IR beam is detected by a detector. The main processes of FTIR are demonstrated in Figure 2.23.

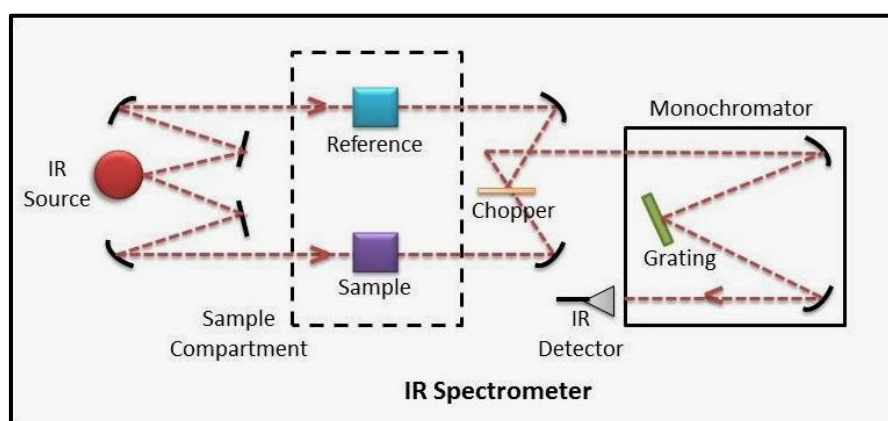
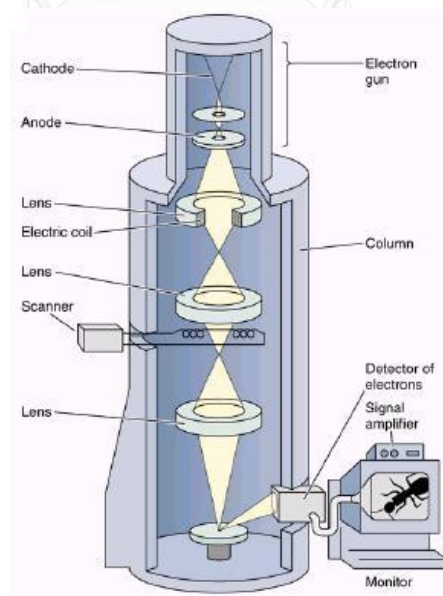


Figure 2.23 The main processes of FTIR [69].

## 2.8.2 Scanning electron microscope (SEM)

The scanning electron microscope (SEM) is a technique used for analyzing surfaces and morphology of sample. The electron microscope produces images of a sample by scanning it with a focused beam of electrons. The electrons interact with atoms in the sample, producing various signals that can be detected and obtain information about the sample's surface and morphology. The electron beam is generally scanned in a raster scan pattern, and the beam's position is combined with the detected signal to produce an image. SEM can achieve resolution better than 1 nanometer. Specimens can be observed in high vacuum, in low vacuum, in wet conditions and at a wide range of cryogenic or elevated temperatures. The most common SEM mode is detection of secondary electrons emitted by atoms excited by the electron beam. The number of secondary electrons depends on the angle at which beam meets surface of specimen. By scanning the sample and collecting the secondary electrons with a special detector, an image displaying the topography of the surface is created. The main processes of SEM are exhibited in Figure 2.24.



**Figure 2.24** The main processes of SEM [70].

### 2.8.3 Proton Nuclear Magnetic Resonance Spectroscopy ( $^1\text{H}$ NMR)

$^1\text{H}$  NMR is a powerful method used in the determination of hydrogen-1 nuclei within the molecules of sample in order to determine the structure of its molecules. In samples where natural hydrogen (H) is used, practically all the hydrogen consists of the isotope  $^1\text{H}$  (hydrogen-1; i.e. having a proton for a nucleus). A full  $^1\text{H}$  atom is called protium.

Simple NMR spectra are recorded in solution, and solvent protons must not be allowed to interfere. The solvents for use in NMR are deuterated water ( $\text{D}_2\text{O}$ ), deuterated acetone,  $(\text{CD}_3)_2\text{CO}$ , deuterated methanol ( $\text{CD}_3\text{OD}$ ), deuterated dimethyl sulfoxide  $(\text{CD}_3)_2\text{SO}$ , and deuterated chloroform ( $\text{CDCl}_3$ ). On the other hand, a solvent without hydrogen, such as carbon tetrachloride ( $\text{CCl}_4$ ) or carbon disulphide ( $\text{CS}_2$ ) may also be used.

TMS is a tetrahedral molecule with all protons being chemically equivalent giving one single signal that used to deuterated solvents permit the use of deuterium frequency-field lock to offset the effect of the natural drift of the NMR's magnetic field fine a chemical shift = 0 ppm. It is volatile and making sample recovery easy as well. In order to provide deuterium lock, the NMR constantly monitors the deuterium signal resonance frequency from the solvent and makes changes to the NMR's magnetic field to keep the resonance frequency constant. Moreover, the deuterium signal may be used to accurately define 0 ppm as the resonant frequency of the lock solvent and the difference between the lock solvent and 0 ppm (TMS) are well known. Proton NMR spectra of most organic compounds are characterized by chemical shifts in the range +14 to -4 ppm and by spin-spin coupling between protons. The integration curve for each proton reflects the abundance of the individual protons.

The chemical shift is not the only indicator used to assign a molecule. Because nuclei themselves possess a small magnetic field, they influence each other, changing the energy and hence frequency of nearby nuclei as they resonate that is known as spin-spin coupling. The most important type in basic NMR is scalar



coupling. This interaction between two nuclei occurs through chemical bonds, and can typically be seen up to three bonds away. The effect of scalar coupling can be understood by examination of a proton which has a signal at 1 ppm. This proton is in a hypothetical molecule where three bonds away exists another proton (in a CH-CH group for instance), the neighbouring group (a magnetic field) causes the signal at 1 ppm to split into two, with one peak being a few hertz higher than 1 ppm and the other peak being the same number of hertz lower than 1 ppm. These peaks each have half the area of the former singlet peak. The magnitude of this splitting (difference in frequency between peaks) is known as the coupling constant. The lignin of spectrum is illustrated in Figure 2.25.

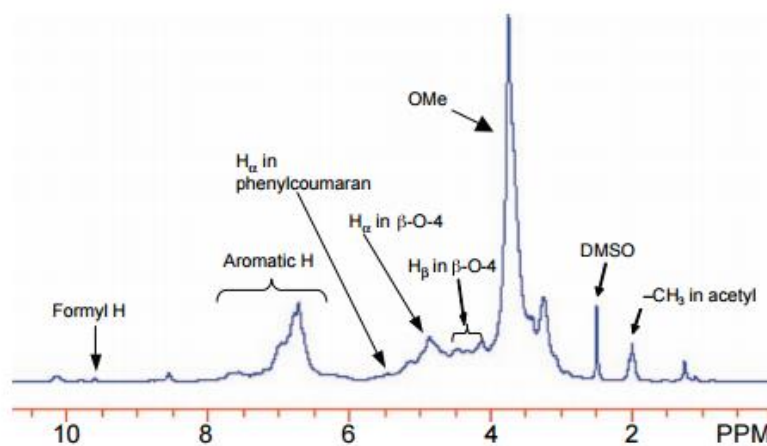


**Figure 2.25** An example of  $^1\text{H}$  NMR spectrum of a poplar mill-wood lignin using DMSO as solvent [71].

#### 2.8.4 Proton Nuclear Magnetic Resonance Spectroscopy ( $^{13}\text{C}$ NMR) [87]

The carbon-13 nuclear magnetic resonance the most commonly known as  $^{13}\text{C}$  NMR. It is analogous to proton NMR ( $^1\text{H}$  NMR) and allows the identification of carbon atoms in sample just as proton NMR identifies hydrogen atoms. As such  $^{13}\text{C}$  NMR is an important tool in chemical structure elucidation in organic chemistry.  $^{13}\text{C}$  NMR detects only the  $^{13}\text{C}$  isotope of carbon. The  $^{13}\text{C}$  NMR is generated in the same fundamental was as proton NMR spectrum. Only 1.1 % of naturally occurring carbon is  $^{13}\text{C}$  and actually an advantage because of less coupling. The chemical shift in  $^{13}\text{C}$  NMR spectrum is in range 0-250 ppm.

Each carbon nucleus has its own electronic environment, different from the environment of other, non-equivalent nuclei; it feels a different magnetic field, and absorbs at different applied fields strength. Proton-coupled spectrum shows splitting of the carbon signal only by protons attached to that carbon itself. The sample of  $^{13}\text{C}$  NMR spectrum compares to  $^1\text{H}$  NMR spectrum is showed in Figure 2.26.

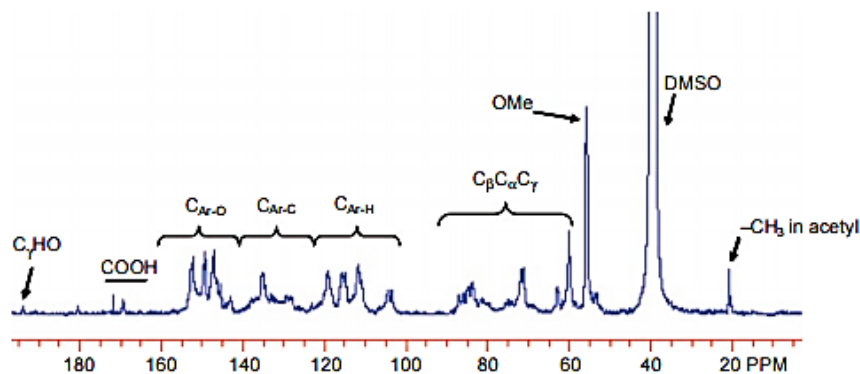


**Figure 2.26**  $^{13}\text{C}$  NMR spectrum of a milled wood lignin isolated from a hardwood *Buddleja davidii* [71].

### 2.8.5 Thermogravimetric analysis (TGA)

The thermogravimetric analysis (TGA) is one of the techniques used to determine the thermal properties of wood. The TGA technique composes to record the lost weight during the increase in temperature from 20°C until 600°C with a 10°C/min heating rate. The thermogram presented a departure phase of free water (from room temperature to 100°C) before the degradation process of the wood constituents. The experimental protocols depend on the quality of the material and the ordinary physical characteristic.

### 2.8.6 Elemental analysis (C, H, O and N)

The elemental analysis always refers to carbon, hydrogen, nitrogen, and oxygen of a sample as biomass. This information is important to help determine the structure of an unknown compound, as well as to help ascertain the structure

and purity of a synthesized compound. Elemental analysis provides the information that is percentage of each element in biomass.



## CHAPTER III

### EXPERIMENTS

#### 3.1 Chemicals, Gases and Materials

1. EDTA,  $C_{16}H_{14}N_2Na_2O_8 \cdot 2H_2O$  (Merck)
2. Sodium tetraborate decahydrate,  $Na_2B_4O_7 \cdot 10H_2O$  (Sigma-Aldrich)
3. Sodium dodecyl sulfate,  $CH_3(CH_2)_{11}SO_4Na$  (Ommipur)
4. 2-Ethoxyethanol,  $C_2H_5OCH_2OH$  (Sigma-Aldrich)
5. Cethyltrimethyl ammonium bromide, CTAB (Aldrich)
6. Potassium permanganate,  $KMnO_4$  (BDH)
7. Silver nitrate,  $AgNO_3$  (Merck)
8. Silver sulfate,  $Ag_2SO_4$  (Merck)
9. Iron (III) nitrate nanohydrate,  $Fe(NO_3)_3 \cdot 9H_2O$  (Merck)
10. Potassium acetate,  $C_2H_3KO_2$  (Fluka)
11. Tertiary butyl alcohol,  $C_4H_{10}O$  (Fluka)
12. Oxalic acid dihydrate (Merck)
13. Hydrochloric acid, HCl (Merck, 37%)
14. Acetic acid glacial,  $CH_3COOH$  (Merck, 100%)
15. Sulfuric acid,  $H_2SO_4$  (Merck, 95-97%)

16. Nitric acid,  $\text{HNO}_3$  (Merck, 65%)
17. Deionized water
18. Tetraethyl orthosilicate, TEOS (Fluka,  $\geq 98\%$ )
19. Triblock copolymer pluronic P123, PEO20-PPO70-PEO20, average molecular weight = 5800 (Aldrich)
20. Sodium aluminate,  $\text{NaAlO}_2$  (Riedel-deHaën)
21. Ammonium chloride,  $\text{NH}_4\text{Cl}$  (Riedel-deHaën)
22. Chloroform-D1,  $\text{CDCl}_3$  (Merck)
23. Dimethyl sulfoxide-D6,  $d_6$ -DMSO (Merck, 99.8%)
24. 2-Chloro-4,4,5,5-tetramethyl-1,3,2-dioxaphospholane, (Sigma-Aldrich)
25. Pyridine,  $\text{C}_5\text{H}_5\text{N}$  (Merck)
26. Cyclohexanol,  $\text{C}_6\text{H}_{12}\text{O}$  (Merck)
27. Chromium(III)-acetylacetonate,  $\text{C}_{15}\text{H}_4\text{CrO}_6$  (Merck)
28. Ethanol,  $\text{C}_2\text{H}_5\text{OH}$  (Merck, 99.9%)
29. Amberlyst-15 in dry (Rohm & Hass, France)
30. ZSM-5 Si/Al = 14.1 (ZEOCHEM)
31. Zeolite-HBEA Si/Al = 15 (ZEOCHEM)
32. Diethyl ether,  $(\text{C}_2\text{H}_5)_2\text{O}$  (Merck)
33. Liquid nitrogen,  $\text{N}_2$  (Linde, highly pure grade)

34. Nitrogen gas, N<sub>2</sub> (Thai Industrial Gases (TIG), highly pure grade)
35. Giant sensitive plant from Hunka district, Chainat province
36. Corncob from Nakhon Sawan Field Crop Research Center in Thailand
37. Rice straw from Nong saeng district, Saraburi province
38. Sugarcane bagasse from Nong saeng district Saraburi province

## 3.2 Instruments and Apparatus

### 3.2.1 Oven

Crystallization of SBA-15 during synthesis was carried out at temperature of 100 °C in static condition using UM-500 oven as heater.

### 3.2.2 Furnace

Calcination of SBA-15 at elevated temperature was achieved in a Carbonite RHF 1600 muffle furnace in air with programmable heating rate of 1 °C/min. Calcination method was conducted to remove template, moisture and some impurities from SBA-15. The temperature program used for the calcination of SBA-15 sample was shown in Figure 3.1.

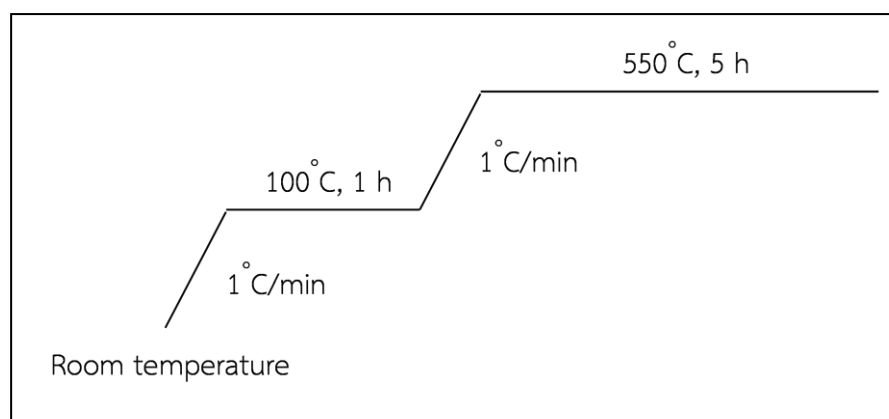


**Figure 3.1** The temperature program for the calcination of SBA-15 catalyst.

### 3.2.3 X-ray powder diffraction (XRD)

The structure of prepared sample was characterized using a Rigaku D/MAX-2200 Ultima<sup>+</sup> X-ray diffractometer (XRD) equipped with Cu K $\alpha$  radiation (40 kV, 30 mA) and a monochromator at 2 theta angle between 0.5 to 3.0 degree for SBA15 and Al-SBA-15. The scattering slit, divergent slit and receiving were fixed at 0.5 degree, 0.5 degree and 0.15 mm, respectively.

### 3.2.4 Surface area analysis

Characterization of catalyst porosity in terms of nitrogen adsorption-desorption isotherm, BET specific surface area, and pore size distribution of the catalyst was carried out using a BET Japan, BELSORP-mini instrument. Before analysis, the calcined sample was weighed about 40 mg that was pretreated at 400 °C for 2-3 h under vacuum. Adsorption isotherms were measured at 77 K (liquid N<sub>2</sub>) using highly pure nitrogen as an adsorbate.

### 3.2.5 Aluminium-27 Nuclear Magnetic Resonance (<sup>27</sup>Al-NMR)

The spectra of aluminum tetrahedral in catalyst was analyzed by <sup>27</sup>Al-magnetic angle spinning nuclear magnetic resonance using <sup>27</sup>Al-MAS-NMR, Bruker advance DPX-300 spectroscopy operating at 78 MHz.

### 3.2.6 Inductively Coupled Plasma-Mass Spectroscopy (ICP-MS)

Aluminium content in Al-SBA-15 was analyzed by using the Thermo Scientific iCAP<sup>TM</sup> Q inductively coupled plasma-quadruples mass spectrometer (ICP-QMS).

### 3.2.7 PARR reactor

The lignin separation was performed in 100 mL of PARR reactor. The temperatures for the reaction are 180-300 °C.

### 3.2.8 Fourier transform infrared spectroscopy (FTIR)

The functional groups of isolated lignin from biomass were analyzed by FTIR, NICOLET 6700 mode ATR.

### 3.2.9 Nuclear Magnetic Resonance Spectroscopy ( $^1\text{H}$ and $^{13}\text{C}$ NMR )

$^1\text{H}$  and  $^{13}\text{C}$  NMR spectra of lignin were obtained in hexadeuterated dimethylsulfoxide ( $d_6$ -DMSO) on Varian Mercury NMR spectrometer (Varian, USA) at 400 MHz

### 3.2.10 Scanning electron microscope (SEM)

The morphology of lignin was analyzed by JSM-5410 LV scanning electron microscope with 15 kV of acceleration voltage. All samples were coated with sputtering gold under vacuum for conductivity.

### 3.2.11 Thermogravimetric analysis (TGA)

The thermogravimetric analysis (TGA) of lignin sample was performed by Netzsch-TG 209 F3 Tarsus thermogravimetric analyzer. The sample was heated to 800°C in air at 10°C/min heating rate.

### 3.2.12 Elemental analyzer (C, H, O and N)

The element analysis of biomass sample was analyzed the elemental carbon (C), hydrogen (H), oxygen (O) and nitrogen (N) composition using C, H, O and N analyzer; Perkin Elmer-PE2400 Series II at Scientific and Technological Research Equipment Centre of Chulalongkorn University.

### 3.2.13 Centrifuge

The separation and collection of prepared solid sample after lignin pyrolysis were processed by a Sanyo Centaur 2 centrifuge at speed of 4,000 rpm for 10 min.



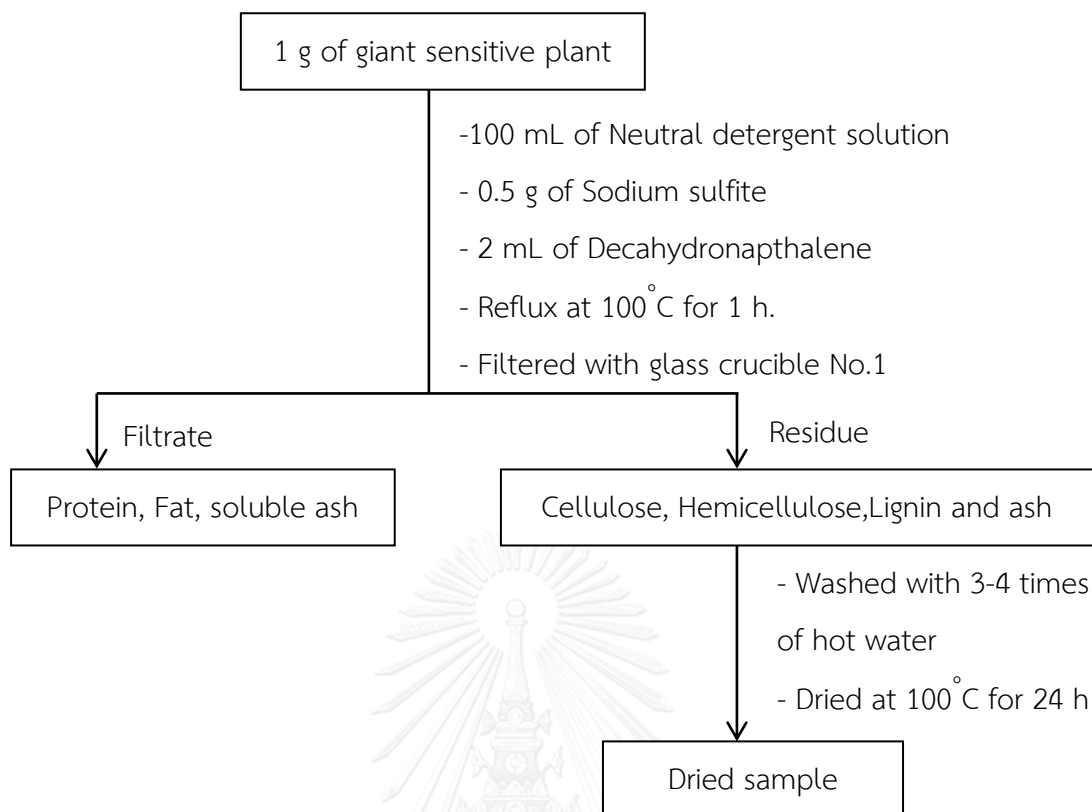
### 3.2.14 Gas chromatograph-mass spectrometer (GC-MS)

The components of liquid products were analyzed by a gas chromatography-mass spectrometry (GC-MS) using an Agilent 7890B GC interfaced with an Agilent 7000C triple quadruples mass spectrometer, equipped with an Agilent HP-5ms capillary column (30 m x 0.25 mm x 0.25  $\mu$ m). The 0.5  $\mu$ L sample was injected by the Agilent 7633 ALS autosampler with the split ratio of 120:1 and helium was used as a carrier gas at a constant flow of 1.0 ml/min. Mass spectrometer was operated in the electron impact ionization mode at 70 eV. The interface and source temperatures were 300°C and 230°C, respectively. Mass spectra were collected by automatic scanning in the mass range m/z 35 - 750 and the compound identification was achieved by matching the unknown mass spectra with a NIST.11.

## 3.3 Determine component of giant sensitive plant [20].

### 3.3.1 Neutral detergent fiber (NDF) method

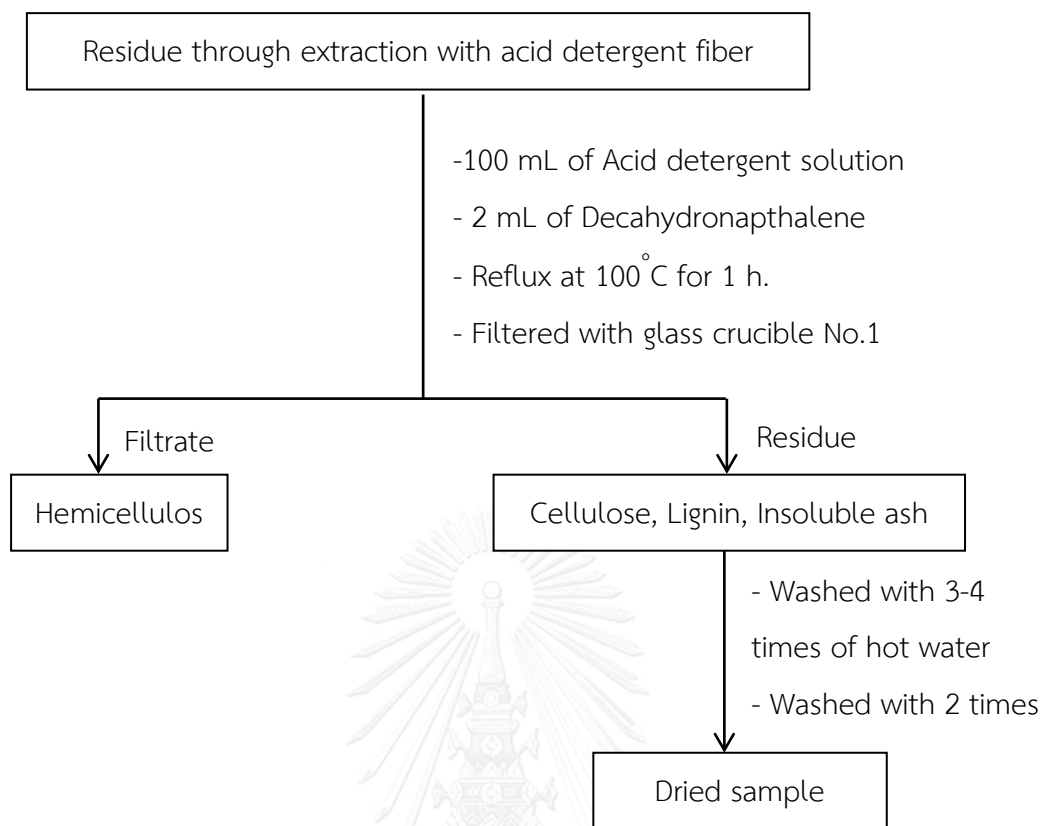
The neutral detergent fiber (NDF) procedure method is the most common measurement for the structural components in plant cells such as lignin, cellulose and hemicellulose. Other components in plant cells such as proteins, sugars and lipids are dissolved by a neutral detergent solution. Firstly, giant sensitive plant was milled and sieved to particle size of 0.5 mm, followed by drying at 100°C for 24 h. Then, 1.0 g giant sensitive plant was refluxed with mixture solution (100 mL of neutral detergent solution, 0.5 g of sodium sulfite and 2 mL of decahydronaphthalene) in the round bottom flask at 100°C for 1 h. The residue was filtered through glass crucible No.1 and washed with 3-4 times of hot water. Finally, the residue was dried at 80°C for 24 h to use as substrate in further step. The calculation of neutral detergent is shown in appendix as equation A-1. The NDF method was shown in Scheme 3.1.



**Scheme 3.1** The process of neutral detergent fiber.

### 3.3.2 Acid detergent fiber (ADF) method

The residue as through extraction with neutral detergent method was continuously refluxed with mixture solution (100 mL acid detergent solution and 2 mL decahydronaphthalene) at 100 °C for 1 h. Next, the residue was filtered through glass crucible No.1 and washed with 3-4 times of hot water and 2 times of 80% ethanol. Lastly, the residue was dried at 80 °C for 24 h to use as substrate in further step. The calculation of acid detergent and percentage of hemicellulose are shown in appendices as equation A-2 and A-3. The ADF method was shown in Scheme 3.2.



**Scheme 3.2** The process of acid detergent fiber.

### 3.3.3 Permanganate detergent (PML) method

The glass crucible containing the residue as through extraction with ADF was placed in pan with 2-3 cm cold water and sequentially extracted with 25 mL of combined  $\text{KMnO}_4$  solution and a demineralizing solution. After that, the residue the residue was vacuum filtered and washed with 2 times 80% ethanol and acetone. Lastly, the residue was dried at  $80^\circ\text{C}$  for 24 h to use as substrate in further step. The percentage of hemicellulose was calculated by using equation that is shown in appendix as equation A-4.

### 3.3.4 Analysis of cellulose with calcination

The glass crucible containing the residue as through extraction with PML was calcined at 500 °C for 3 h. The percentage of cellulose was calculated by using equation that is shown in appendix as equation A-5.

## 3.4 Biomass pretreatment

### 3.4.1 Hardwood

Firstly, the giant sensitive plant was milled and sieved to particle size of 0.5 mm and pretreated with ratio 20:1 (w/v) of 0.25, 0.75, 0.5, 1.0 and 2.0 %wt H<sub>2</sub>SO<sub>4</sub>. Then, the mixture solution was pretreated by reflux at 100 °C for 8 h. The pretreated giant sensitive plant was filtered and washed with deionized water until neutral pH. Lastly, the pretreated giant sensitive plant was dried at 80 °C for 24 h.

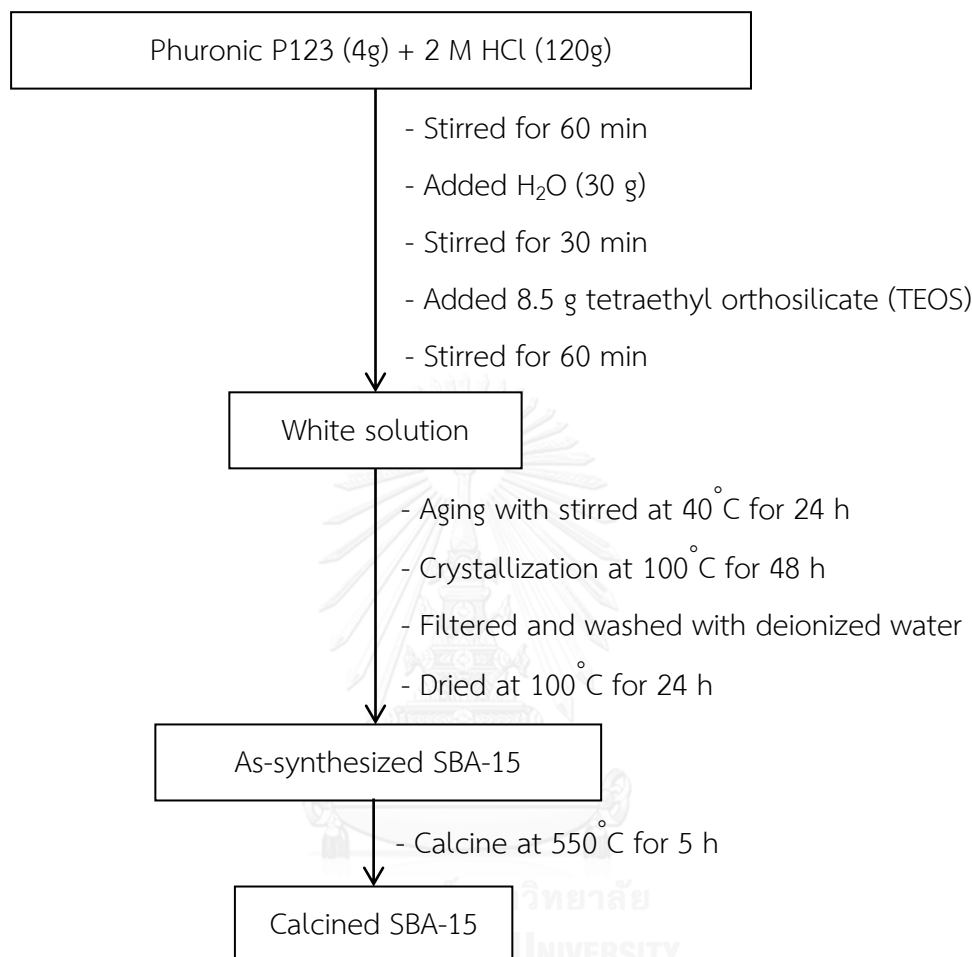
### 3.4.2 Agricultural residue

The agricultural residue such as corncob, rice straw and sugarcane bagasse was milled and sieved to particle size of 0.5 mm and dried at 100 °C for 8 h to use as substrate in further lignin separation.

## 3.5 Synthesis of SBA-15

SBA-15 synthesis was performed by hydrothermal method reported by [72]. The gel mole composition of 1.0 TEOS: 0.0165P123: 5.88HCl: 192H<sub>2</sub>O was prepared by dissolving 4.0 g phuronic P123 as template that was dissolved with stirring in 30 g of deionized water and 120 g of 2.0 M of HCl solution at room temperature. Then, 8.5 g of tetraethyl orthosilicate (TEOS) was added and stirred for 60 min. The mixture solution illustrates as white. The solution was aged at 40 °C for 8 h under stirring. The white gel solution was transferred into a Teflon-PARR autoclave for crystallization at 100 °C for 48 h without stirring. Finally, the obtained white solid was filtered and washed with deionized water to neutral pH value. The template in SBA-15 was

removed by calcination at 550 °C for 5h. The synthesis of SBA-15 was shown in Scheme 3.3.

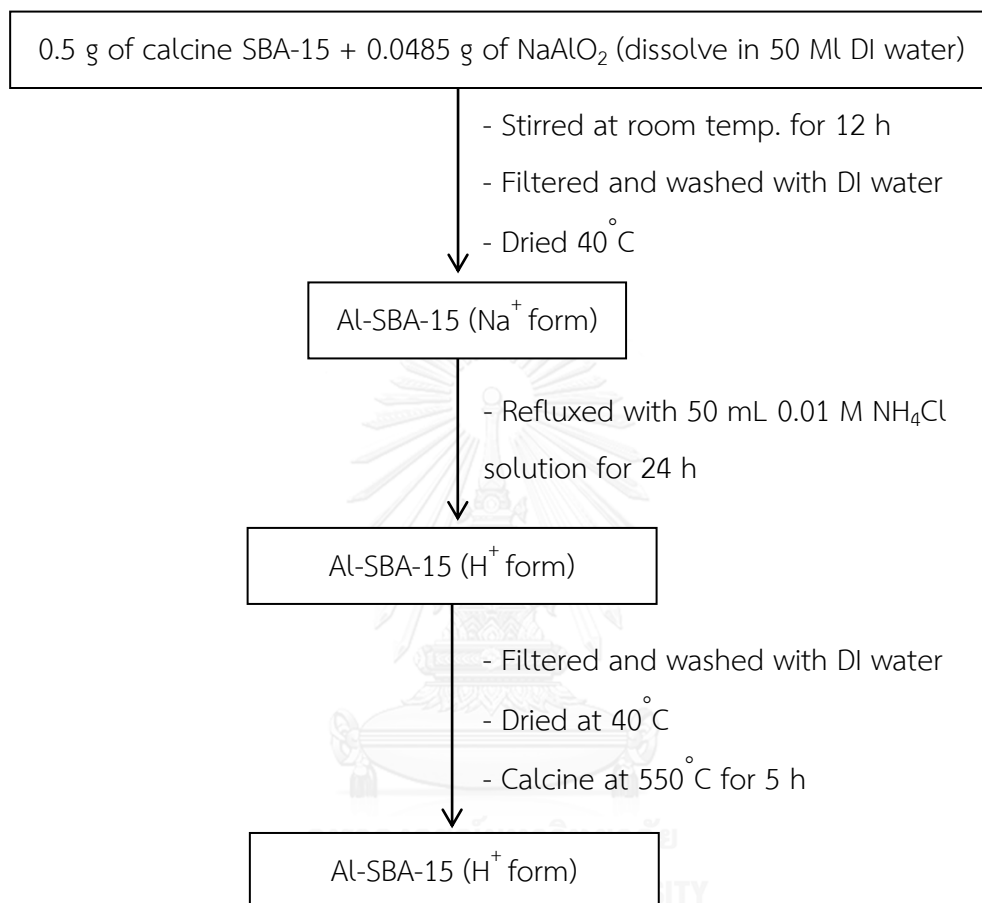


**Scheme 3.3** Diagram of SBA-15 synthesis.

### 3.5.1 Synthesis of Al-SBA-15

The Al-containing SBA-15 material consist of SiO<sub>2</sub>/Al<sub>2</sub>O<sub>3</sub> mole ratio in gel of 14 which were prepared by post-synthesis method [73]. The alumination of calcined SBA-15 was conducted by stirring 50 mL of dionized water and sodium aluminate at room temperature for 12 h. The solid material was isolated by filtration, washed with deionized water and dried at 40 °C. Next, the obtained solid material is called as-synthesized Al-SBA-15 that existed Na ion form. The Na ion form was

removed by ion exchange with 0.01 M  $\text{NH}_4\text{Cl}$  that was filtered and repeatedly washed with deionized water. In the end, this material was calcined at  $550^\circ\text{C}$  for 5 h. The synthesis of Al-SBA-15 was shown in Scheme 3.4.



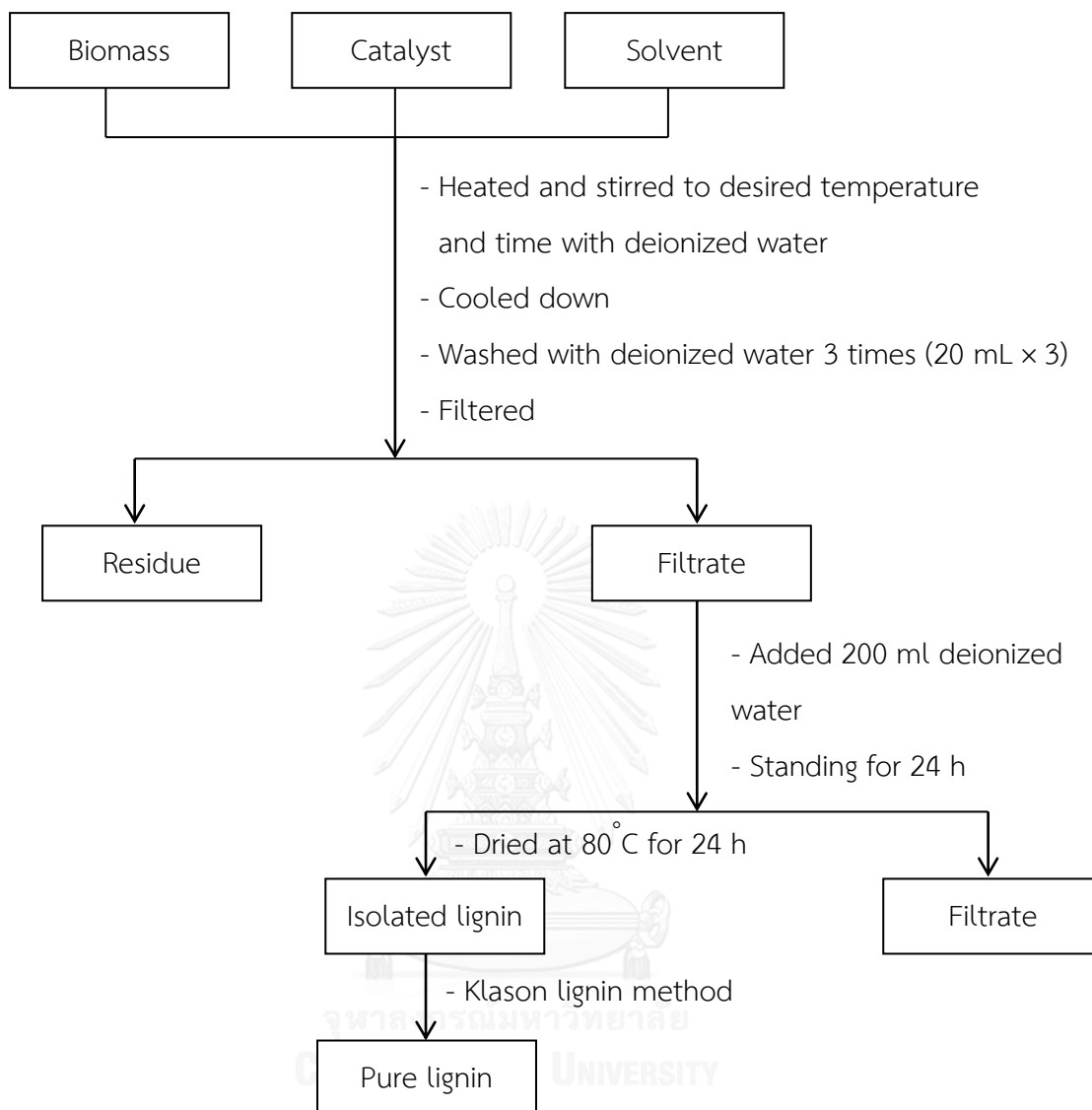
**Scheme 3.4** Diagram of Al-SBA-15 by post-synthesis method.

### 3.6 Acid-base titration

The acid amount of catalyst was measured by using 2 M NaCl solution that was the ion-exchange agent. Approximately 0.05 g of the catalyst was added into 15 ml of NaCl solution to equilibrate for 30 min under stirred at room temperature. After that, it was titrated by using 0.01 M NaOH as titrant and phenolphthalein as indicator. Finally, The end point of solution was light pink [74].

### 3.7 Lignin separation from biomass

In each experiment, 3 grams of dry pretreated hardwood (giant sensitive plant) and agricultural residue (corn cob, rice straw and sugarcane bagasse), 0.63 g of catalyst and EtOH:H<sub>2</sub>O (80:20 v/v, 50 mL) were carried out in 100 mL pressure Parr reactor equipment. The reaction was heated to desired reaction temperature and kept constant for a period of time. After completion of the reaction, the reaction mixture was cooled down. The residue was filtered with filter paper Whatman<sup>®</sup> No.2 and washed with deionized water three times (20 mL × 3). Then, the filtrate was added 200 mL of deionized water in order to precipitate lignin and set for 24 h. Finally, the lignin was filtered through a filter paper and dried at 80 °C for 24 h. The obtained lignin was purified with Klason lignin method and confirmed using FTIR, <sup>1</sup>H NMR, <sup>13</sup>C NMR and <sup>31</sup>P NMR. The %yield of isolated crude lignin was calculated based on equation that was shown in appendices as equation B-1. The process of lignin separation was shown in Scheme 3.5.



**Scheme 3.5** Diagram of lignin separation.

### 3.8 Parameters affecting biomass pretreatment

#### 3.8.1 Acid pretreatment of giant sensitive plant

##### 3.8.1.1 Effect of amount of $\text{H}_2\text{SO}_4$

The reaction was studied at different amount of  $\text{H}_2\text{SO}_4$  of 0.25, 0.75, 0.5, 1.0 and %wt. The giant sensitive plant was pretreated by reflux at  $100^\circ\text{C}$ .



### 3.8.1.2 Effect of temperature

The pretreated giant sensitive plant temperature was varied to 1-8 °C.

## 3.8.2 Parameters affecting lignin separation

### 3.8.2.1 Effect of EtOH/H<sub>2</sub>O ratio

The EtOH/H<sub>2</sub>O ratio as solvent in lignin separation was varied to 50:50, 60:40, 70:30, 80:20, 90:10 and 100:0 (v/v).

### 3.8.2.2 Effect of reaction temperature

The reaction temperature was varied to 180, 200, 220 and 240 °C

### 3.8.2.3 Effect of reaction time

The reaction time was varied to 15, 30, 45 and 60 min.

### 3.8.2.4 Effect of catalyst type

The effect of catalytic lignin separation from hardwood and agricultural residue was performed by using catalysts that were included two microporous materials (e.g. ZSM-5 and Zeolite-β), mesoporous material (e.g. Al-SBA-15) and resin material (e.g. Amberlyst-15).

## 3.9 Determine pure isolated lignin with Klason method

The isolated lignin was purified by using Klason lignin from TAPPI test method T222 om-88. 1 g of dried biomass sample was weighed in a 50 mL breaker. 10 mL of 72% H<sub>2</sub>SO<sub>4</sub> were added carefully with a pipetted and the mixture was stirred with a small glass lod. During this process, the mixture was frequently stirred and maintained in a water bath at 20 ± 1 °C for 2 h. After that, the mixture solution was transferred into a autoclave and added 560 mL of deionized water. The mixture

solution was heated at 121 °C for 1 h. After completion of the reaction, the reaction mixture was cooled down. The lignin was filtered through a glass crucible No.3 and washed with 250 mL of hot water. The pure lignin-containing crucible was dried at 100 °C for 24 h. The Klason lignin content was calculated as using equation that is shown in appendix as equation C-1.

### 3.10 Lignin transformation to fine chemicals with optimal condition

Klason lignin and crude lignin from hardwood (giant sensitive plant) and agricultural residue (corn cob, rice straw and sugarcane bagasse) were carried out in 100 mL stainless steel autoclave bath reactor equipment with an electromagnetic driven stirrer. In reaction, one gram of lignin (Klason lignin or crude lignin) was load into the autoclave. The reactor was purged with N<sub>2</sub> gas and heated up to desired pyrolysis temperature at 300 °C for 30 min. After pyrolysis, the products such as gas, liquid and solid were collected for determination of the conversion, yield and selectivity. The percentage of gaseous product was calculated by subtraction of the weight of liquid products and residues from the starting material. The amount of solid residue in the reactor was measured by direct weight. The components of liquid products were analyzed by gas chromatography-mass spectrometer (GC-MS).

## CHAPTER IV

### RESULTS AND DISCUSSIONS

#### 4.1 The component of biomass

Table 4.1 was shown the composition of biomass using in experiment. Giant sensitive plant was investigated using Forage fiber analysis. The components of another biomass (e.g. rice straw, sugarcane bagasse and corncob) were obtained by several references ( He, Y. *et al.* [17]; Han, Y.W. *et al* [18]; and Funda, A. [19])

**Table 4.1** The component of biomass.

Biomass	Composition (wt%)				
	Cellulose	Hemicellulose	Lignin	Ash	Others
Rice straw	33.40	28.20	7.40	12.80	18.20
Sugarcane bagasse	50.40	28.50	14.90	2.00	4.20
Corn cob	52.90	32.10	13.10	1.20	0.70
Giant sensitive plant [20]	36.87	15.51	20.68	0.58	26.35

#### 4.2 Giant sensitive pretreatment with dilute acid

The giant sensitive pretreatment was important process that affected to the structure of biomass such as reduced the crystallinity of structure and increased the porosity of the biomass. This part was investigated influence of concentration of dilute acid (0.25, 0.5, 0.75, 1.0 and 2.0 wt%) and reflux temperature (1, 4 and 8 h). It is apparent that both different acid concentration and temperature were playing a key role of giant sensitive pretreatment. Table 4.2 and Figure 4.1 showed result of isolated lignin that was pretreated without dilute acid solution. Table 4.3 and Figure

4.2 shown result of isolated lignin that was pretreated with various concentration of dilute acid solution.

The results indicated isolated lignin from giant sensitive plant that was pretreated only refluxed with water (giant sensitive plant : water = 1 : 15 w/v) for 1, 4 and 8 h, the yield of separated lignin was increased from only 6.89% to 7.78%. On the other hand, the separated lignin was pretreated in range of 0.25-1 wt% H<sub>2</sub>SO<sub>4</sub> at 100 °C for 8 h, gave the highest isolated lignin 15.67% yield under pretreatment with 1wt% of H<sub>2</sub>SO<sub>4</sub>.

**Table 4.2** Effect of time on giant sensitive plant pretreatment without dilute acid solution at 100 °C.

Biomass	Time (h)	Yield (wt%)	
		Isolated lignin	Residue
Giant sensitive plant	1	6.89	57.33
	4	7.22	53.33
	8	7.78	52.45

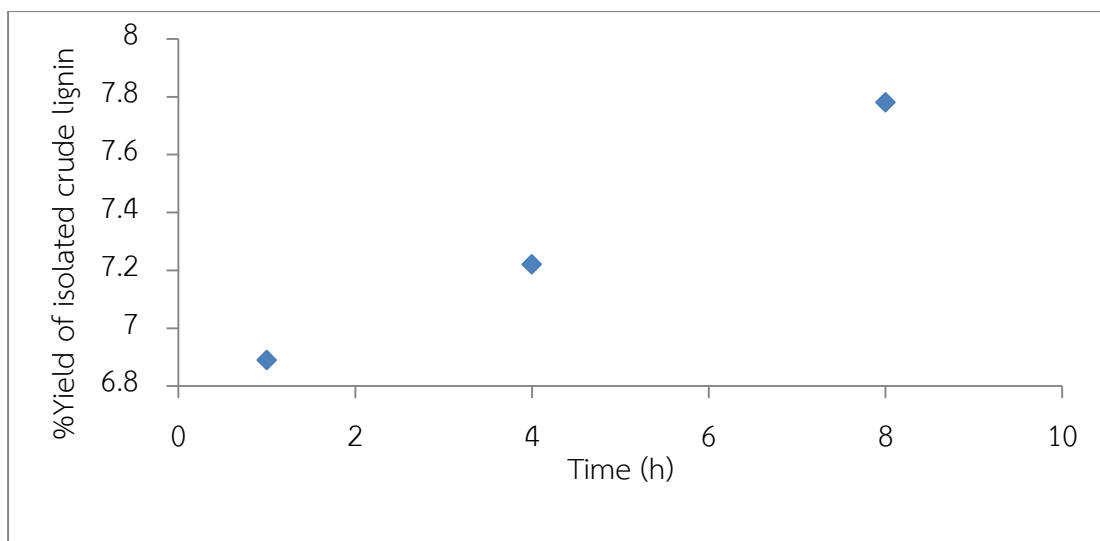


**Figure 4.1** %Yield of isolated crude lignin from giant sensitive plant pretreatment without dilute acid solution at 100 °C for 1-8 h.

**Table 4.3** Effect of various concentration of dilute acid on giant sensitive plant pretreatment at 100 °C for 8 h.

Biomass	H <sub>2</sub> SO <sub>4</sub> (wt%)	Yield (wt%)	
		Isolated lignin	Residue
Giant sensitive plant	0.25	12.50	59.00
	0.5	12.00	44.84
	0.75	14.65	40.93
	1	15.67	30.00
	2	11.31	45.83

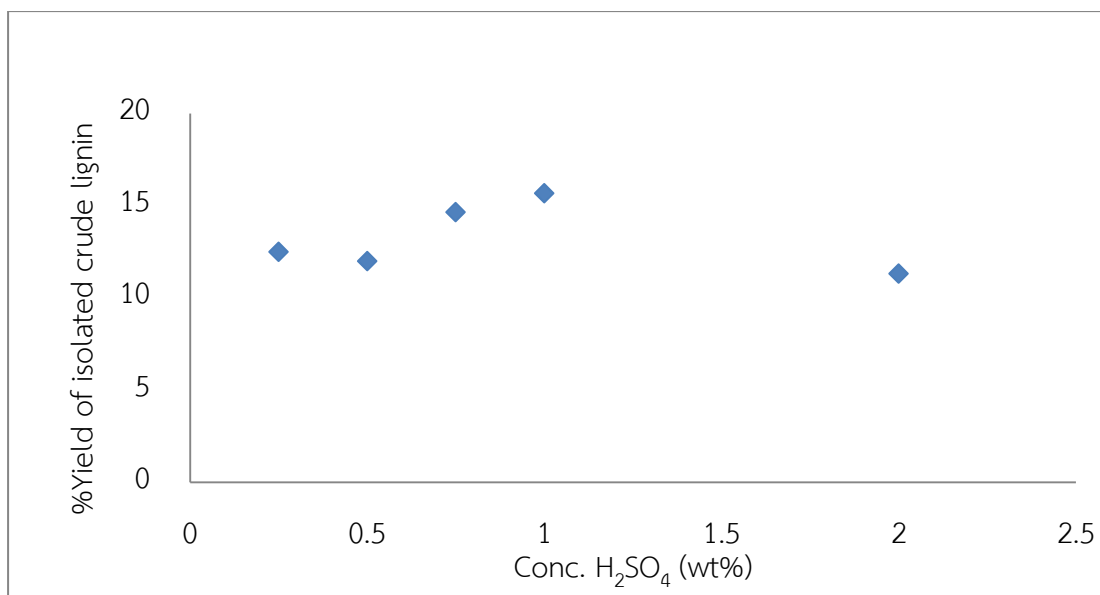


**Figure 4.2** %Yield of isolated crude lignin from giant sensitive plant pretreatment with 0.25-2% H<sub>2</sub>SO<sub>4</sub> at 100 °C for 8 h.

### 4.3 Characterization of catalysts

#### 4.3.1 Pure SBA-15 and Al-SBA-15

##### 4.3.1.1 X-ray powder diffraction (XRD)

The pure SBA-15 was prepared using hydrothermal method whereas Al was added by alumination of SBA-15 using post synthesis. The Si/Al ratio was 14. The low angle XRD pattern of SBA-15 showed peaks index to (100), (110) and (200). These peaks reveal the characteristic pattern of hexagonal mesoporous material. After Al loading, the 3 characteristic peaks still showed hexagonal mesoporous structure. However, the peak intensity at (100) plane of Al-SBA-15 was decreased because the hexagonal structure was destroyed by Al insertion or recalcination process.

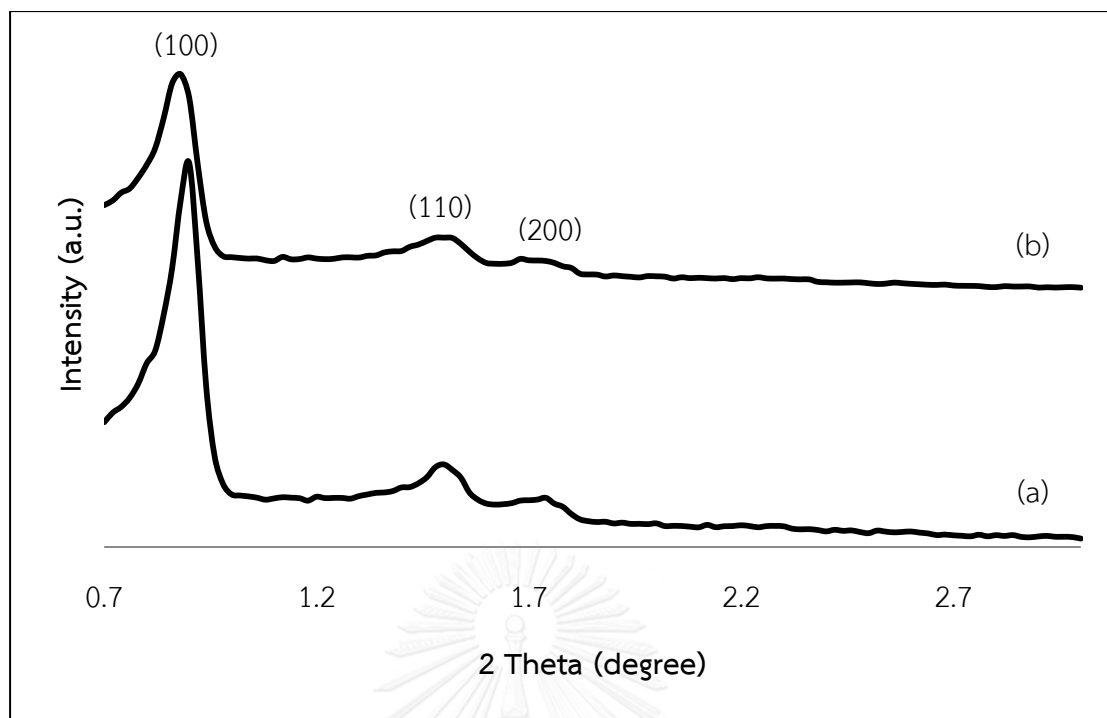


**Figure 4.3** XRD patterns of (a) pure SBA-15 and (b) Al-SBA-15.

#### 4.3.1.2 Nitrogen adsorption-desorption

The N<sub>2</sub> adsorption/desorption isotherm of SBA-15 and Al-SBA-15 was shown in Figure 4.4. The sample illustrated the type IV isotherm of mesoporous material that involve to SBA-15 materials. In addition, textural properties of SBA-15 and Al-SBA-15, with Si/Al ratio as 14, was indicated in Table 4.4. Aluminium was loaded in SBA-15 framework that decreased the amount of nitrogen up take in SBA-15 owing to the decreasing of pore volume [75] as  $0.98 \text{ cm}^3 \text{ g}^{-1}$ . In addition, the loading Al into SBA-15 framework affected to decrease the BET surface area ( $515 \text{ m}^2 \text{ g}^{-1}$ ) and internal surface area ( $450 \text{ m}^2 \text{ g}^{-1}$ ).

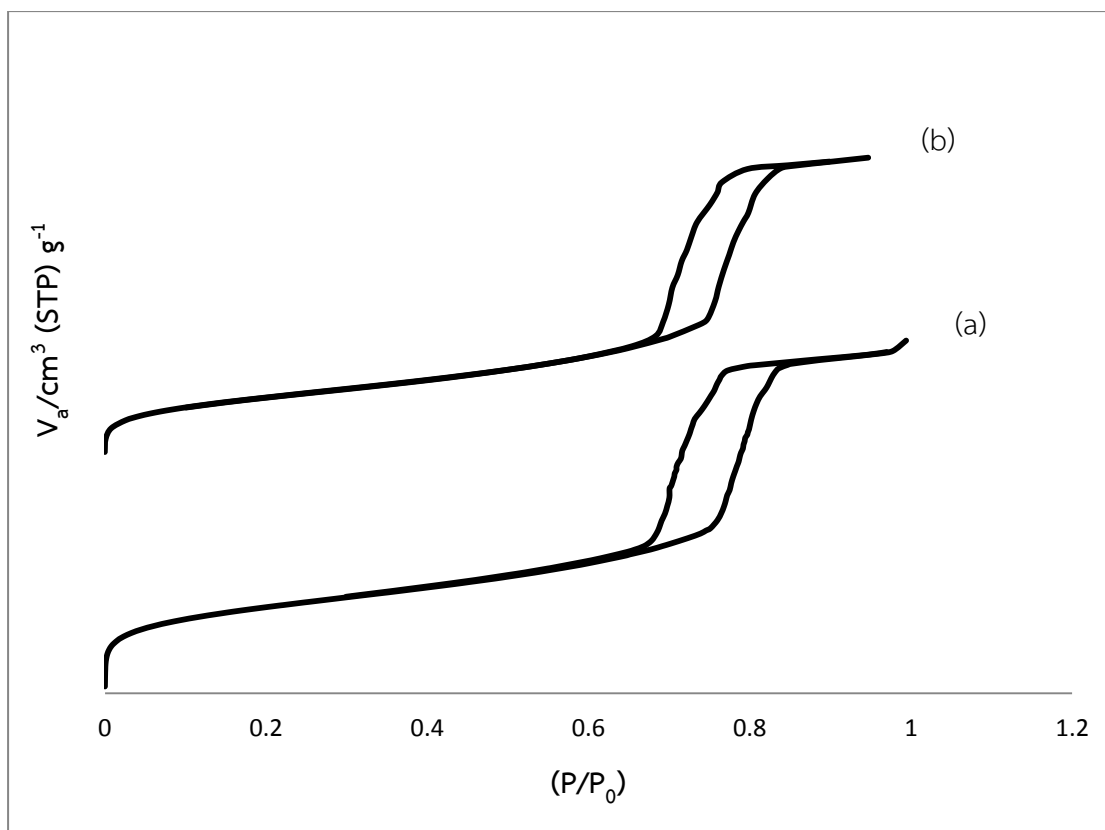


**Figure 4.4** Nitrogen adsorption-desorption isotherms of (a) pure SBA-15 and (b) Al-SBA-15.

**Table 4.4** Properties of pure SBA-15 and Al-SBA-15.

Catalyst	N <sub>2</sub> Adsorption/desorption			
	BET surface area (m <sup>2</sup> g <sup>-1</sup> ) <sup>a</sup>	Internal surface area (m <sup>2</sup> g <sup>-1</sup> ) <sup>b</sup>	Total pore volume (cm <sup>3</sup> g <sup>-1</sup> ) <sup>c</sup>	Average pore diameter (nm) <sup>c</sup>
SBA-15	675	478	1.09	9.36
Al-SBA-15	515	450	0.98	9.36

<sup>a</sup>Reported by BET method,

<sup>b</sup>Reported by t-plot,

<sup>c</sup>Reported by BJH-plot method



### 4.3.2 $^{27}\text{Al}$ -MAS-NMR spectra of Al-SBA-15

The  $^{27}\text{Al}$ -MAS-NMR spectrum of Al-SBA-15 was shown in Figure 4.5. The  $^{27}\text{Al}$ -MAS-NMR spectrum could allow the information of the aluminium atoms which they were located at framework or non-framework site. The result showed that Al-SBA-15 illustrated only one strong peak at about 56 ppm. This peak was indicated to tetrahedral ( $T_d$ ) coordination framework aluminium formed in the mesoporous material [76]. However, the peak at 0 ppm of octahedral ( $O_h$ ) characteristic was octahedral ( $O_h$ ) was not observed, showing the absence of octahedrally coordination non-framework aluminium.

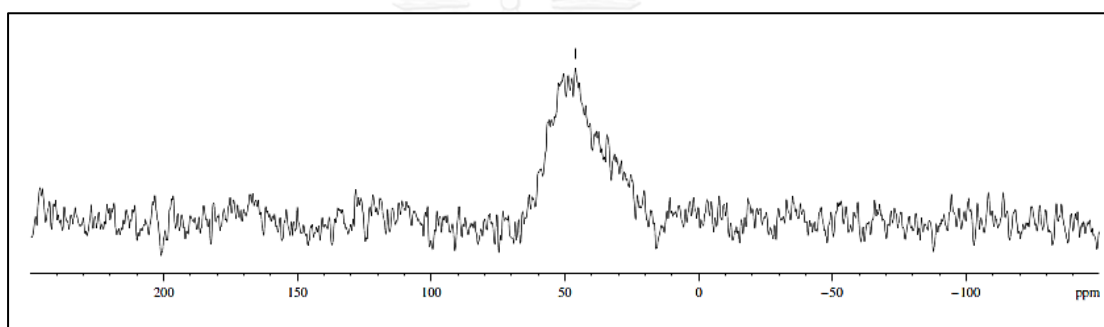


Figure 4.5  $^{27}\text{Al}$ -MAS-NMR spectra of Al-SBA-15.

### 4.3.3 Elemental analysis of Al-SBA-15

The number of aluminium atoms in catalysts was determined by ICP-MS. The Si was calculated by deduction of Al from the total number of tetrahedral atoms. It was found that Al contents in the catalyst that was not significant difference between Si/Al mol ratio in Al-SBA-15, ZSM-5 and Zeolite- $\beta$  which are in a range of 14.1-15.0 as shown in Table 4.5. However, the data from ICP-MS technique cannot illustrate the structure of aluminium atom, whether it located in framework or extra-framework. Thus, data from  $^{27}\text{Al}$ -NMR was needed for this identification.

**Table 4.5** Si/Al mole ratio of Al-SBA-15.

Catalyst	Si/Al mole ratio in catalyst
Al-SBA-15 <sup>a</sup>	14.1
ZSM-5 <sup>a</sup>	14.6
Zeolite- $\beta$ <sup>b</sup>	15.0

<sup>a</sup>Calculated from ICP-QMS.

<sup>b</sup>Si/Al mole ratio in catalyst provide by the ZEOCHEM supplier.

#### 4.3.4 Physical properties of Amberlyst-15, ZSM-5 and Zeolite- $\beta$

The physical properties of the catalysts were characterized by N<sub>2</sub> adsorption/desorption as shown in Table 4.6. The BET specific surface area and internal surface area of ZSM-5 were higher than Zeolite- $\beta$ . Moreover, the ZSM-5 provided the highest pore volume as 0.28 cm<sup>3</sup> g<sup>-1</sup>. The Zeolite- $\beta$  exhibited higher pore diameter than ZSM-5 and Amberlyst-15

**Table 4.6** Properties of Amberlyst-15, ZSM-5 and Zeolite- $\beta$ .

Catalyst	N <sub>2</sub> Adsorption/desorption			
	BET surface area (m <sup>2</sup> g <sup>-1</sup> ) <sup>a</sup>	Internal surface area (m <sup>2</sup> g <sup>-1</sup> ) <sup>b</sup>	Total pore volume (cm <sup>3</sup> g <sup>-1</sup> ) <sup>c</sup>	Average pore diameter (nm) <sup>c</sup>
Amberlyst-15	37	12	0.06	2.40
ZSM-5	435	445	0.28	2.59
Zeolite- $\beta$	210	212	0.18	3.36

<sup>a</sup>Reported by BET method,

<sup>b</sup>Reported by t-plot,

<sup>c</sup>Reported by BJH-plot method

#### 4.3.5 Acid-base titration

The acid value quantities of all catalysts were determined by acid-base titration using sodium chloride as ion-exchange reagent. The acid value of all catalysts was shown in Table 4.7. The acid amount of catalysts followed in the order: Amberlyst-15 > Al-SBA-15 > ZSM-5 > Zeolite- $\beta$ . Particularly, Amberlyst-15 showed the highest acid amount because the structure consisted of strongly acidic sulfonic group. Thus, it illustrated as high acid content.

**Table 4.7** Acid amount of catalysts.

Catalyst	H <sup>+</sup> Content (mmol/g)
Amberlyst-15	4.72
ZSM-5	0.69
Zeolite- $\beta$	0.56
Al-SBA-15	0.78

#### 4.4 Lignin separation from hardwood and agricultural residue

The results of lignin separation were presented in Table 4.8. The lignin isolation of biomass followed in the order: giant sensitive plant > corncob > sugarcane bagasse > rice straw. The pretreated giant sensitive plant gave the highest lignin separation because it was hardwood. So, the pretreated giant sensitive plant was chosen for studying parameters such as solvent ratio, reaction temperature, reaction time and type of catalyst.

**Table 4.8** Lignin separation from hardwood and agricultural residue.

Biomass	Yield (wt%)		%Separation
	Lignin component	Lignin separation	
Rice straw	7.4	6.7	90.6
Sugarcane bagasse	14.9	11.2	75.2
Corn cob	13.1	11.6	88.6
Pretreated giant sensitive plant	20.7	16.8	81.2

#### 4.5 Lignin Separation from pretreated giant sensitive plant

The lignin from pretreated giant sensitive plant was separated by organosolv method by varying various reaction parameters, i.e. solvent ratio, reaction temperature, reaction time and type of catalyst, as the following study.

##### 4.5.1 Effect of solvent ratio

The effect of solvent ratio was studied following the method explained in part 3.8.2.1. The Amberlyst-15 as catalyst, temperature and time were fixed at 0.63 g, 200°C and 30 min, respectively. The results were shown that using EtOH:H<sub>2</sub>O

ratios as 80:20 was an optimum solvent mixture that the isolated lignin from pretreated giant sensitive plant obtained the highest of Klason lignin yield (95.80%) as shown in Table 4.9.

**Table 4.9** Effect of solvent ratio on isolated lignin from pretreated giant sensitive plant.

Biomass	EtOH:H <sub>2</sub> O ratio (50 mL)	Yield (wt%)			%Klason lignin
		Crude lignin	Pure lignin	others	
Pretreated giant sensitive plant	50:50	6.50	5.54	0.96	85.30
	60:40	10.67	9.21	1.46	86.35
	70:30	13.83	12.71	1.12	91.91
	80:20	16.83	16.12	0.71	95.80
	90:10	10.67	9.02	1.65	84.55
	100:0	6.83	6.04	0.79	88.35

Data were shown as the mean  $\pm$  0.23SD, derived from 3 independent repeats.

#### 4.5.2 Effect of reaction temperature

The effect of temperature was studied following the method explained in part 3.8.2.2. The Amberlyst-15 as catalyst, EtOH:H<sub>2</sub>O and time were fixed at 0.63 g, 80:20 (50 ml) and 30 min, respectively. The temperature at 240 °C gave the highest crude lignin (17.17%). However, this temperature gave only 90.13% of Klason lignin that compared with the same condition using temperature at 200 °C (95.77%) as shown in Table 4.10.

**Table 4.10** Effect of temperature on isolated lignin from pretreated giant sensitive plant.

Biomass	Temperature (°C)	Yield (wt%)			%Klason lignin
		Isolated lignin	Pure lignin	others	
Pretreated giant sensitive plant	180	5.17	4.91	0.26	95.01
	200	16.83	16.12	0.71	95.77
	220	16.50	14.59	1.91	88.41
	240	17.17	15.47	1.70	90.13

Data were shown as the mean  $\pm$  0.24SD, derived from 3 independent repeats.

#### 4.5.3 Effect of reaction time

The effect of reaction time was studied following the method explained in part 3.8.2.3. The Amberlyst-15 as catalyst, EtOH:H<sub>2</sub>O and temperature were fixed at 0.63 g, 80:20 (50 ml) and 200°C, respectively. The reaction time 30 min gave high crude lignin as 16.83%. In addition, this temperature also exhibited the highest 95.77% of Klason lignin when compare with other reaction times as shown in Table 4.11.

**Table 4.11** Effect of time on isolated lignin from pretreated giant sensitive plant.

Biomass	Time (min)	Yield (wt%)			%Klason lignin
		Isolated lignin	Pure lignin	others	
Pretreated giant sensitive plant	15	14.83	13.75	1.08	92.70
	30	16.83	16.12	0.71	95.77
	45	14.67	13.65	1.02	93.05
	60	14.17	12.83	1.34	90.55

Data were shown as the mean  $\pm$  0.23SD, derived from 3 independent repeats.

#### 4.5.4 Effect of catalyst

The lignin from pretreated giant sensitive plant and corncob was separated over various catalysts which distributed as two groups that composed of heterogeneous (i.e. Amberlyst-15, ZSM-15, Zeolite- $\beta$ , Al-SBA-15) and homogeneous (i.e.  $H_2SO_4$ , HCl,  $HNO_3$ ) catalysts to compare their efficiency of lignin separation. The results displayed that the lignin separation without a catalyst using  $C_2H_5OH:H_2O$  (80:20 v/v, 50 ml) at 200°C for 30 min obtained a yield of only 4.17 % of lignin, whereas using Amberlyst-15 under the same condition gave a yield 16.84% of lignin. In addition, this condition gave 95.80% of the highest Klason lignin as the lignin purity as shown in Table 4.12. Sulfuric acid as homogeneous catalyst gave the highest yield of lignin. However, this homogeneous catalyst gave a yield 87.90% of Klason lignin.

**Table 4.12** Effect of various catalysts on isolated lignin from pretreated giant sensitive plant.

Biomass	Catalyst	Yield (wt%)			%Klason lignin
		Isolated lignin	Pure lignin	others	
Pretreated giant sensitive plant	None	4.17	3.52	0.65	84.36
	Amberlyst-15	16.83	16.12	0.71	95.80
	ZSM-5	5.83	5.02	0.81	86.10
	Zeolite- $\beta$	5.50	5.22	0.28	94.89
	Al-SBA-15	4.50	3.41	1.09	85.20
	$H_2SO_4$	20.67	18.17	2.50	87.90
	HCl	3.83	3.48	0.35	90.86
	$HNO_3$	4.33	3.20	1.13	73.73

Data were shown as the mean  $\pm$  0.24SD, derived from 3 independent repeats.

Isolated lignin condition: 3.0 g of sample, 0.63 g of catalyst, EtOH:H<sub>2</sub>O (v/v) at 200°C for 30 min.

#### 4.6 Lignin separation from corncob

The comparison of isolated lignin both pretreated giant sensitive plant and corncob under the same condition (3.0 g of biomass, 0.63 g of Amberlyst-15, EtOH:H<sub>2</sub>O = 80:20 v/v at 200°C for 30 min.) was illustrated in Table 4.13. The isolated lignin from corncob gave isolated lignin and Klason lignin only 11.60 and 72.49%, respectively. While, pretreated giant sensitive plant gave isolated lignin and Klason lignin as 16.80 and 95.80%, respectively

**Table 4.13** The comparison of isolated lignin from pretreated giant sensitive plant and corncob.

Biomass	Yield (wt%)			%Klason lignin
	Isolated lignin	Pure lignin	others	
Pretreated giant sensitive plant	16.83	16.12	0.71	95.80
Corn cob <sup>a</sup>	11.60	9.79	3.71	72.49

<sup>a</sup> Data were shown as the mean  $\pm$  0.28SD, derived from 3 independent repeats.

#### 4.7 Characterization of isolated lignin

##### 4.7.1 Fourier transform infrared spectroscopy (FTIR)

##### 4.7.1.1 Isolated lignin from giant sensitive plant

The functional groups of all samples were determined by NICOLET 6700 Fourier transform infrared spectroscopy in ATR mode. FTIR spectra in Figure 4.6 showed the peak pattern of residue, isolated crude lignin, Klason lignin and raw material of giant sensitive plant. The spectra of four samples illustrated the similar peak patterns in range 3645-2837 cm<sup>-1</sup> that were stretching vibration of C-H and OH groups. These are peaks could be commonly found in residue, isolated crude lignin, Klason lignin and raw material of giant sensitive plant.



The raw giant sensitive plant exhibited the characteristic peak of hemicellulose at  $1725\text{ cm}^{-1}$  [77] as the characteristic stretching vibration of the carbonyl. Moreover, the bands at  $1395\text{ cm}^{-1}$ ,  $1364\text{ cm}^{-1}$  and  $896\text{ cm}^{-1}$  as characteristic bands of cellulose [78]. After raw giant sensitive plant was pretreated with 1%  $\text{H}_2\text{SO}_4$ , the characteristic peaks of hemicellulose and cellulose demonstrated the decreased in intensity of peaks.

After the crude isolated lignin from giant sensitive plant was purified with Klason method under optimum condition, the characteristic peaks of hemicellulose was disappeared as shown the shoulder at  $1698$  and  $1669\text{ cm}^{-1}$  originated from conjugated carbonyl stretches [79]. Aromatic skeletal vibrations gave three strong peaks at  $1591$ ,  $1590$  and  $1491\text{ cm}^{-1}$ . A band at  $1460\text{ cm}^{-1}$  was indicated to C-H deformations and aromatic ring vibration [80]. In addition, the band at  $1265\text{ cm}^{-1}$  was assigned to guaiacyl ring mixing with C=O stretching [81]. Moreover, the band for aromatic in plane bending, and out of-plane C-H bending were observed at  $1210$  and  $1149\text{ cm}^{-1}$  for syringyl unit, and at  $1027$  and  $847\text{ cm}^{-1}$  for guaiacyl unit, respectively. Although, the familiar peak pattern of Klason lignin were similar with isolated crude lignin. The peaks of Klason lignin gave the decreased intensity at in range  $3631\text{-}3038\text{ cm}^{-1}$  due to the removal of cellulose and hemicellulose in both the structure.

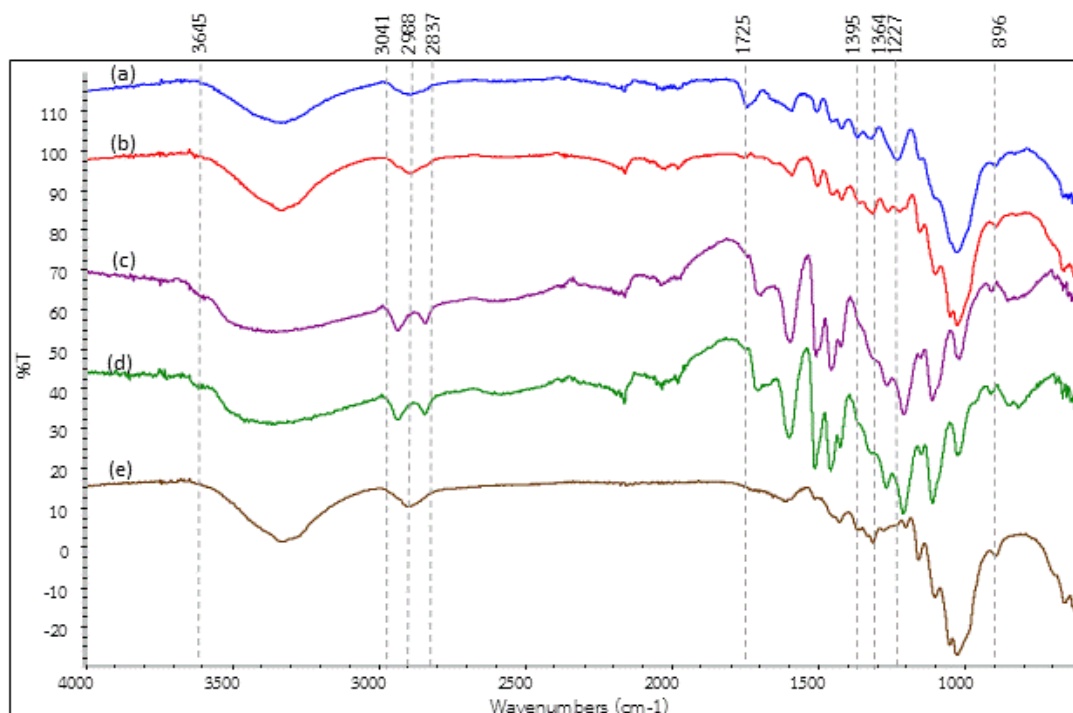


**Figure 4.6** FTIR spectra of (a) raw giant sensitive plant, (b) pretreated giant sensitive plant with 1% H<sub>2</sub>SO<sub>4</sub> at 100 °C for 8 h, (c) isolated crude lignin, (d) Klason lignin and (e) residue. Separation condition: 3.0 g of pretreated giant sensitive plant, 0.63 g of Amberlyst-15, C<sub>2</sub>H<sub>5</sub>OH:H<sub>2</sub>O = 80:20 (v/v) at 200 °C for 30 min.

#### 4.7.1.2 Isolated lignin from corncob

FTIR spectra of raw corncob, isolated crude lignin, Klason lignin and residue after lignin separation were presented in Figure 4.7. The raw corncob illustrated the peak of hemicellulose was shifted from 1725 to 1716 due to the lack of pretreatment step [77]. Besides, the bands at 1364 cm<sup>-1</sup>, 1236 cm<sup>-1</sup>, 1155 and 890 cm<sup>-1</sup> as characteristic bands of cellulose [78]. The band at 1236 cm<sup>-1</sup> was appeared in isolated crude lignin that demonstrated isolated crude lignin as non-pure lignin due to the contaminated from cellulose. This result was confirmed by Klason method that the percentage of Klason lignin of corncob was illustrated only 72.49%.

The isolated lignin from corncob was purified with Klason method under the similar optimum condition. The characteristic peaks of lignin were shown in Figure 4.7 (c). The band at  $1652\text{ cm}^{-1}$  was attributed to conjugated carbonyl stretching in lignin. The aromatic skeleton in the lignin as assigned at 1594, 1590 and  $1422\text{ cm}^{-1}$  [79]. The band at  $1459\text{ cm}^{-1}$  related to C-H deformation and aromatic ring vibration. The aliphatic C-H stretching in  $\text{CH}_3$  gave a small band at  $1352\text{ cm}^{-1}$ . Moreover, the band at 1249 and  $1210\text{ cm}^{-1}$  was indicated as benzene ring hmixing with C-O stretching in lignin structure. The band 1120 and  $1024\text{ cm}^{-1}$  raised from the aromatic C-H in plane deformation for S type and G type, respectively [80]. The aromatic C-H out of plane demonstrated at  $835\text{ cm}^{-1}$  [81].

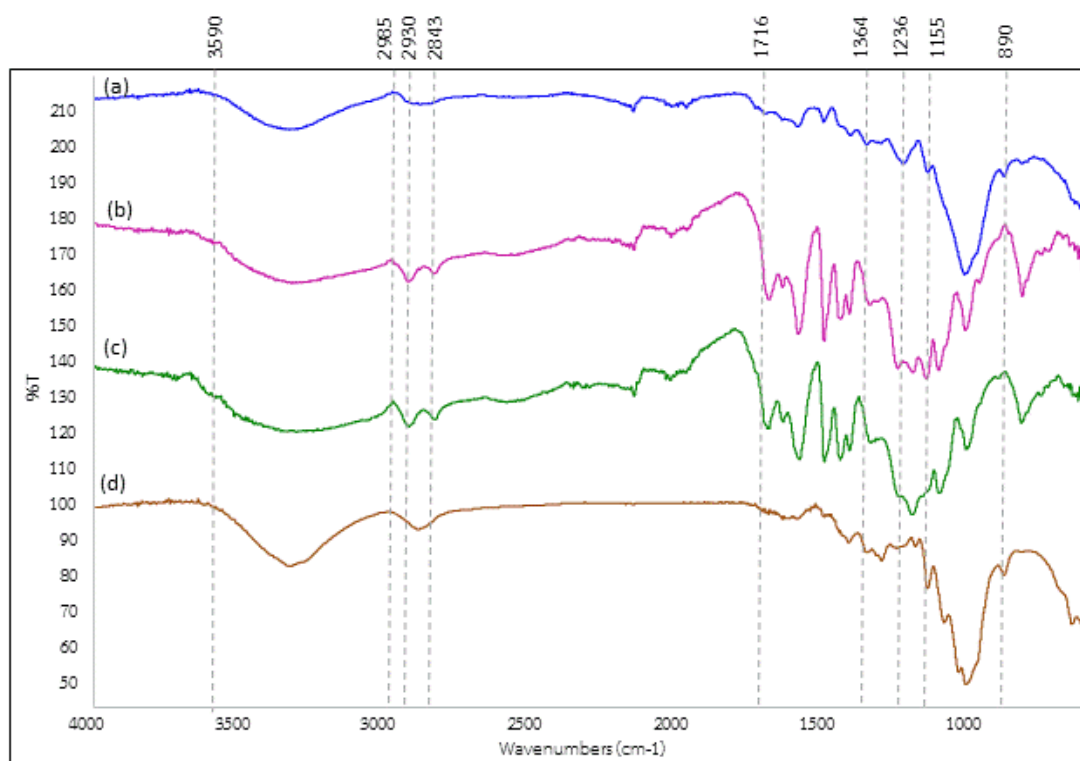
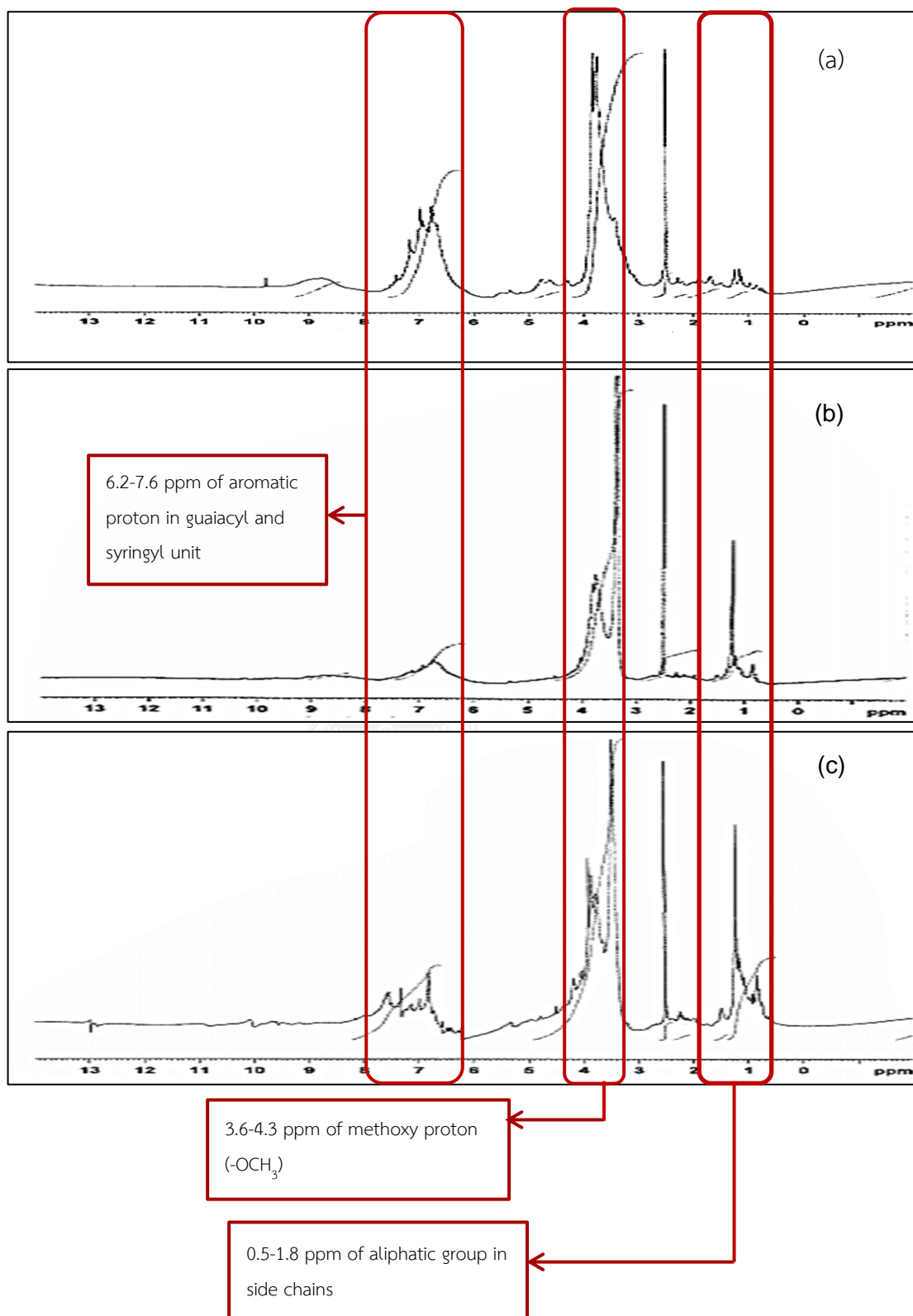


**Figure 4.7** FTIR spectra of (a) raw corncob, (b) isolated crude lignin, (c) Klason lignin and (d) residue. Separation condition: 3.0 g of corncob, 0.63 g of Amberlyst-15,  $\text{C}_2\text{H}_5\text{OH}:\text{H}_2\text{O} = 80:20$  (v/v) at  $200^\circ\text{C}$  for 30 min.

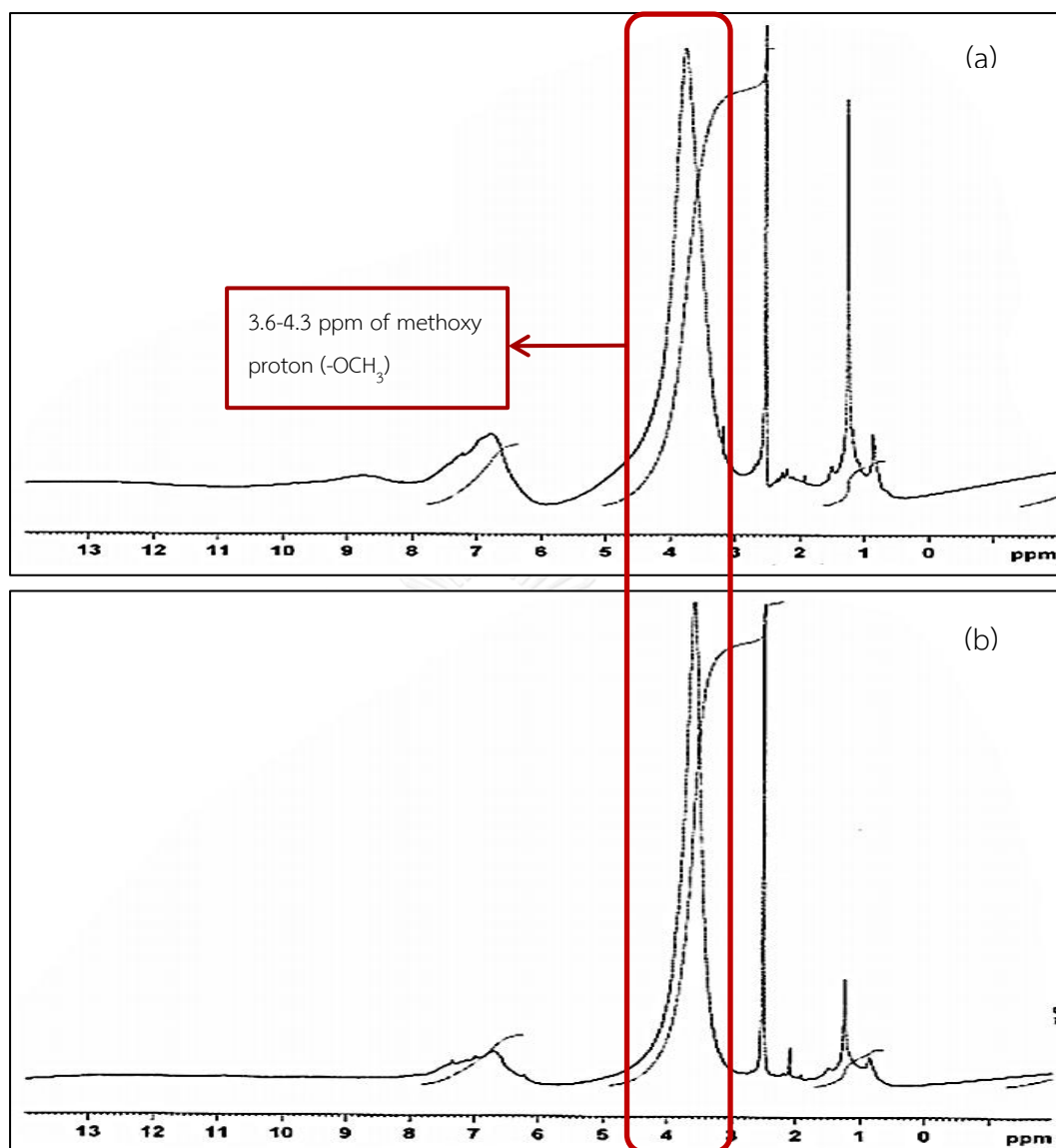
#### 4.7.2 Proton-1 Nuclear Magnetic Resonance Spectroscopy ( $^1\text{H}$ NMR)

Figure 4.8 compared  $^1\text{H}$  NMR spectra of crude lignin from commercial (Figure D-1), pretreated giant sensitive plant (Figure D-2) and corncob (Figure D-3). The  $^1\text{H}$  NMR spectra of three samples gave signals in the range 7.6-6.2 ppm that were assigned to the aromatic proton in G and S units. The methoxy proton gave signals in range 4.3-3.6 ppm. The intense signal at 3.3 ppm was due to proton in water in  $d_6$ -DMSO. The signal at 2.5 ppm was indicative of proton in  $d_6$ -DMSO. Moreover, the protons in aliphatic group such as in the side chains of crude lignins were identified by signals at 1.8-0.5 ppm [82].

After that, crude lignin from three samples was purified with Klason lignin method. The  $^1\text{H}$  NMR spectra of pure lignin from Klason purification of crude commercial lignin (Figure D-4), pretreated giant sensitive plant (Figure D-5) and corncob (Figure D-6) were illustrated in Figure 4.9. The all signals of three samples showed increased sharp peaks at 3.4-5.1 ppm because the cellulose backbone signals were removed from crude lignins [83]. Particularly, the strong peak at 3.7 ppm showed a signal of methoxyl proton ( $-\text{OCH}_3$ ) in lignin structure.



**Figure 4.8**  $^1\text{H}$  NMR spectrums of crude lignin from commercial, pretreated giant sensitive plant and corncob.



**Figure 4.9** <sup>1</sup>H NMR spectra of Klason lignin from crude lignin of pretreated giant sensitive plant (Figure D-4) and corn cob (Figure D-5).

#### 4.7.3 Carbon-13 Nuclear Magnetic Resonance Spectroscopy (<sup>13</sup>C NMR)

From Figure 4.11 showed a comparison of the <sup>13</sup>C NMR spectra of crude lignin from commercial (Figure D-7), pretreated giant sensitive plant (Figure D-8) and corn cob (Figure D-9). The <sup>13</sup>C NMR spectra of three samples illustrated chemical shift assignments for <sup>13</sup>C spectra of crude lignin that were difficult to interpret because lignin is a very heterogeneous polymer, and many signals were overlapped [84].

The signals in the range of 100-165 ppm were attributed to aromatic carbon, while the aliphatic carbons were identified by signals at 15-90 ppm. The strong signals at 55-56 ppm corresponded to methoxyl carbon ( $-\text{OCH}_3$ ) in syringyl and guaiacyl units. In addition, the signals occurred between 14-34 ppm region were assigned to saturated hydrocarbon structures in the aliphatic side-chains. Especially, the signals at 145-160 ppm were attributed to the major signals of lignin that were C-3, C-4 carbon in guaiacyl phenolic units and C-3, C-5 carbon in syringyl units as shown Figure 4.10.

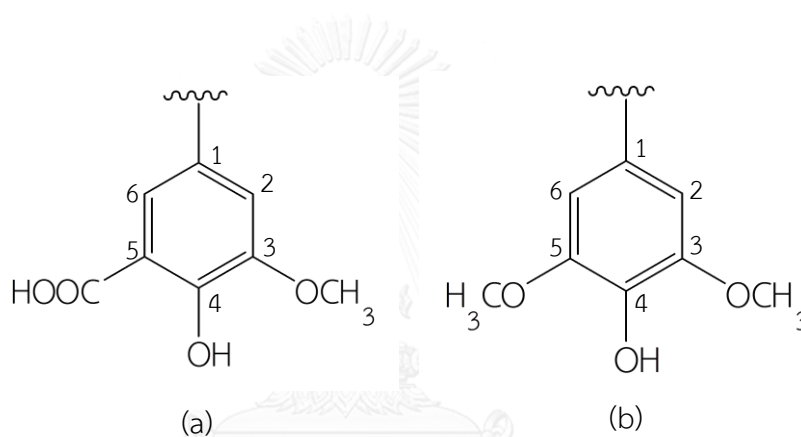


**Figure 4.10** Guaiacyl phenolic unit (a) and syringyl unit (b).

However, the signals about 60 ppm were identified to all unsubstituted the C-6 carbons and methyl groups in cellulose structure [85]. These result illustrated that crude lignins from three samples were contaminated with cellulose, while Klason lignin of crude lignin from commercial (Figure D-10), giant sensitive plant (Figure D-11) and corncob (Figure D-12) had disappeared this signal because it was removed from lignin structure as shown in Figure 4.12.

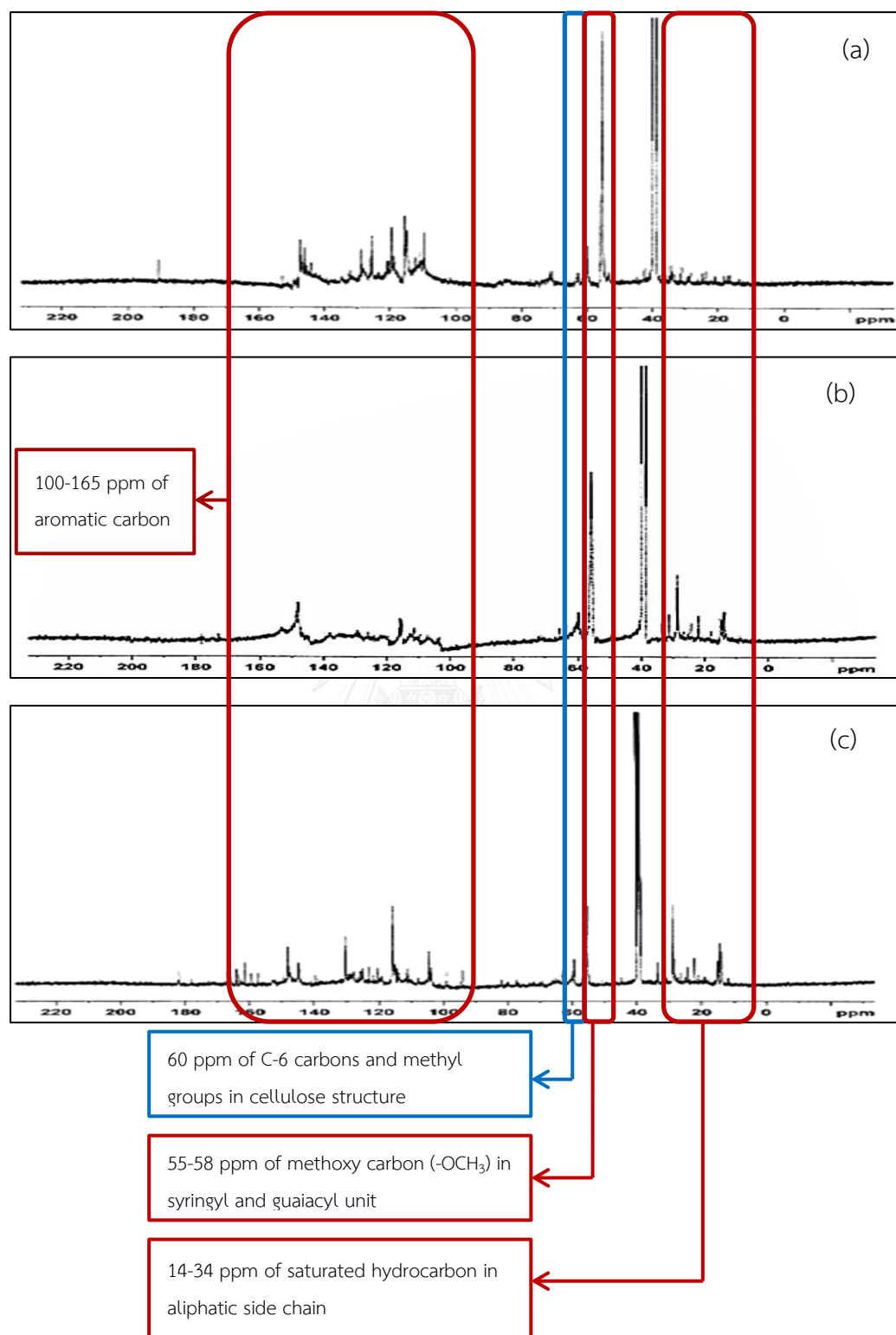


**Figure 4.11**  $^{13}\text{C}$  NMR spectrums of crude lignin from commercial (Figure D-6), pretreated giant sensitive plant (Figure D-7) and corncob (Figure D-8).



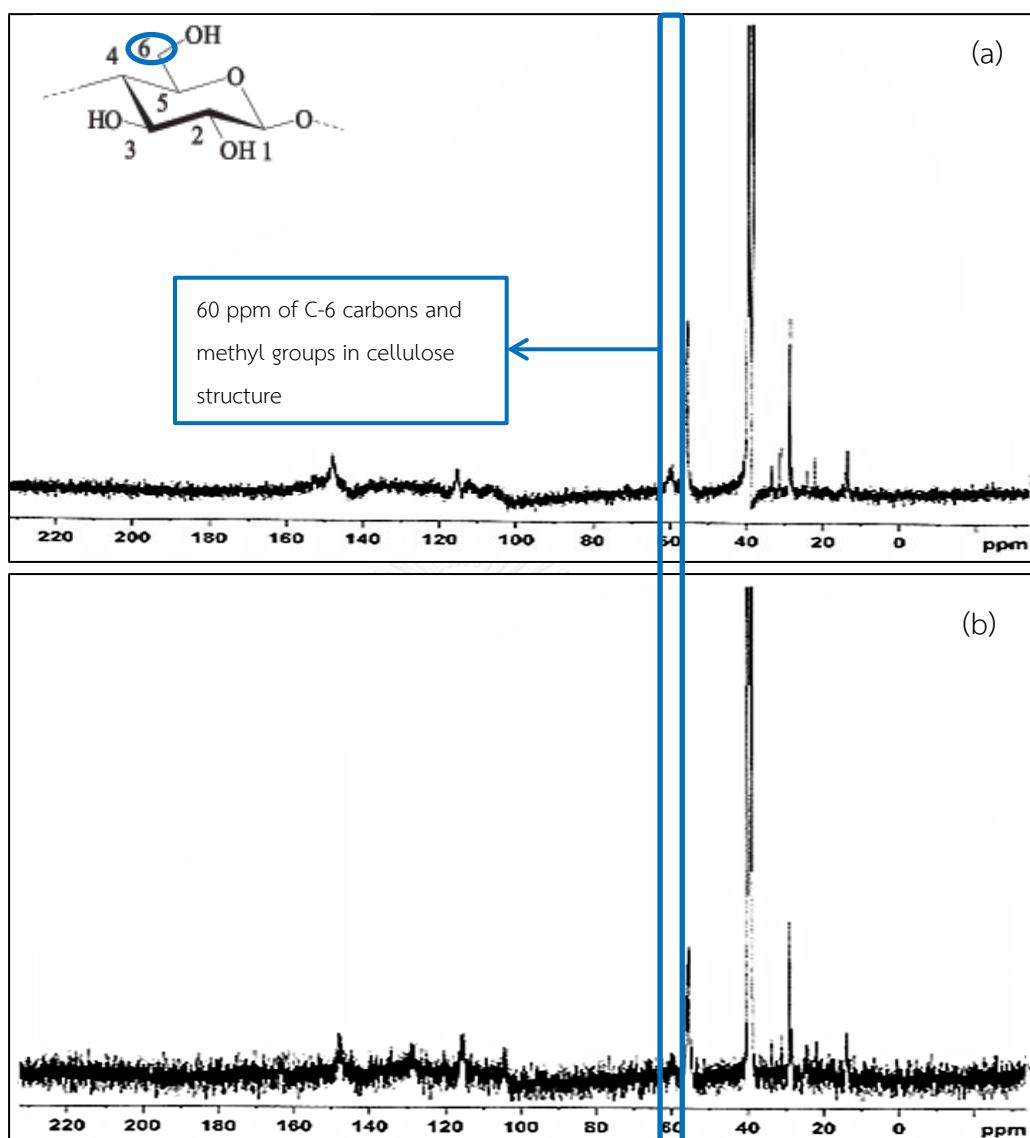
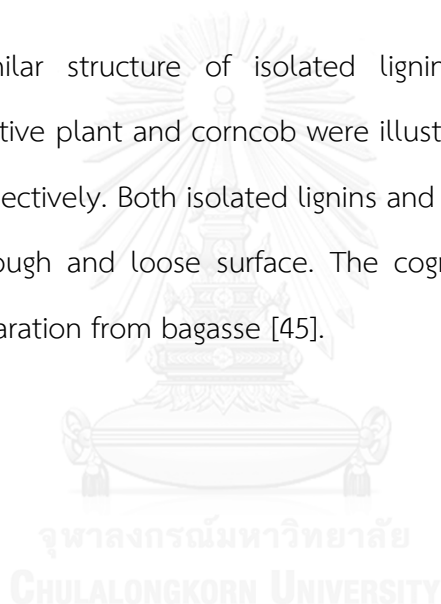


**Figure 4.12**  $^{13}\text{C}$  NMR spectrums of Klason lignin from crude lignin from giant sensitive plant (Figure D-9) and corncob (Figure D-10).

#### 4.7.4 Scanning electron microscope (SEM)

The SEM images of raw giant sensitive plant and corncob were shown in Figure 4.13 (a) and Figure 4.14 (a), respectively that were exhibited smooth and non-porous and uniform surfaces. The SEM image of the 1% (w/w) H<sub>2</sub>SO<sub>4</sub> pretreated giant sensitive plant displayed hole on its biomass surface due to partly hemicellulose and cellulose removal and crystallinity reducing as shown in Figure 4.18 (b). On the other hand, the raw corncob was not necessary to pretreat with 1% (w/w) H<sub>2</sub>SO<sub>4</sub> due to weaker plant structure.

The similar structure of isolated lignins and Klason lignins from pretreated giant sensitive plant and corncob were illustrated in Figure 4.13 (d, e) and Figure 4.14 (c, d), respectively. Both isolated lignins and Klason lignins of two samples were distributed a rough and loose surface. The cognate structure of lignin were reported in lignin separation from bagasse [45].



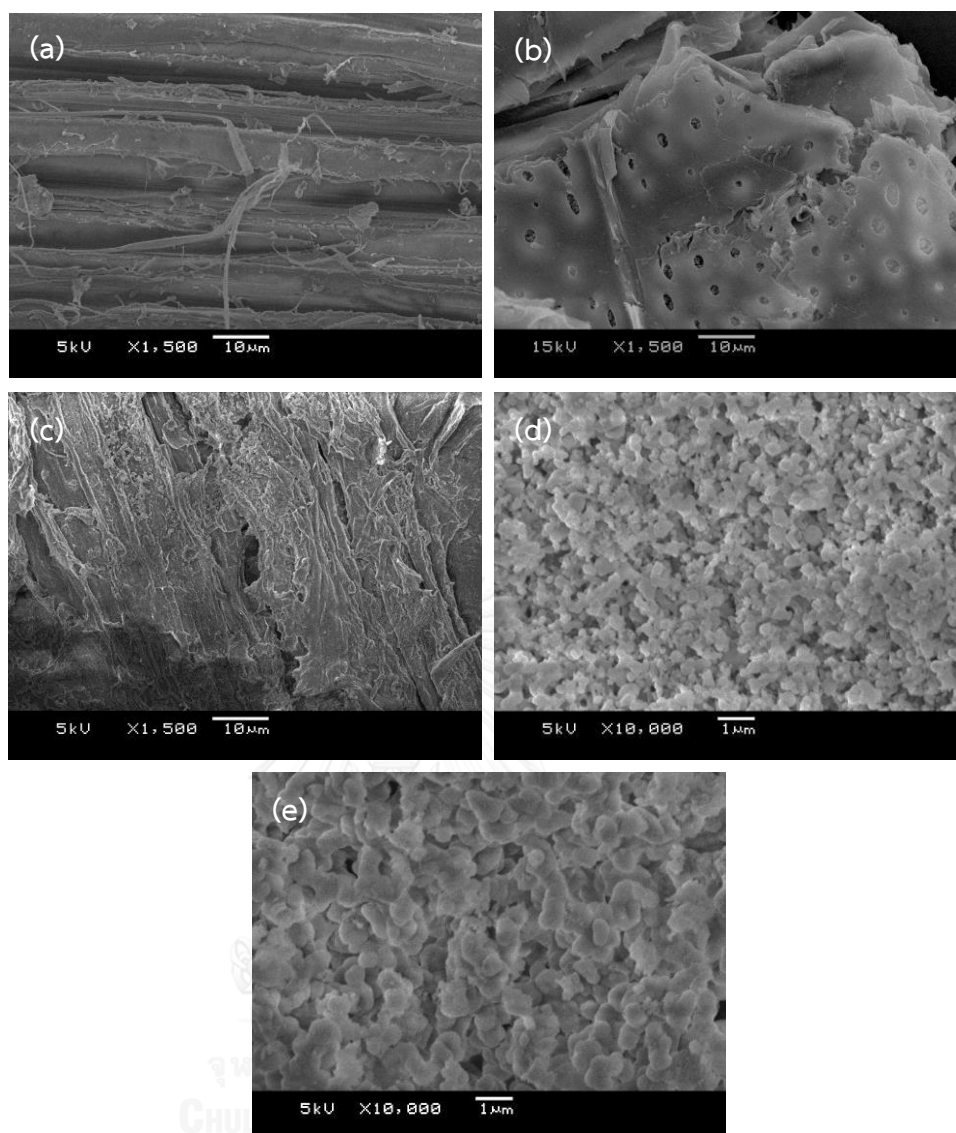


**Figure 4.13** SEM images (1,500 × magnification) of (a) raw giant sensitive plant, (b) pretreatment with 1% (w/w) H<sub>2</sub>SO<sub>4</sub> as 15:2 ratio of raw giant sensitive plant to H<sub>2</sub>SO<sub>4</sub> and (c) residue from separated lignin, (10,000 × magnification) of (d) isolated lignin and (e) Klason lignin; Separation condition: 3.0 g of pretreated giant sensitive plant, 0.63 g of Amberlyst-15, C<sub>2</sub>H<sub>5</sub>OH:H<sub>2</sub>O = 80:20 (v/v) at 200°C for 30 min.

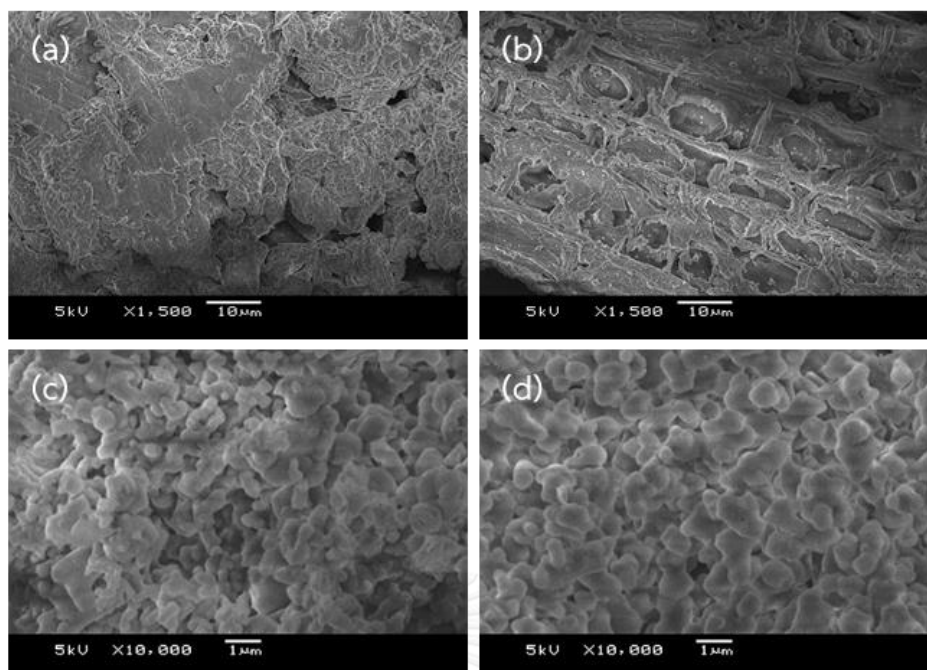


**Figure 4.14** SEM images (1,500 × magnification) of (a) raw corn cob and (b) residue from separated lignin, of (c) isolated lignin (10,000 × magnification) and (d) Klason lignin; Separation condition: 3.0 g of corn cob, 0.63 g of Amberlyst-15, C<sub>2</sub>H<sub>5</sub>OH:H<sub>2</sub>O = 80:20 (v/v) at 200°C for 30 min.

## 4.7.5 Thermogravimetric analysis (TGA)

### 4.7.5.1 Raw giant sensitive plant and corncob

The thermal decomposition of raw giant sensitive plant and corncob is commonly investigated by thermogravimetric analysis (TGA) under nitrogen atmosphere. TGA thermograms were shown the weight loss of both biomasses into the temperature of thermal decomposition, while the first derivative of that DTG thermogram was illustrated corresponding rate of weight loss. The temperature at  $327.4^{\circ}\text{C}$  was expressed the highest temperature that raw giant sensitive plant withstand decomposition more than the temperature of corncob ( $324.9^{\circ}\text{C}$ ) as shown in Figure 4.15 (a) and (b).

Both TGA thermogram of raw giant sensitive plant and corncob were revealed that in the first step were the decomposition of water molecules in raw giant sensitive plant and corncob at  $70\text{--}100^{\circ}\text{C}$  as 2.30 wt% and 2.36 wt%, respectively. The second step was the disintegration of cellulose, hemicellulose in raw giant sensitive plant and corncob in range of  $200\text{--}360^{\circ}\text{C}$  in order to light volatile and gases such as  $\text{H}_2\text{O}$ ,  $\text{CO}$  and  $\text{CO}_2$  [86] at about 74.34 wt%, while corncob was 73.62 wt%. The char product of raw giant sensitive plant and corncob was 25.36 wt% and 24.02 wt%, respectively. From the Figure 4.15 (a) and (b) included that the temperature of decomposition of raw giant sensitive plant was higher than raw corncob.

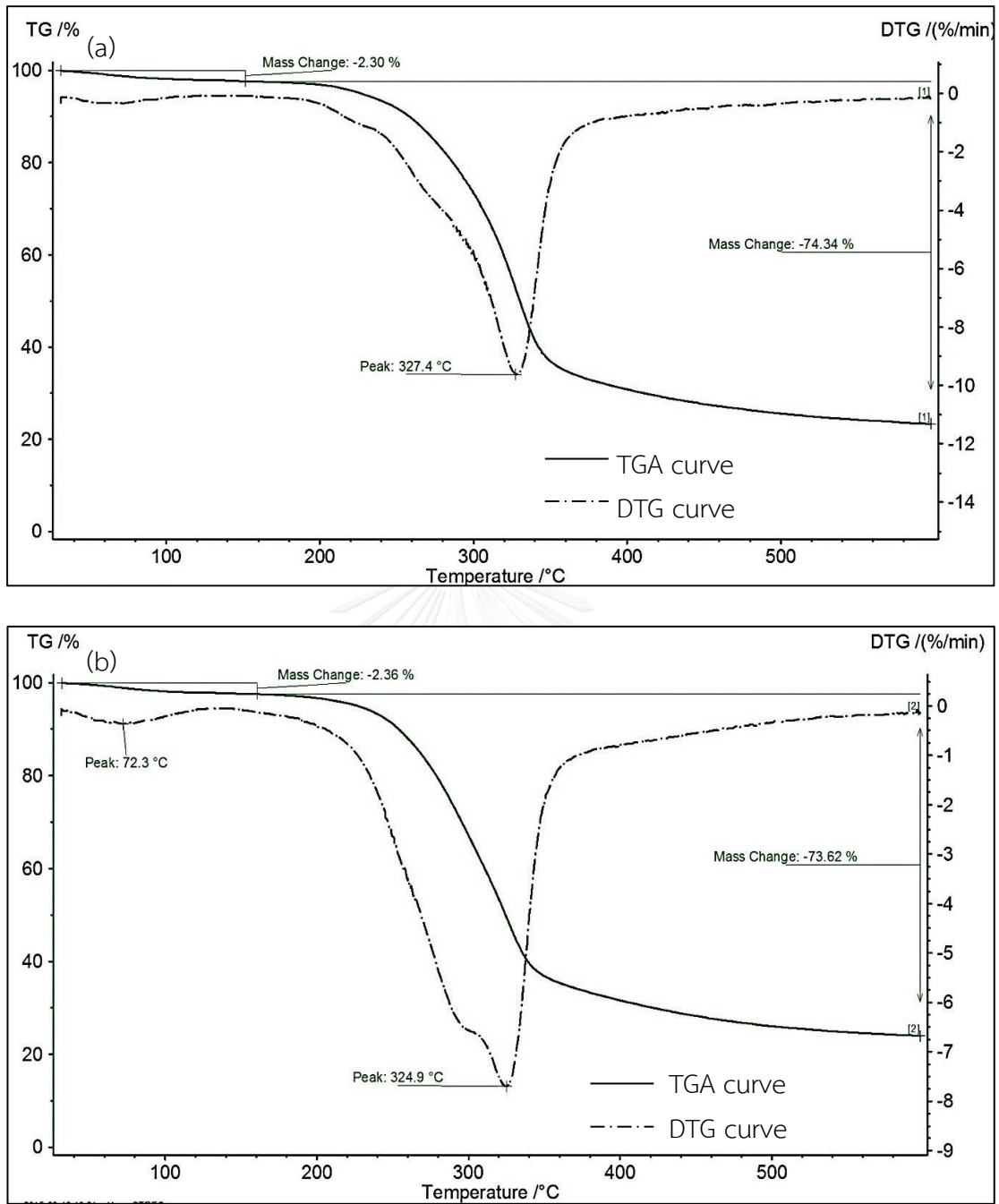
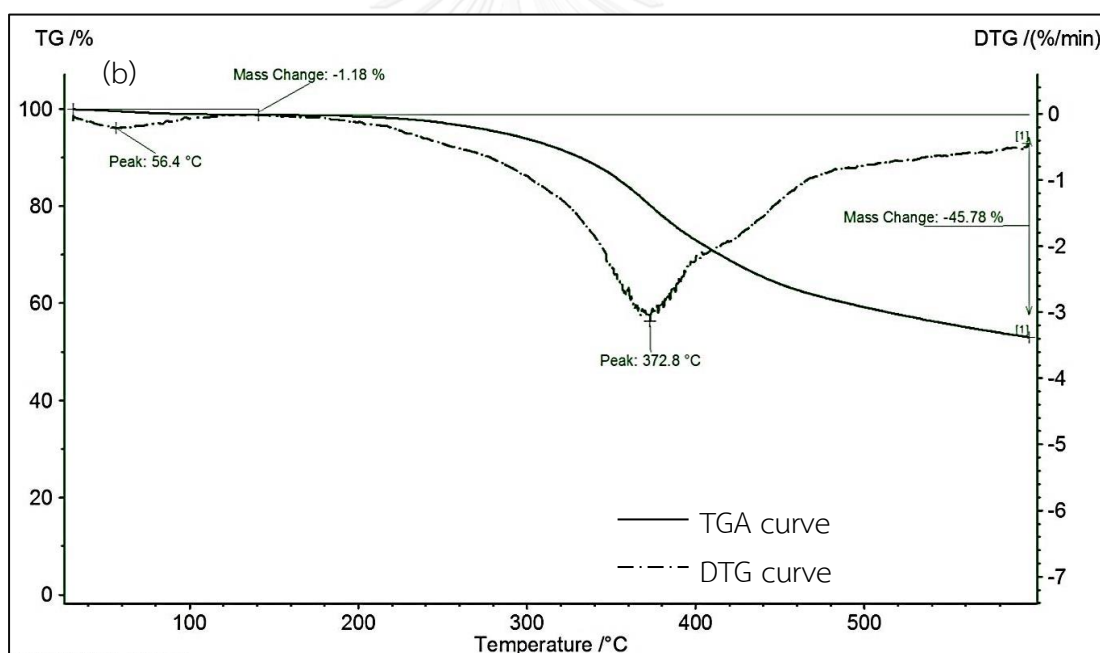
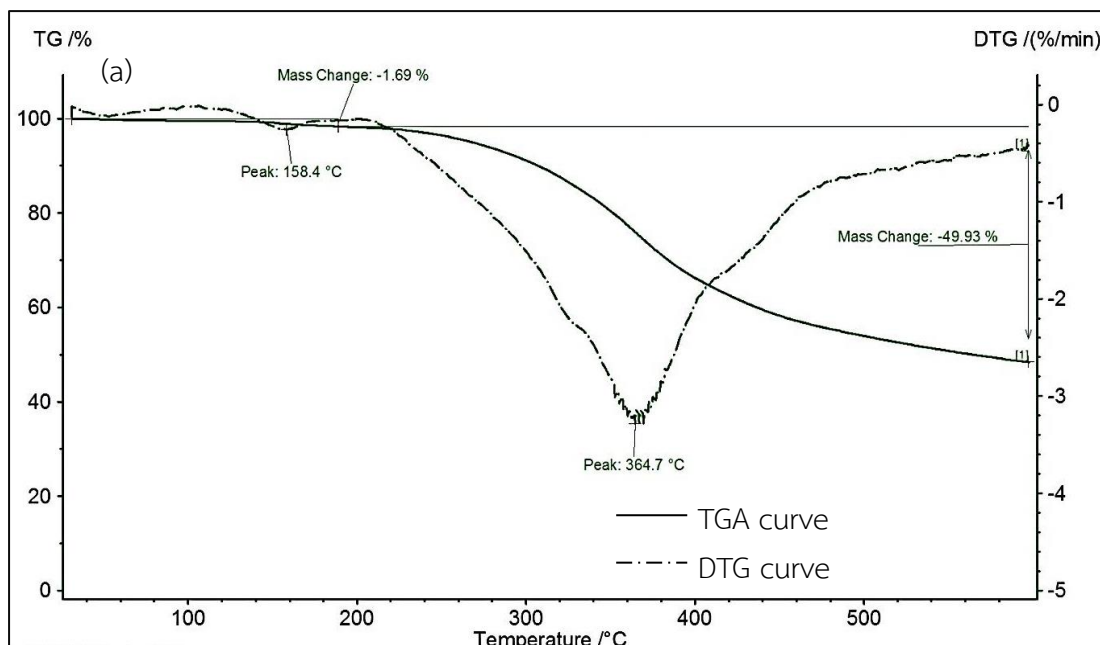


Figure 4.15 TGA and DTG curves of (a) raw giant sensitive plant and (b) corncob.

#### 4.7.5.2 Isolated crude lignin and Klason lignin from pretreated giant sensitive plant

The thermal properties of the isolated lignin and Klason lignin were studied by TGA and DTG. The thermal stabilities of both isolated crude lignin and Klason lignin were included two steps that the first step 1.69 wt% and 1.18 wt%, respectively. This weight loss was shown as moisture evaporation (e.g. H<sub>2</sub>O) occurred at range 40-160 °C. In the second step, 49.93 wt% and 45.78 wt% of both samples at range 220-500 °C as weight loss was degradation of inter-unit linkages, releasing monomeric phenol into the vapour phase as shown in Figure 4.16 (a) and (b) [87].

The DTG thermograms of both isolated lignin and Klason lignin in Figure 4.16 (a) and (b) were demonstrated a single weight loss peak at 364.7 °C and 372.8 °C, respectively. Their temperatures were confirmed the unique composition of isolated lignin that were related to FTIR and NMR characterizations. However, The DTG thermograms of Klason lignin was illustrated the higher temperature than isolated lignin because Klason lignin was measuring only lignin as composition in biomass while isolated crude lignin might be degradation other substances.



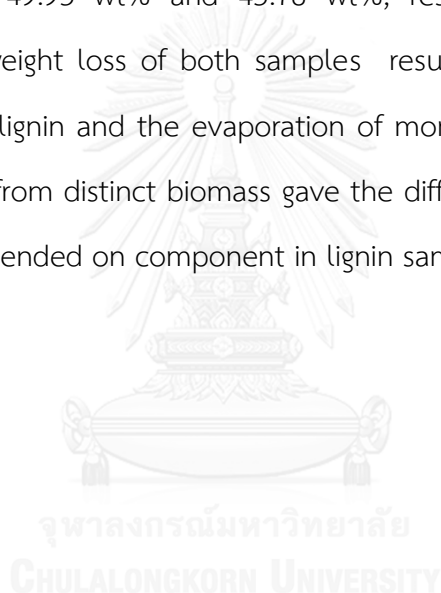
**Figure 4.16** TGA and DTG curves of crude lignin and Klason lignin from pretreated giant sensitive plant.



#### 4.7.5.3 Isolated crude lignin and Klason lignin from corncob

The thermal stability of isolated crude lignin and Klason lignin from corncob was determined by TGA and DTG. The TGA thermogram were found 1.69 wt% and 1.18 wt% of the humidity that was removed in rang 70-160 °C as shown in Figure 4.17 (a) and (b).

The decomposition process of both isolated crude lignin and Klason lignin covered a large temperature range between 210 and 500 °C that weight loss was shown as 49.93 wt% and 45.78 wt%, respectively. The results were demonstrated that weight loss of both samples results from the cleavage of the inter-unit linkages of lignin and the evaporation of monomer phenol [79]. Thus, the isolated crude lignin from distinct biomass gave the different thermal decomposition temperature that depended on component in lignin sample.



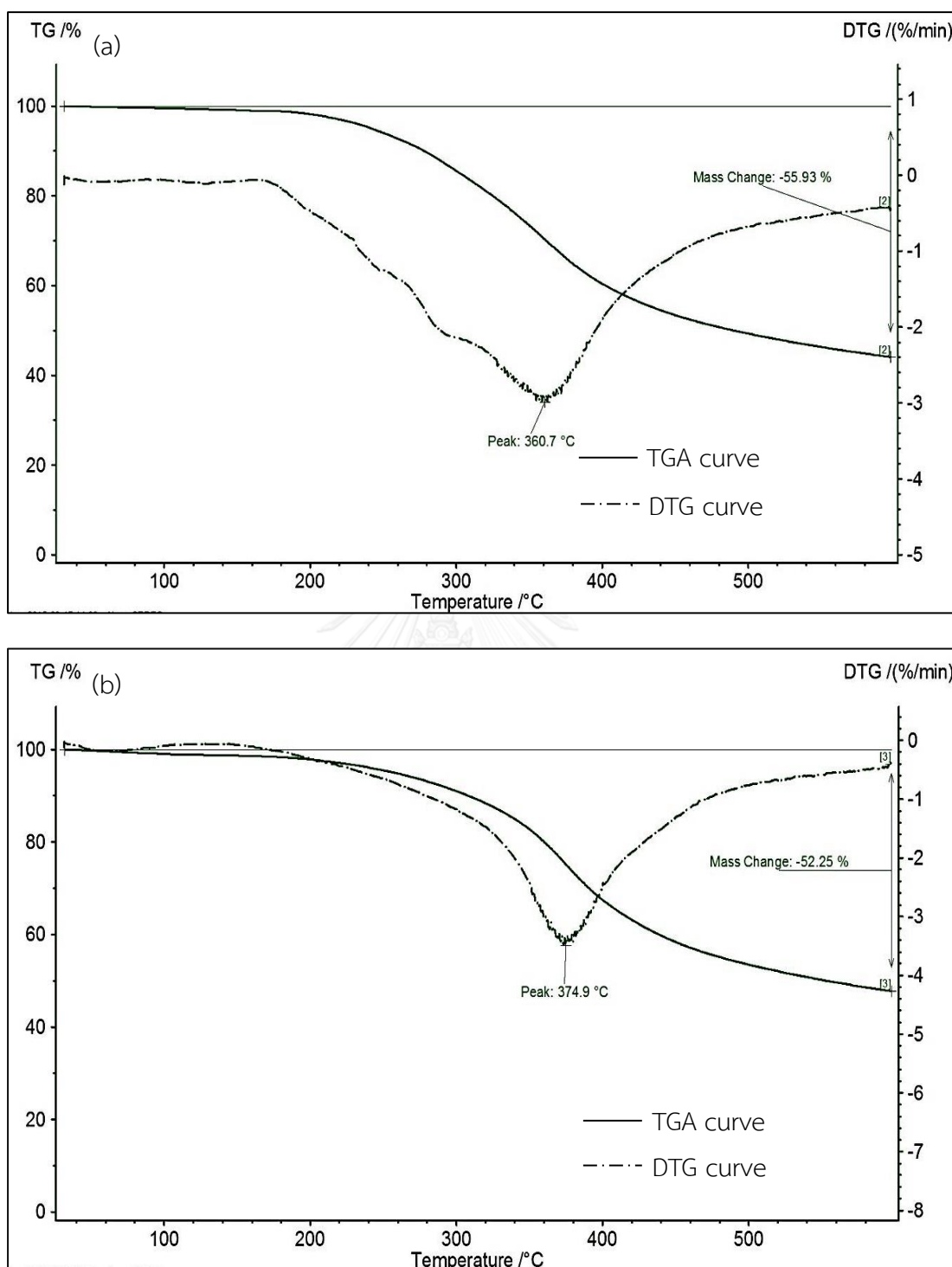


Figure 4.17 TGA and DTG curves of isolated lignin and Klason lignin from corncob.

#### 4.7.6 Elemental analysis (C, H, O and N)

The elemental analysis from six samples was shown in Table 4.12. After the Klason lignin process, the results illustrated the decreasing of carbon amount due to the removal cellulose and hemicellulose from the isolated crude lignin, while the number of oxygen increased as a result of the main structure of lignin that mostly consisted of methoxyl group (-OCH<sub>3</sub>).

**Table 4.14** Elemental analysis

Biomass	C (%)	H (%)	O (%)	N (%)
Raw giant sensitive plant	48.70	7.04	43.64	0.62
Isolated crude lignin <sup>a</sup>	67.77	6.64	25.35	0.24
Klason lignin <sup>b</sup>	66.95	6.07	26.71	0.27
Raw corncob	46.80	6.54	45.87	0.79
Isolated crude lignin <sup>a</sup>	65.40	6.42	27.24	0.94
Klason lignin <sup>b</sup>	64.06	6.13	28.87	0.94

<sup>a</sup>From reaction using 0.63 of Amberlyst-15, 3.0 g of pretreated giant sensitive plant, EtOH:H<sub>2</sub>O ratio = 80:20 (v/v%) at 30 °C for 30 min.

<sup>b</sup>TAPPI Test Method T222 om-88

#### 4.8 Lignin transformation to fine chemicals with optimal condition

All liquid products after catalytic pyrolysis of isolated lignin and Klason lignin with optimum condition were determined by GC-MS analysis

##### 4.8.1 Gas chromatograph-mass spectrometer (GC-MS)

##### 4.8.1.1 Commercial lignin and Klason commercial lignin

The comparison between commercial lignin and Klason lignin in catalytic pyrolysis gave many products as shown in Table 4.13 and Table 4.14.

**Table 4.15** Compound identified by GC-MS in catalytic pyrolysis of commercial lignin.

Peak	Retention time (min)	Compound name	%Selectivity
1	19.5	Catechol	30.3
2	22.1	1,2-Benzenediol, 4-methyl-	17.8
3	16.1	Phenol, 2-methoxy-	16.3
4	19.3	2-Methoxy-5-methylphenol	6.4
5	21.3	1,2-Benzenediol, 3-methyl-	6.0
6	12.5	Phenol	3.3
7	24.6	1,3-Benzenediol, 4-ethyl-	3.3
8	21.8	Phenol, 4-ethyl-2-methoxy-	2.9
9	15.7	p-Cresol	2.5
10	15.0	Phenol, 2-methyl-	2.3
11	25.0	Vanillin	2.0
12	23.8	1,4-Benzenediol, 2,5-dimethyl-	1.8
13	28.4	2-Propanone, 1-(4-hydroxy-3-methoxyphenyl)-	1.6
14	23.5	1,3-Benzenediol, 4-ethyl-	1.2
15	17.9	Phenol, 3,5-dimethyl-	1.0
16	27.3	Apocynin	0.9
17	23.6	1,4-Benzenediol, 2-methyl-	0.7

**Table 4.16** Compound identified by GC-MS in catalytic pyrolysis of Klason commercial lignin.

Peak	Retention time (min)	Compound name	%Selectivity
1	12.5	Phenol	19.2
2	15.0	Phenol, 2-methyl-	14.6
3	19.5	Catechol	14.3
4	15.7	p-Cresol	14.0
5	21.4	Phenol, 2,3,5-trimethyl-	6.3
6	18.0	Phenol, 3,5-dimethyl-	5.8
7	21.3	1,2-Benzenediol, 3-methyl-	4.7
8	22.1	1,2-Benzenediol, 4-methyl-	4.7
9	28.0	1-Naphthalenol	3.7
10	2.8	Propanoic acid	2.7
11	23.8	1,4-Benzenediol, 2,5-dimethyl-	2.2
12	23.6	1,4-Benzenediol, 2-methyl-	1.8
13	21.7	3,4-Dimethoxytoluene	1.7
14	30.4	1-Naphthalenol, 2-methyl-	1.2
15	16.0	Phenol, 2-methoxy-	1.2
16	24.6	1,3-Benzenediol, 4-ethyl-	1.1
17	30.4	1-Naphthalenol, 2-methyl-	1.0

Table 4.13 and Table 4.14 showed the seventeen major products of commercial lignin and Klason lignin that were mainly phenol derivatives. The results of products in distilled liquid were presented in the mean values of percentage area. The peak area of catechol gave the highest as 30.29% (retention time = 19.5 min in Figure 4.18 (a)) from catalytic pyrolysis of commercial lignin. On the other hand, the phenol product gave the highest as 19.2% of Klason lignin (retention time = 12.5 min in Figure 4.18 (b)) because commercial lignin obtained from various commercial pulp trees.

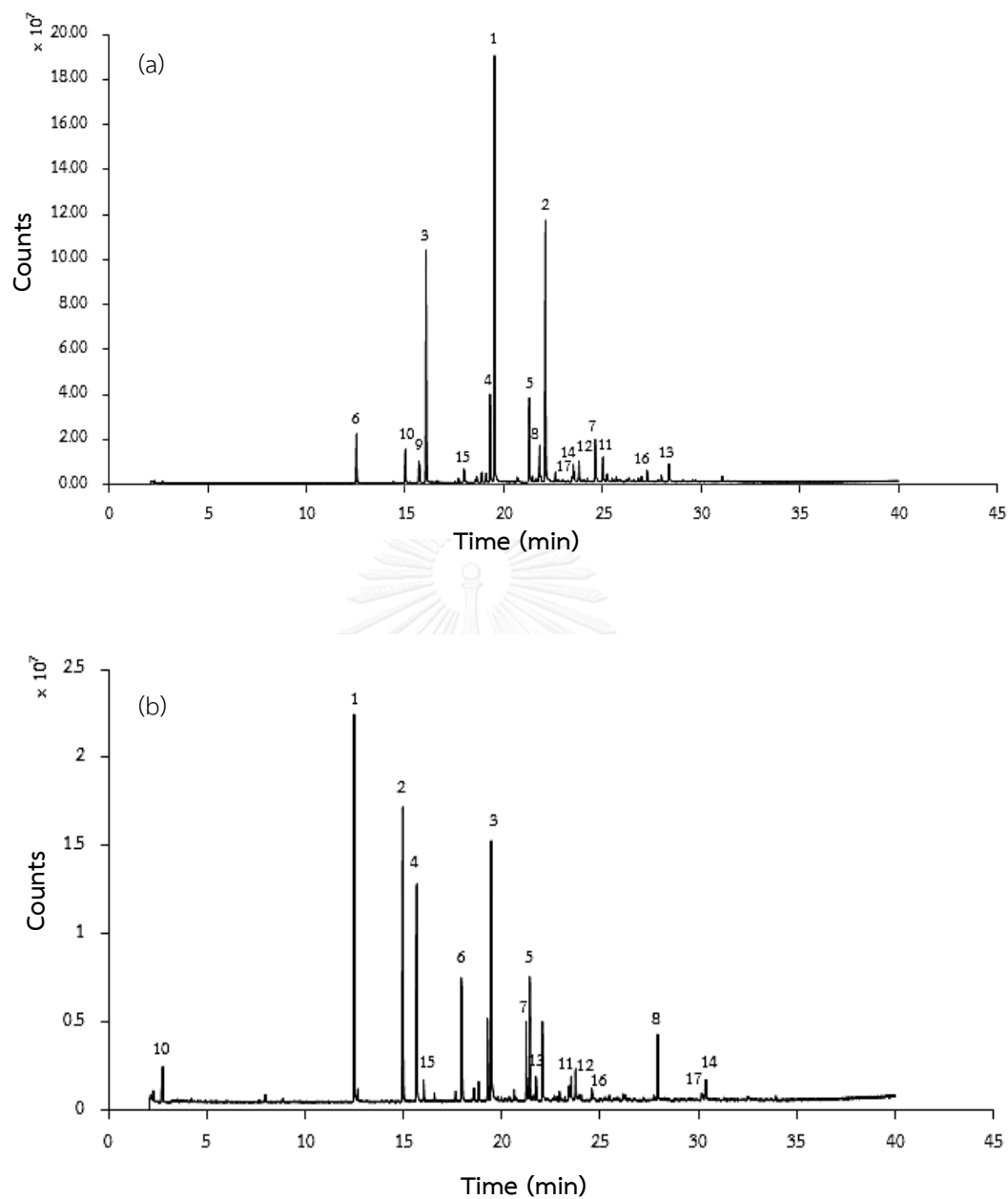


**Figure 4.18** Total ion chromatograms of (a) commercial lignin and (b) Klason commercial lignin catalytic pyrolysis of lignin at 300°C for 30 min, ZSM-5 to lignin ratio of 0.75:1 with 10 g of DI water. Refer to Table 4.13 and Table 4.14 for the names of identified compounds.

#### 4.8.1.2 Isolated crude lignin and Klason lignin from pretreated giant sensitive plant

The catalytic pyrolysis between isolated crude lignin and Klason lignin gave many products as shown in Table 4.15 and Table 4.16.

**Table 4.17** Compound identified by GC-MS in catalytic pyrolysis of isolated crude lignin from pretreated giant sensitive plant.

Peak	Retention time (min)	Compound name	%Selectivity
1	26.3	1,2,4-Trimethoxybenzene	15.4
2	15.0	Phenol, 2-methyl-	10.5
3	15.7	p-Cresol	10.2
4	12.5	Phenol	9.4
5	19.5	Catechol	8.9
6	16.1	Phenol, 2-methoxy-	8.4
7	19.3	Creosol	7.1
8	18.0	Phenol, 3,5-dimethyl-	5.5
9	28.3	5-tert-Butylpyrogallol	4.7
10	23.8	Phenol, 2,6-dimethoxy-	3.9
11	22.1	1,2-Benzenediol, 3-methyl-	3.0
12	21.8	Phenol, 4-ethyl-2-methoxy-	2.8
13	21.5	Phenol, 2,3,5-trimethyl-	2.7
14	18.6	Phenol, 3-ethyl-	2.1
15	28.0	1-Naphthalenol	2.0
16	2.8	Propanoic acid	1.9
17	24.6	4-Ethylcatechol	1.7

**Table 4.18** Compound identified by GC-MS in catalytic pyrolysis of Klason lignin from pretreated giant sensitive plant.

Peak	Retention time (min)	Compound name	%Selectivity
1	26.3	1,2,4-Trimethoxybenzene	14.5
2	19.5	Catechol	14.2
3	12.5	Phenol	9.8
4	15.0	Phenol, 2-methyl-	8.7
5	21.5	Phenol, 2,3,5-trimethyl-	8.7
6	28.3	5-tert-Butylpyrogallol	7.8
7	21.3	1,2-Benzenediol, 3-methyl-	5.9
8	18.0	Phenol, 3,5-dimethyl-	5.6
9	23.8	Phenol, 2,6-dimethoxy-	5.2
10	15.8	p-Cresol	3.9
11	28.0	Butylated Hydroxytoluene	3.9
12	23.6	1,4-Benzenediol, 2-methyl-	3.4
13	21.6	Hydroquinone	2.9
14	21.8	Phenol, 4-ethyl-2-methoxy-	2.2
15	30.3	Benzene, 1,1'-propylidenebis-	1.6
16	16.1	Phenol, 2-methoxy-	1.0
17	30.4	1-Naphthalenol, 2-methyl-	1.0

The result illustrated the relationship between pretreated giant sensitive plant lignin and Klason pretreated giant sensitive plant lignin that also gave the various products such as 1,2,4-trimethoxybenzene catechol phenol and other products. The highest product of both samples was 1,2,4-trimethoxybenzene about 14.45-15.37% that were illustrated as retention time at 26.3 min as in Figure 4.19 (a) and (b). The application of 1,2,4-trimethoxybenzene can be used as a precursor to produce the mellitic anhydride in the manufacture of dyes. The trimethoxybenzene might be decomposed mainly from guaiacyl, G unit of lignin.



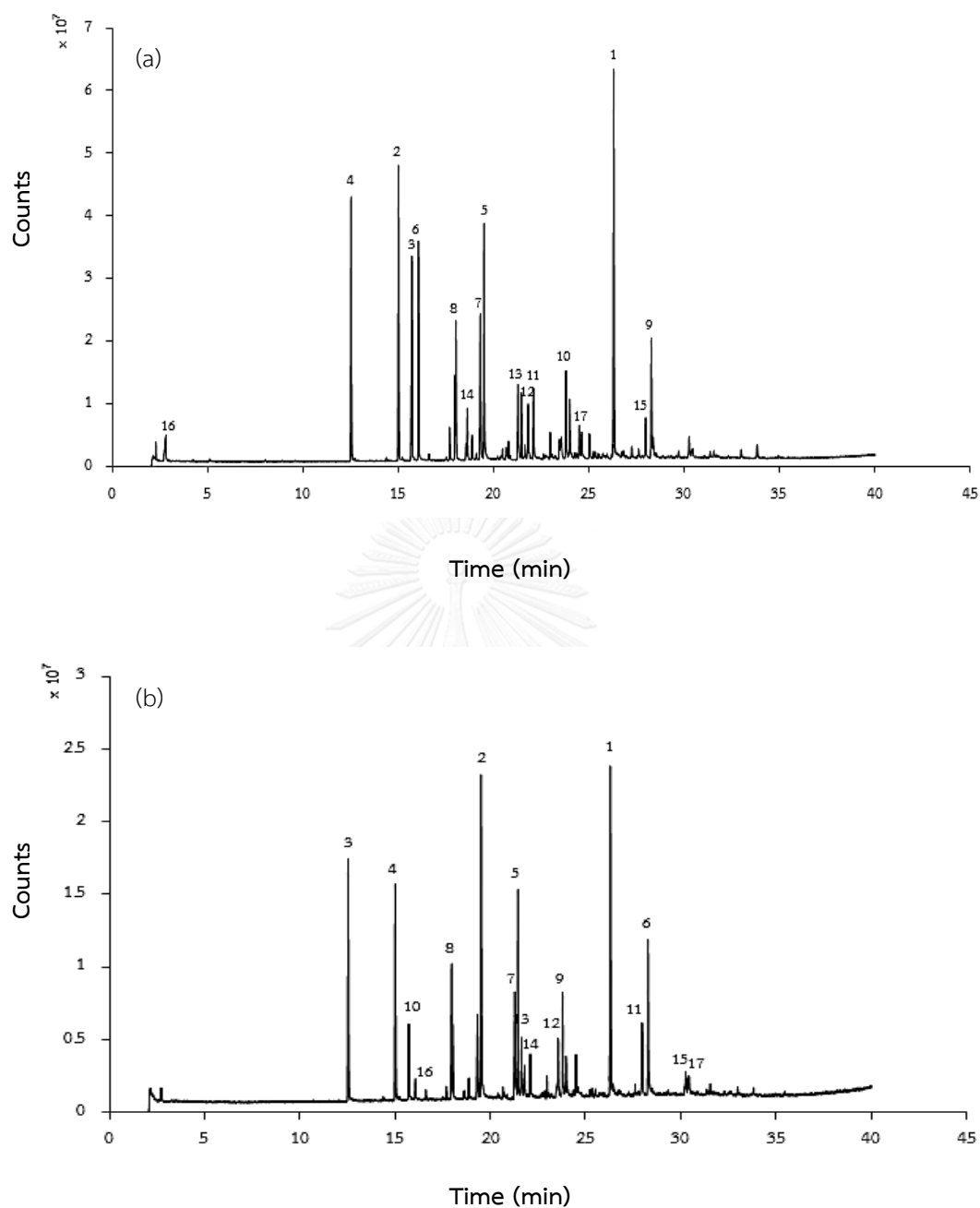


**Figure 4.19** Total ion chromatograms of (a) isolated crude lignin and (b) Klason lignin from pretreated giant sensitive plant catalytic pyrolysis of lignin at 300°C for 30 min, ZSM-5 to lignin ratio of 0.75:1 with 10 g of DI water. Refer to Table 4.15 and Table 4.16 for the names of identified compounds.

#### 4.8.1.3 Isolated crude lignin and Klason lignin from corncob

The catalytic pyrolysis between isolated crude lignin and Klason lignin gave many products as shown in Table 4.17 and Table 4.18.

**Table 4.19** Compound identified by GC-MS in catalytic pyrolysis of isolated crude lignin from corncob.

Peak	Retention time (min)	Compound name	%Selectivity
1	19.5	Catechol	26.6
2	12.5	Phenol	19.3
3	22.1	1,2-Benzenediol, 3-methyl-	10.7
4	15.7	p-Cresol	6.9
5	26.3	1,2,4-Trimethoxybenzene	5.5
6	24.6	4-Ethylcatechol	4.9
7	15.0	Phenol, 2-methyl-	4.6
8	23.8	Phenol, 2,6-dimethoxy-	3.4
9	18.6	Phenol, 3-ethyl-	3.4
10	16.1	Phenol, 2-methoxy-	2.7
11	28.3	5-tert-Butylpyrogallol	2.2
12	23.5	1,3-Benzenediol, 4-ethyl-	1.8
13	23.6	1,4-Benzenediol, 2-methyl-	1.7
14	19.3	Creosol	1.7
15	18.6	Phenol, 4-ethyl-	1.7
16	18.0	Phenol, 3,5-dimethyl-	1.4
17	24.0	3-Amino-2,6-dimethoxy pyridine	1.4

**Table 4.20** Compound identified by GC-MS in catalytic pyrolysis of Klason lignin from corncob.

Peak	Retention time (min)	Compound name	%Selectivity
1	19.5	Catechol	30.3
2	12.5	Phenol	26.8
3	22.1	1,2-Benzenediol, 3-methyl-	6.4
4	23.8	Phenol, 2,6-dimethoxy-	6.1
6	16.1	Phenol, 2-methoxy-	4.4
7	26.3	1,2,4-Trimethoxybenzene	4.0
8	21.8	Phenol, 4-ethyl-2-methoxy-	3.7
9	15.0	Phenol, 2-methyl-	3.3
10	24.6	4-Ethylcatechol	2.5
11	19.3	Creosol	2.3
12	18.6	Phenol, 3-ethyl-	2.0
13	15.7	p-Cresol	1.7
14	28.3	5-tert-Butylpyrogallol	1.7
15	28.0	Butylated Hydroxytoluene	1.3
16	23.6	1,4-Benzenediol, 2-methyl-	1.3
17	30.3	N-[3,5-Dinitropyridine-2-yl]phenylalanine	1.2

The results shown that the various products both isolated crude lignin and Klason lignin from corncob such as catechol, phenol, 1,2-Benzenediol, 3-methyl- and other products. The highest product was found in liquid of both samples were similar result that was catechol as 26.64 and 30.30% (retention time = 19.5 min as shown in Figure 4.20 (a) and (b)). The catechol main product might occur from syringyl lignin unit cracking.

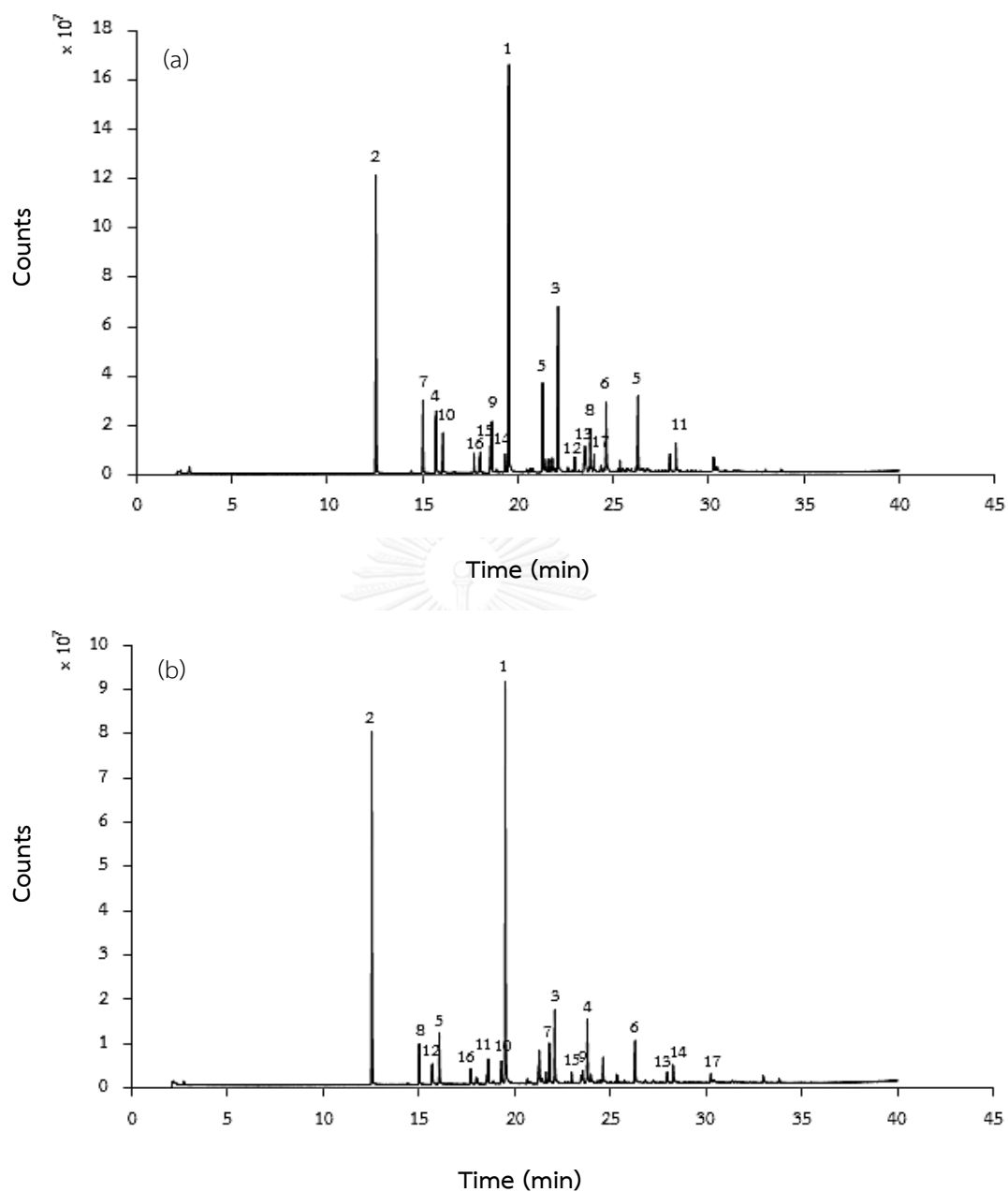


**Figure 4.20** Total ion chromatograms of (a) isolated crude lignin and (b) Klason lignin from corncob catalytic pyrolysis of lignin at 300°C for 30 min, ZSM-5 to lignin ratio of 0.75:1 with 10 g of DI water. Refer to Table 4.17 and Table 4.18 for the names of identified compounds.

#### 4.9 Catechol selectivity from lignin pyrolysis

Catechol is mainly used as an intermediate in pharmaceutical, perfume and food industry. Thus, the part of lignin pyrolysis was focused on catechol selectivity. The result showed in Figure 4.21. The isolated lignin and pure lignin pyrolysis from corncob gave the highest catechol selectivity as 26.6 and 30.3%, respectively. Moreover, the lignin and pure lignin pyrolysis from commercial and pretreated giant sensitive plant gave catechol selectivity as 30.3, 14.3 and 8.9, 4.2%, respectively. This result illustrated that type of lignin affected on catechol selectivity.

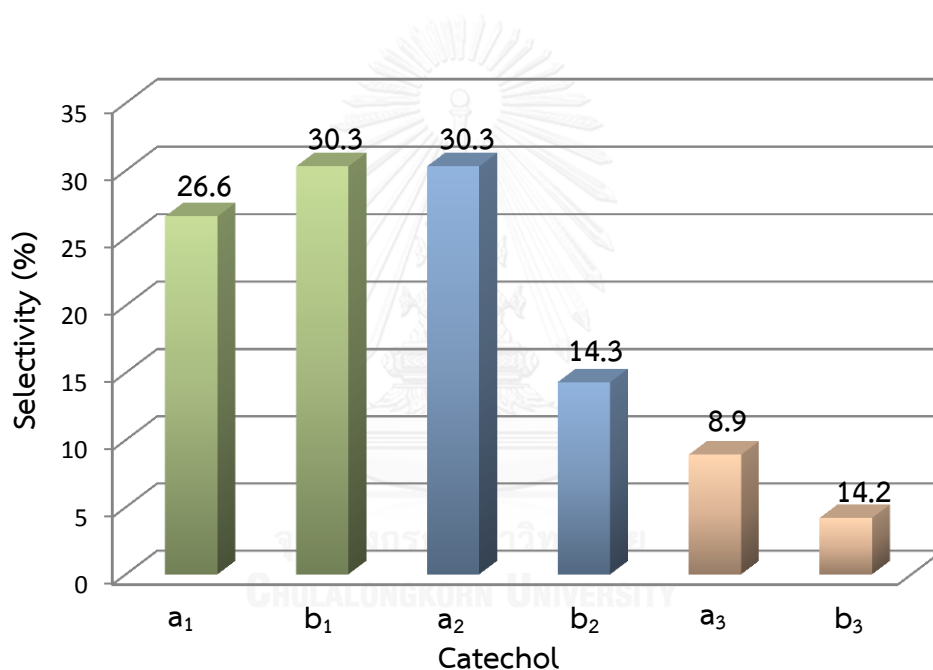


**Figure 4.21** %Selectivity based on peak area of products in liquid obtained by pyrolysis from lignin<sup>a</sup> and pure lignin<sup>b</sup> of corncob, commercial and pretreated giant sensitive plant.

a<sub>1</sub>: catechol from isolated lignin pyrolysis of corncob,

b<sub>1</sub>: catechol from pure lignin pyrolysis of corncob,

a<sub>2</sub>: catechol from lignin pyrolysis of commercial,

b<sub>2</sub>: catechol from pure lignin pyrolysis of commercial,

a<sub>3</sub>: catechol from isolated lignin pyrolysis of pretreated giant sensitive plant,

b<sub>3</sub>: catechol from pure lignin pyrolysis of pretreated giant sensitive plant



## CHAPTER V

### CONCLUSION

From this research, the giant sensitive plant is a hardwood that should be pretreated in order to remove hemicellulose and reduce the crystallinity of cellulose, while corncob was not necessary pretreated due to its softwood nature. The optimum condition for giant sensitive plant pretreatment was refluxing with 1wt% H<sub>2</sub>SO<sub>4</sub> at 100 °C for 8 h that gave the highest isolated crude lignin as 15.67 wt%.

Moreover, the optimum condition for lignin separation was carried out with 0.63: 3 by weight ratio of Amberlyst-15: lignin sample, 80: 20 by volume ratio of ethanol: H<sub>2</sub>O at 200 °C for 30 min. It could be concluded that lignin separation from pretreated giant sensitive plant and corncob with organosolv method, obtained yield of isolated crude lignin as 16.83 wt% and 11.60 wt%, respectively. Then, both samples were purified with Klason lignin method that gave yield of pure lignin as 16.12 wt% and 9.79 wt%, respectively.

The major parameters affected on isolated crude lignin that were reaction temperature, time, solvent ratio and types of catalyst. The catalyst was the most influencing parameter for lignin separation because Amberlyst-15 gave the highest acidity as 4.72 mmol/g. The increased acidity affected to rising isolated crude lignin due to the strong structure of lignin. It was difficult to remove from biomass because the most common linkage was  $\beta$ -O-4 ether bond. When the comparison of isolated crude lignin yield between giant sensitive plant and corncob found that pretreated giant sensitive plant gave isolated crude lignin yield more than corncob due to giant

sensitive plant as hardwood. Generally, the lignin component of hardwood was more than agricultural residue.

The isolated crude lignin and Klason lignin from pretreated giant sensitive plant and corncob were pyrolyzed in a stainless steel autoclave with optimum condition as 0.75: 1: 10 by weight ratio of ZSM-5: lignin sample: H<sub>2</sub>O at 300 °C for 30 min. The result could be concluded that the highest product of commercial lignin and Klason commercial lignin provided the different product selectivity as catechol (30.3 %) and phenol (19.1 %), respectively. On the other hand, isolated crude lignin and Klason lignin from pretreated giant sensitive plant shown the highest similar selectivity product as 1,2,4-trimethoxybenzene (14.5-15.4%). In addition, isolated crude lignin and Klason lignin from corncob gave the highest similar product as selectivity catechol (26.6-30.3%). The different products might be due to the inherent variance among the various chemical structure of lignin that major component of hardwood is syringyl unit, while softwood consisted of *p*-hydroxyphenyl as a main unit. However, commercial lignin was used in this research that was produced from Kraft pulping. It was contaminated with hemicellulose, lead to the different products both commercial lignin and Klason commercial lignin.

### **The suggestions for future work**

The structure of isolated lignin in this research suggested that it can be a valuable source of chemicals. Therefore, in future work should be converted isolated lignin into high-value chemical with lignin oxidation that might give vanillin product. This product is a major flavor constituent of vanilla. It has a wide range of application in food industry (e.g. a flavor agent). In addition, in the future should study the optimum condition for lignin oxidation such as types of catalyst, reaction temperature, time and solvent that may affect to vanillin yield.



## REFERENCES

- [1] Devi, L., Ptasiński, K.J., and Janssen, F.J.J.G. A review of the primary measures for tar elimination in biomass gasification processes. Biomass and Bioenergy 24(2) (2003): 125-140.
- [2] Saxena, R.C., Seal, D., Kumar, S., and Goyal, H.B. Thermo-chemical routes for hydrogen rich gas from biomass: A review. Renewable and Sustainable Energy Reviews 12(7) (2008): 1909-1927.
- [3] Suwannakhanthi, N. overview for thailand's renewable energy focusing on biomass energy. Department of alternative energy development and efficiency, 2004.
- [4] Boudet, A.-M. Lignins and lignification: Selected issues. Plant Physiology and Biochemistry 38(1–2) (2000): 81-96.
- [5] Khokhar, Z.-U., Syed, Q., Nadeem, M., Baig, S., Irfan, M., Gull, I., Tipu, I., Aslam, S., Samra, Z.Q., and Athar, M.A. Delignification of Wheat Straw with Acid and Hydro-Steam under Pressure. World Applied Sciences Journal 11(12) (2010): 1524-1530.
- [6] Obama, P., Ricochon, G., Muniglia, L., and Brosse, N. Combination of enzymatic hydrolysis and ethanol organosolv pretreatments: Effect on lignin structures, delignification yields and cellulose-to-glucose conversion. Bioresource Technology 112 (2012): 156-163.
- [7] El Hage, R., Brosse, N., Sannigrahi, P., and Ragauskas, A. Effects of process severity on the chemical structure of Miscanthus ethanol organosolv lignin. Polymer Degradation and Stability 95(6) (2010): 997-1003.
- [8] Kadam, S.T., Thirupathi, P., and Kim, S.S. Amberlyst-15: an efficient and reusable catalyst for the Friedel–Crafts reactions of activated arenes and heteroarenes with  $\alpha$ -amido sulfones. Tetrahedron 65(50) (2009): 10383-10389.

- [9] Park, Y.-M., et al. Esterification of used vegetable oils using the heterogeneous WO<sub>3</sub>/ZrO<sub>2</sub> catalyst for production of biodiesel. Bioresource Technology 101(1, Supplement) (2010): S59-S61.
- [10] Tadesse, H., and Luque, R. Advances on biomass pretreatment using ionic liquids: An overview. Energy and Environmental Science. 4(10) (2011): 3913-3929.
- [11] Nantapipat, J., Luengnaruemitchai, A., and Wongkasemjit, S. A Comparison of Dilute Sulfuric and Phosphoric Acid Pretreatments in Biofuel Production from Corncobs World Academy of Science, Engineering and Technology 7(4) (2013): 477-481.
- [12] El Hage, R., Brosse, N., Chrusciel, L., Sanchez, C., Sannigrahi, P., and Ragauskas, A. Characterization of milled wood lignin and ethanol organosolv lignin from miscanthus. Polymer Degradation and Stability 94(10) (2009): 1632-1638.
- [13] Sannigrahi, P., Ragauskas, A.J., and Miller, S.J. Lignin Structural Modifications Resulting from Ethanol Organosolv Treatment of Loblolly Pine. Energy Fuels 24 (2010): 683-689.
- [14] Hallac, B.B., Pu, Y., and Ragauskas, A.J. Chemical Transformations of *Buddleja davidii* Lignin during Ethanol Organosolv Pretreatment. Energy Fuels 24 (2010): 2723-2732.
- [15] Ye, Y., Zhang, Y., Fan, J., and Chang, J. Selective production of 4-ethylphenolics from lignin via mild hydrogenolysis. Bioresource Technology 118 (2012): 648-651.
- [16] Huber, G.W. and Dumesic, J.A. An overview of aqueous-phase catalytic processes for production of hydrogen and alkanes in a biorefinery. Catalysis Today 111(1-2) (2006): 119-132.
- [17] He, Y., Pang, Y., Liu, Y., Li, X., and Wang, K. Physicochemical Characterization of Rice Straw Pretreated with Sodium Hydroxide in the Solid State for Enhancing Biogas Production. Energy & Fuels 22 (2008): 2775-2781.
- [18] Han, Y.W., Catalano, E.A., and Ciegler, A. . Chemical and Physical Properties of Sugarcane Bagasse Irradiated with  $\gamma$  Rays Journal of Agricultural and Food Chemistry 31 (1983): 34-38.

- [19] Ateş, F. and Işıkdağ, M.A. Influence of temperature and alumina catalyst on pyrolysis of corncob. Fuel 88(10) (2009): 1991-1997.
- [20] Goering, H.K., and Soest, P.J.V. FORAGE FIBER ANALYSES (Apparatus, Reagents, Procedures, and Some Applications). U. S. Government Printing Office, 1970.
- [21] Wild, P., Reitha, H., and Heeresb, E. Biomass pyrolysis for chemicals. Biofuels 2(2) (2011): 185-208.
- [22] Mohan, D., Pittman, C.U., and Steele, P.H. Pyrolysis of Wood/Biomass for Bio-oil: A Critical Review. Energy & Fuels 20 (2006): 848-889.
- [23] Turner, M.B., Spear, S.K., Holbrey, J.D., and Rogers, R.D. Production of bioactive cellulose films reconstituted from ionic liquids. Biomacromolecules 5(4) (2004): 1379-1384.
- [24] Swatloski, R.P., Spear, S.K., Holbrey, J.D., and Rogers, R.D. Dissolution of Cellose with Ionic Liquids. Journal of the American Chemical Society 124(18) (2002): 4974-4975.
- [25] Folch-Mallol, J.L., and Quiroz-Castañeda, R.E. Plant cell wall degrading and remodeling proteins:  
current perspectives Biotechnologia Aplicada 28 (2011): 205-215.
- [26] Boerjan, W., Ralph, J., and Baucher, M. Lignin Biosynthesis. Annual Review of Plant Biology 54 (2003): 519-546.
- [27] Chabannes, M., Ruel, K., Yoshinaga, A., Chabbert, B., Jauneau, A., Joseleau, J.P., and Boudet, A.M. In situ analysis of lignins in transgenic tobacco reveals a differential impact of individual transformations on the spatial patterns of lignin deposition at the cellular and subcellular levels. The Plant Journal 28(3) (2001): 271-282.
- [28] Zakzeski, J., Bruijninx, P.C.A., Jongerius, A.L., and Weckhuysen, B.M. The Catalytic Valorization of Lignin for the Production of Renewable Chemicals. Chemical Reviews 110 (2010): 3552-3599.
- [29] Hossain, M.M., and Aldous, L. Ionic Liquid for Lignin Processing: Dissolution, Isolation, and Conversion. Australian Journal of Chemistry 65 (2012): 1465-1477.

- [30] Lange, H., Decina, S., and Crestini, C. Oxidative upgrade of lignin – Recent routes reviewed. European Polymer Journal 49(6) (2013): 1151-1173.
- [31] Chaula, Z., Said, M., John, G., Manyele, S., and Mhilu, C. Modelling the Suitability of Pine Sawdust for Energy Production via Biomass Steam Explosion. Smart Grid and Renewable Energy 5 (2014): 1-7.
- [32] Agbor, V.B., Cicek, N., Sparling, R., Berlin, A., and Levin, D.B. Biomass pretreatment: Fundamentals toward application. Biotechnology Advances 29(6) (2011): 675-685.
- [33] Bensah, E.C., and Mensah, M. Chemical Pretreatment Methods for the Production of Cellulosic Ethanol: Technologies and Innovations. International Journal of Chemical Engineering 2013 (2013): 1-21.
- [34] Liu, Z.-S., Wu, X.-L., Kida, K., and Tang, Y.-Q. Corn stover saccharification with concentrated sulfuric acid: Effects of saccharification conditions on sugar recovery and by-product generation. Bioresource Technology 119 (2012): 224-233.
- [35] Zainudin, M.H.M., Rahman, N.A.A., Abd-Aziz1, S., Funaoka, M., Shinano, T., Shirai, Y., Wakisaka, M., and Hassan, M.A. Utilization of Glucose Recovered by Phase Separation System from Acid-hydrolysed Oil Palm Empty Fruit Bunch for Bioethanol Production. Pertanika Journal of Tropical Agricultural Science 35(1) (2012): 117–126.
- [36] Menon, V. and Rao, M. Trends in bioconversion of lignocellulose: Biofuels, platform chemicals & biorefinery concept. Progress in Energy and Combustion Science (2012).
- [37] Xu, J., Zhang, X., and Cheng, J.J. Pretreatment of corn stover for sugar production with switchgrass-derived black liquor. Bioresource Technology 111 (2012): 255-260.
- [38] Tutt, M., Kikas, T., and Olt, J. COMPARISON OF DIFFERENT PRETREATMENT METHODS ON DEGRADATION OF RYE STRAW. ENGINEERING FOR RURAL DEVELOPMENT 24 (2012): 412-416.
- [39] Sun, Y. and Cheng, J. Hydrolysis of lignocellulosic materials for ethanol production: a review. Bioresource Technology 83(1) (2002): 1-11.

- [40] Chum, H.L., Johnson, D.K., Black, S., Baker, J., Grohmann, K., Sarkanen, K.V., Wallace, K., and Schroeder, H.A. Organosolv pretreatment for enzymatic hydrolysis of poplars: I. Enzyme hydrolysis of cellulosic residues. Biotechnology and Bioengineering 31 (1988): 643– 649.
- [41] Thring, R.W., Chornet, E., and Overend, R.P. Recovery of a solvolytic lignin: Effects of spent liquor/acid volume ratio, acid concentration and temperature. Biomass 23(4) (1990): 289-305.
- [42] Guragain, Y.N., De Coninck, J., Husson, F., Durand, A., and Rakshit, S.K. Comparison of some new pretreatment methods for second generation bioethanol production from wheat straw and water hyacinth. Bioresource Technology 102(6) (2011): 4416-4424.
- [43] Kim, J.-Y., et al. Structural features of lignin macromolecules extracted with ionic liquid from poplar wood. Bioresource Technology 102(19) (2011): 9020-9025.
- [44] Sun, Y.-C., Xu, J.-K., Xu, F., and Sun, R.-C. Efficient separation and physico-chemical characterization of lignin from eucalyptus using ionic liquid–organic solvent and alkaline ethanol solvent. Industrial Crops and Products 47 (2013): 277-285.
- [45] Long, J., Li, X., Guo, B., Wang, L., and Zhang, N. Catalytic delignification of sugarcane bagasse in the presence of acidic ionic liquids. Catalysis Today 200 (2013): 99-105.
- [46] Hendriks, A.T.W.M. and Zeeman, G. Pretreatments to enhance the digestibility of lignocellulosic biomass. Bioresource Technology 100(1) (2008): 10-18.
- [47] Ricardo B. Santos, P.H., Hasan Jameel and Hou-min Chang. Wood Based Lignin Reactions Important to the Biorefinery and Pulp and Paper Industries BioResources [Online]. 2013.
- [48] Gierer, J., and Noren, I. Reaction of lignin on sulfate digestion. II. Model experiments on the cleavage of aryl alkyl ethers by alkali. Acta Chemica Scandinavica 16 (1962): 1713-1729.

- [49] Bardet, M., Robert, D.R., and Lundquist, K. On the reactions and degradation of the lignin during steam hydrolysis of aspen wood. Svensk Papperstidn 88(6) (1985): 61-67.
- [50] Lower, S. Catalysts reduce activation energy [Online]. 2015. Available from: [http://chemwiki.ucdavis.edu/Physical\\_Chemistry/Kinetics/Complex\\_Reactions/Catalysis/Catalysts](http://chemwiki.ucdavis.edu/Physical_Chemistry/Kinetics/Complex_Reactions/Catalysis/Catalysts) [October 15]
- [51] Hagen, J. Industrial Catalysis, A Practical Approach. Wiley-VCH, Weinheim, 1999.
- [52] Kaneko, K. Determination of pore size and pore size distribution: 1. Adsorbents and catalysts. Journal of Membrane Science 96(1-2) (1994): 59-89.
- [53] Flanigen, E.M. Chapter 2 Zeolites and Molecular Sieves an Historical Perspective. in H. van Bekkum, E.M.F. and Jansen, J.C. (eds.), Studies in Surface Science and Catalysis, pp. 13-34: Elsevier, 1991.
- [54] Karmen Margeta, N.a.Z.L., Mario Šiljeg and Anamarija Farkas. Natural Zeolites in Water Treatment – How Effective is Their Use [Online]. 2013. Available from: <http://www.intechopen.com/books/water-treatment/natural-zeolites-in-water-treatment-how-effective-is-their-use> [October 20]
- [55] Scott M. Auerbach, K.A.C.a.P.K.D. ZEOLITE SCIENCE AND TECHNOLOGY. Marcel Dekker.
- [56] Mbaraka, I.K., Radu, D.R., Lin, V.S.Y., and Shanks, B.H. Organosulfonic acid-functionalized mesoporous silicas for the esterification of fatty acid. Journal of Catalysis 219(2) (2003): 329-336.
- [57] Zeolite [Online]. Available from: <http://www.ebah.com.br/content/ABAAAfAJIAL/handbook-of-zeolite?part=5> [October 27]
- [58] Newsam, J.M., Treacy, M.M.J., Koetsier, W.T., and Gruyter, C.B.D. Structural Characterization of Zeolite Beta. London: The Royal Society 420 (1988): 375-405.
- [59] Luan, Z., Hartmann, M., Zhao, D., Zhou, W., and Kevan, L. . Alumination and Ion Exchange of Mesoporous SBA-15 Molecular Sieves. Chemistry of Materials 11(6) (1999): 1621-1627.

- [60] Beck, J.S., Vartuli, J.C., Roth, W.J., Leonowicz, M.E., Kresge, C.T., Schmitt, K.D., Chu, C.T.W., Olson, D.H., and Sheppard, E.W. . A new family of mesoporous molecular sieves prepared with liquid crystal templates. Journal of the American Chemical Society 114(27) (1992): 10834–10843.
- [61] Soler-Illia, G.J.d.A.A., Crepaldi, E.L., Grosso, D., and Sanchez, C. Block copolymer-templated mesoporous oxides. Current Opinion in Colloid & Interface Science 8(1) (2003): 109-126.
- [62] Pal, R., Sarkar, T., and Khasnobis, S. Amberlyst-15 in organic synthesis. ARKIVOC (2012): 570-609.
- [63] Moore, U.E.a.E.A. SOLID STATE CHEMISTRY AN INTRODUCTION, ed. 4. New York: CRC Press Taylor & Francis Group, 2005.
- [64] Wostrack, A., Driessen, H., and Tickle, I. Bragg's Law [Online]. Available from: [http://sbio.uct.ac.za/online\\_content/MSD-UCT/diffract/bragg.htm](http://sbio.uct.ac.za/online_content/MSD-UCT/diffract/bragg.htm) [24 October]
- [65] Balbuena, P.B., and Gubbins, K.E. Theoretical interpretation of adsorption behavior of simple fluids in slit pores. Langmuir 9(7) (1993): 1801–1814.
- [66] Sing, K.S.W., Everett, D.H, Haul, R.A.W., Moscou, L., Pierotti, R.A., Rouquerol, J., and Siemieniewska, T. Reporting physisorption data for gas/solid systems with special reference to the determination of surface area and porosity Pure and Applied Chemistry 57(4) (1985): 603-619.
- [67] Batsala, M., Chandu, B., Sakala, B., Nama, S., and Domatoti, S. INDUCTIVELY COUPLED PLASMA MASS SPECTROMETRY (ICP-MS). INTERNATIONAL JOURNAL OF RESEARCH IN PHARMACY AND CHEMISTRY 2(3) (2012): 671-680.
- [68] School of Earth, A.a.E.S. ICP-MS [Online]. Available from: <http://www.seaes.manchester.ac.uk/our-research/facilities/geochemistry/equipmentandfacilities/icp-ms/instrumentdescriptionandtheory/> [24 October]
- [69] Heda, N. Spectrophotometry - IR Spectroscopy - Instrumentation [Online]. 2014. Available from: [http://namrataheda.blogspot.com/2014/01/spectrophotometry-ir-spectroscopy\\_30.html](http://namrataheda.blogspot.com/2014/01/spectrophotometry-ir-spectroscopy_30.html) [24 October]

- [70] Focosi, D. MICROSCOPY [Online]. 2014. Available from: [http://www.ufrgs.br/imunovet/molecular\\_immunology/microscopy.html](http://www.ufrgs.br/imunovet/molecular_immunology/microscopy.html) [October 27]
- [71] Pu, Y., Hallac, B., and Ragauskas, A.J. Plant Biomass Characterization: Application of Solution-and Solid-state NMR Spectroscopy. in Aqueous Pretreatment of Plant Biomass for Biological and Chemical Conversion to Fuels and Chemicals, pp. 370-390: John Wiley & Sons, Ltd., 2013.
- [72] Zhao, D., Feng, J., Huo, Q., Melosh, N., Fredrickson, G.H., Chmelka, B.F., and Stucky, G.D. Triblock Copolymer Syntheses of Mesoporous Silica with Periodic 50 to 300 Angstrom Pores. Science 297 (1998): 548-552.
- [73] Ooi, Y.-S. and Bhatia, S. Aluminum-containing SBA-15 as cracking catalyst for the production of biofuel from waste used palm oil. Microporous and Mesoporous Materials 102(1-3) (2007): 310-317.
- [74] Hermida, L., Abdullah, A.Z., and Mohamed, A.R. Effects of functionalization conditions of sulfonic acid grafted SBA-15 on catalytic activity in the esterification of glycerol to monoglyceride: a factorial design approach. Journal of Porous Materials 19(5) (2012): 835-846.
- [75] Eswaramoorthi, I. and Dalai, A.K. Synthesis, characterisation and catalytic performance of boron substituted SBA-15 molecular sieves. Microporous and Mesoporous Materials 93(1-3) (2006): 1-11.
- [76] Chupas, P.J. and Grey, C.P. Surface modification of fluorinated aluminas: Application of solid state NMR spectroscopy to the study of acidity and surface structure. Journal of Catalysis 224(1) (2004): 69-79.
- [77] Bian, J., Peng, F., Xu, F., Sun, R.-C., and Kennedy, J.F. Fractional isolation and structural characterization of hemicelluloses from *Caragana korshinskii*. Carbohydrate Polymers 80(3) (2010): 753-760.
- [78] Jasiukaitytė, E., Kunaver, M., and Strlič, M. Cellulose liquefaction in acidified ethylene glycol. Cellulose 16 (2009): 393-405.
- [79] Tejado, A., Peña, C., Labidi, J., Echeverria, J.M., and Mondragon, I. Physico-chemical characterization of lignins from different sources for use in phenol-



- formaldehyde resin synthesis. Bioresource Technology 98(8) (2007): 1655-1663.
- [80] Sun, R.C., Fang, J.M., and Tomkinson, J. Delignification of rye straw using hydrogen peroxide. Industrial Crops and Products 12(2) (2000): 71-83.
- [81] SABERIKHAH, E., MOHAMMADI-ROVSHANDEH, J., and MAMAGHANI, M. . SPECTROSCOPIC COMPARISON OF ORGANOSOLV LIGNINS ISOLATED FROM WHEAT STRAW. CELLULOSE CHEMISTRY AND TECHNOLOGY 47 (2013): 409-418.
- [82] MAO, J.Z., ZHANG, L.M. and XU, F. . FRACTIONAL AND STRUCTURAL CHARACTERIZATION OF ALKALINE LIGNINS FROM CAREX MEYERIANA KUNTH. CELLULOSE CHEMISTRY AND TECHNOLOGY 46 (2012): 193-205.
- [83] Osichow, A., and Mecking, S. Alkoxyacylation of Ethylene with Cellulose in Ionic Liquids. Chemical Communications 46 (2010): 4980–4981.
- [84] G. J. Leary, R.H.N. Cross Polarization/Magic Angle Spinning Nuclear Magnetic Resonance (CP/MAS NMR) Spectroscopy. Springer-Verlag, Berlin, 1992.
- [85] Oliveiraa, R.L., Vieirab, J.G., Baruda, H.S., Assunçãoc, R.M.N., Filhob, G.R., Ribeiroa, S.J.L., and Messadeqqa, Y. Synthesis and Characterization of Methylcellulose Produced from Bacterial Cellulose under Heterogeneous Condition. Journal of the Brazilian Chemical Society 26(9) (2015): 1861-1870.
- [86] Cao, Q., Xie, K.-C., Bao, W.-R., and Shen, S.-G. Pyrolytic behavior of waste corn cob. Bioresource Technology 94(1) (2004): 83-89.
- [87] Mansouri, N.E.E., Yuan, Q., and Huang, F. SYNTHESIS AND CHARACTERIZATION OF KRAFT LIGNIN-BASED EPOXY RESINS. BioResources 6(3) (2011): BioResources



A. Determine component of giant sensitive plant with TAPPI test method

T 222 om-88

1.1 Neutral detergent fiber (NDF)

$$\% \text{ of NDF} = \frac{(W_n - W_t)(100)}{S} \quad (\text{A-1})$$

$W_n$  = weight of oven-dry crucible including fiber

$W_t$  = tared weight of oven-dry crucible

$S$  = oven-dry sample weight

1.2 Acid detergent fiber (ADF)

$$\% \text{ADF} = \frac{(W_a - W_t)(100)}{S} \quad (\text{A-2})$$

$$\% \text{hemicellulose} = \frac{(\% \text{NDF} - \% \text{ADF})(100)}{S} \quad (\text{A-3})$$

$W_a$  = weight of residue through extraction with acid detergent fiber

$W_t$  = tared weight of oven-dry crucible

$S$  = oven-dry sample weight

1.3 Permanganate detergent (PML)

$$\% \text{lignin} = \frac{(W_a - W_p)(100)}{S} \quad (\text{A-4})$$

$W_a$  = weight of residue through extraction with acid detergent fiber

$W_p$  = weight of residue through extraction with permanganate detergent

$S$  = oven-dry sample weight

#### 1.4 Analysis of cellulose

$$\% \text{cellulose} = \frac{(W_p - W_c)(100)}{S} \quad (\text{A-5})$$

$W_p$  = weight of residue through extraction with permanganate detergent

$W_c$  = weight of crucible through calcination

$S$  = oven-dry sample weight

#### B. Determine isolated crude lignin

$$\% \text{isolated crude lignin} = \frac{(M - N)(100)}{X} \quad (\text{B-1})$$

$M$  = crude lignin + filter paper

$N$  = weight of filter paper

$X$  = oven-dry raw biomass

#### C. Determine pure isolated lignin with Klason method

$$\% \text{Klason lignin} = \frac{(A)(100)}{W} \quad (\text{C-1})$$

$A$  = weight of Klason lignin

$W$  = oven-dried weigh of biomass

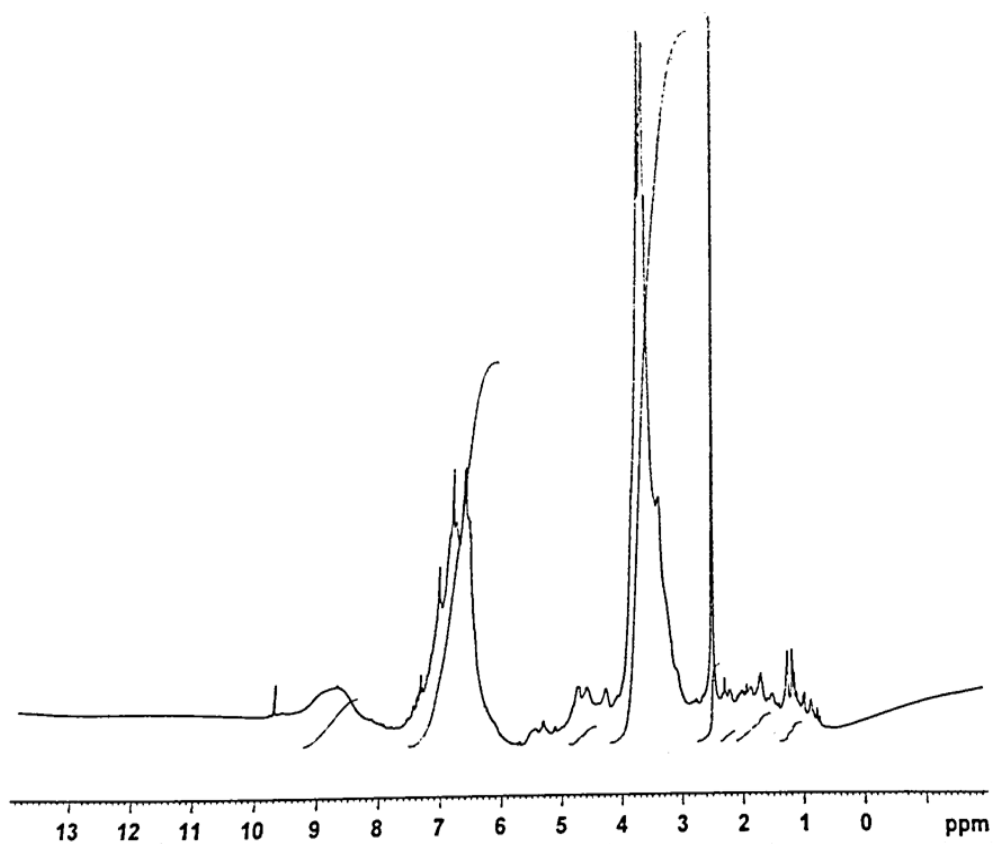


Figure D-1  $^1\text{H}$  NMR spectrums of crude lignin from commercial.

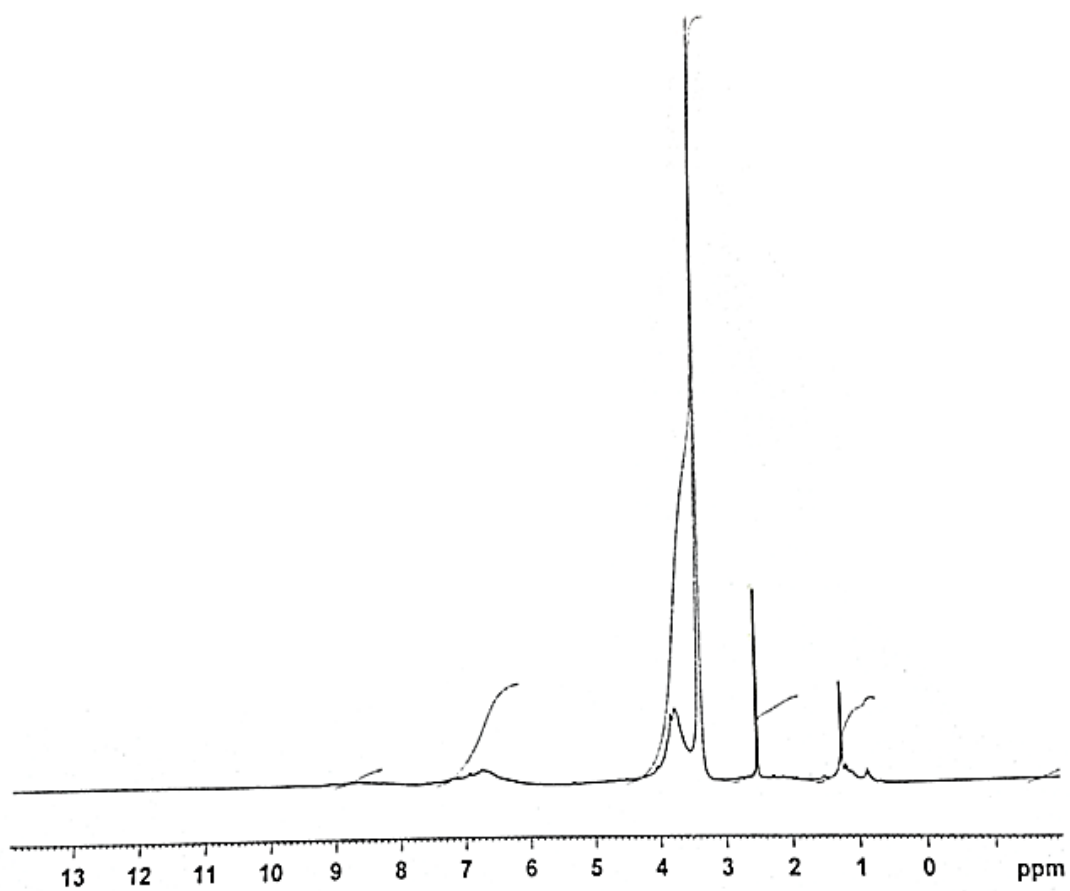


Figure D-2  $^1\text{H}$  NMR spectrums of crude lignin from pretreated giant sensitive plant.

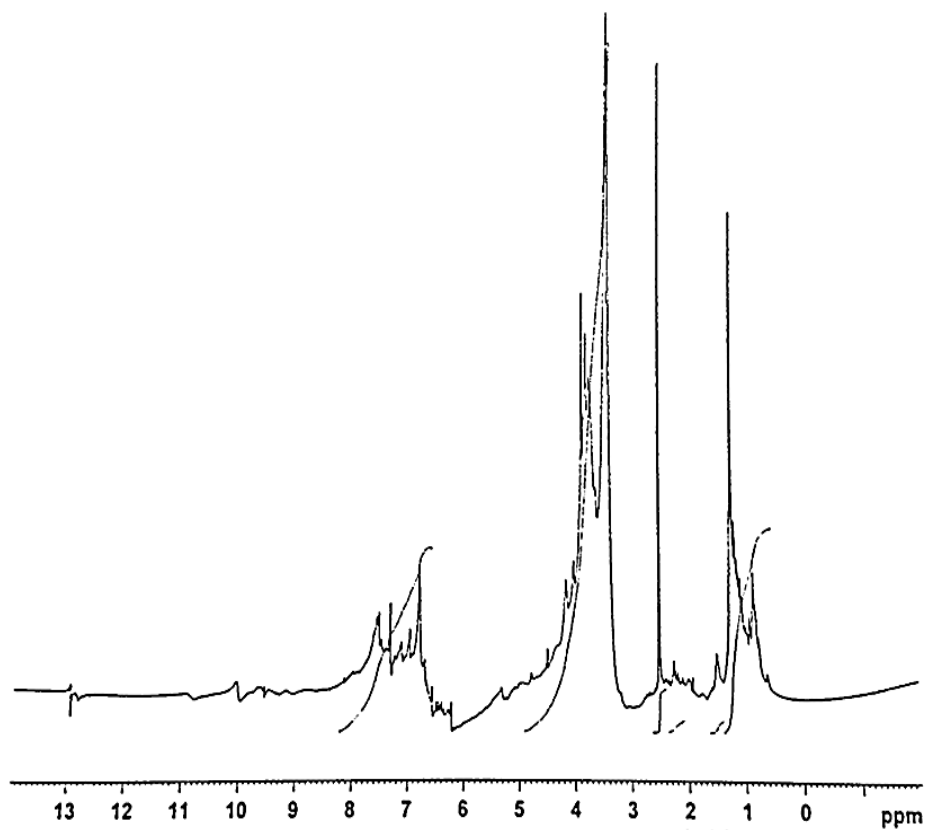


Figure D-3  $^1\text{H}$  NMR spectrums of crude lignin from corncob.

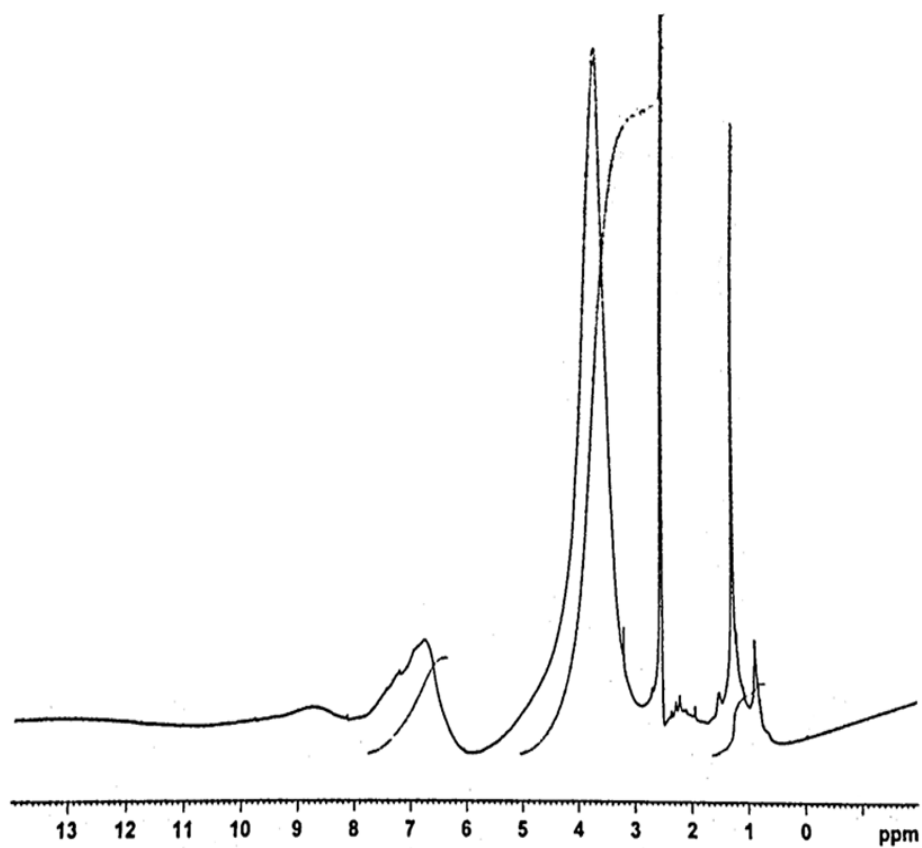


Figure D-4  $^1\text{H}$  NMR spectrums of Klason lignin from pretreated giant sensitive plant.



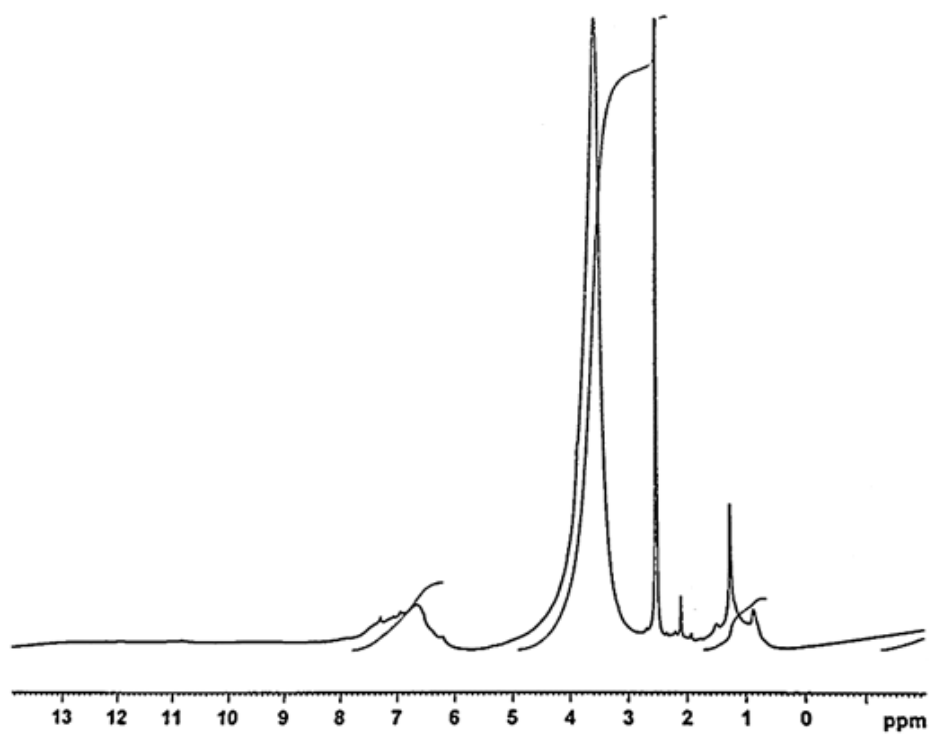


Figure D-5  $^1\text{H}$  NMR spectrums of Klason lignin from corncob.



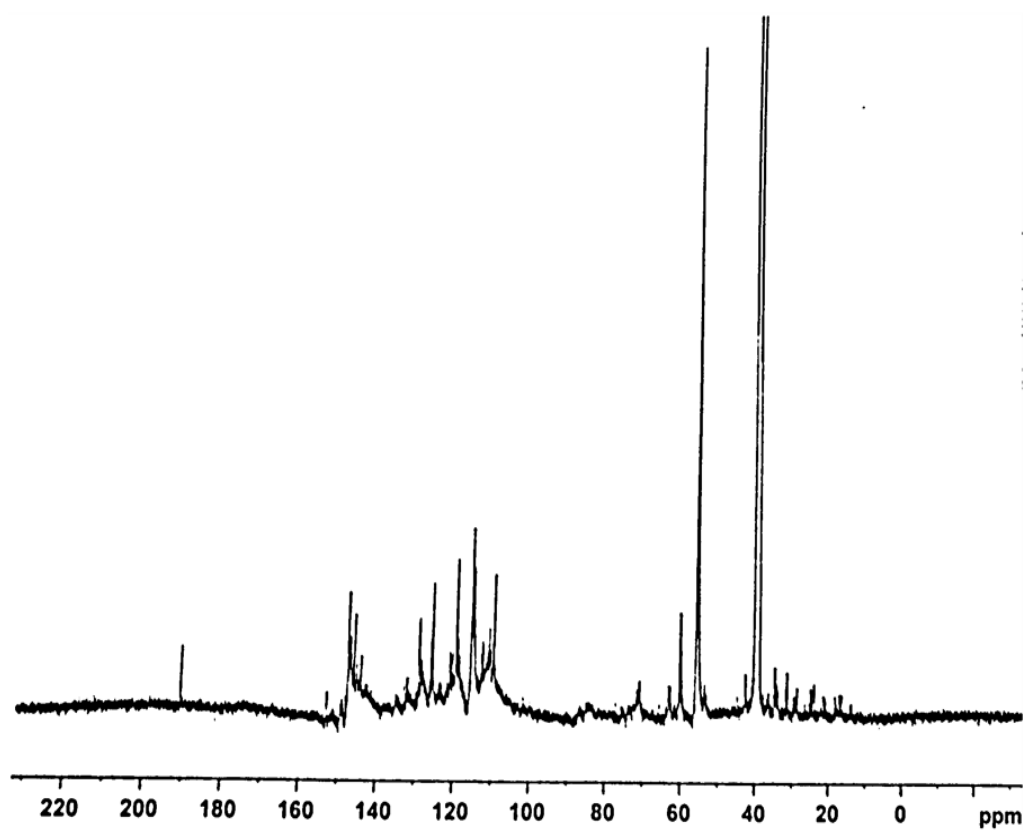


Figure D-6  $^{13}\text{C}$  NMR spectrums of crude lignin from commercial.

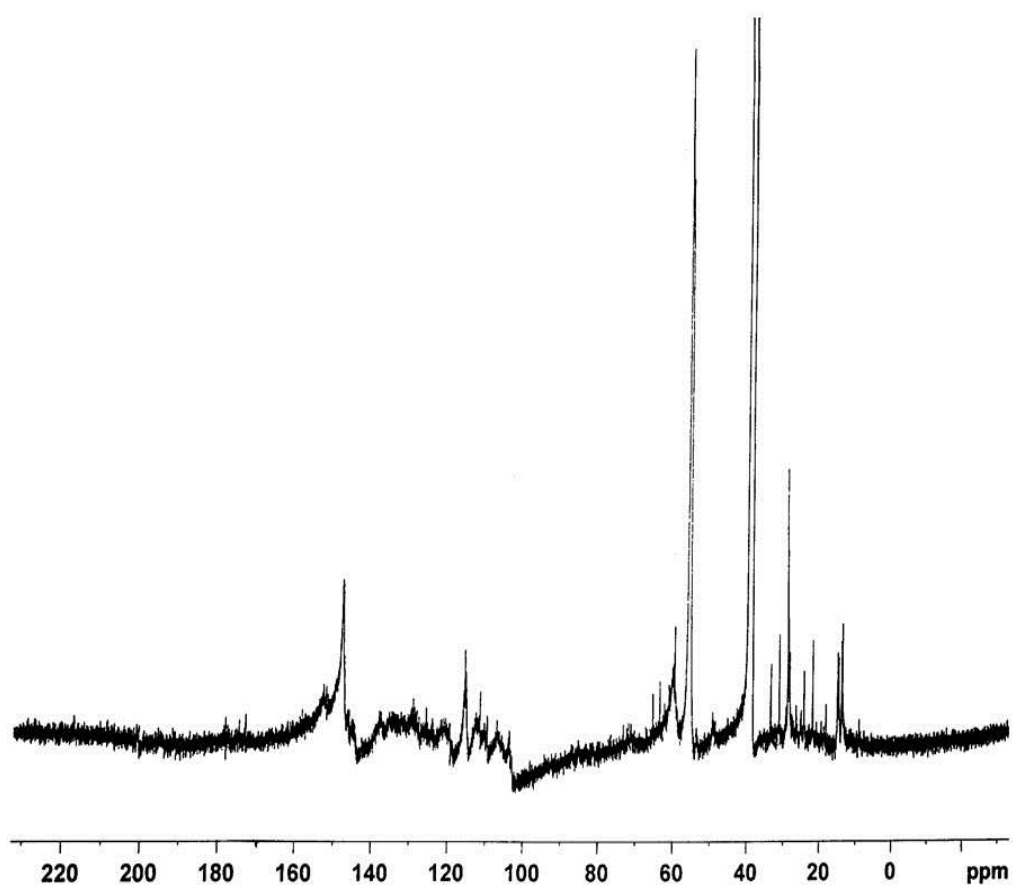


Figure D-7  $^{13}\text{C}$  NMR spectrums of crude lignin from pretreated giant sensitive plant.

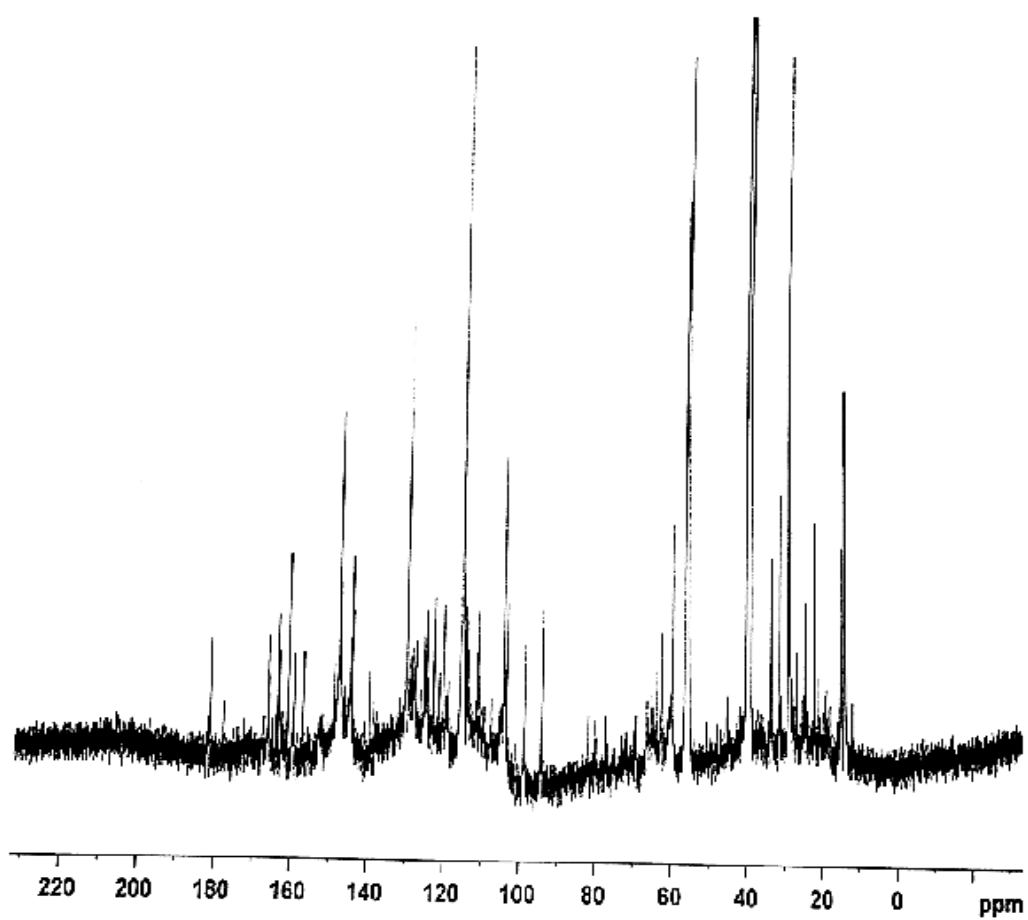


Figure D-8  $^{13}\text{C}$  NMR spectrums of crude lignin from corncob.

CHULALONGKORN UNIVERSITY

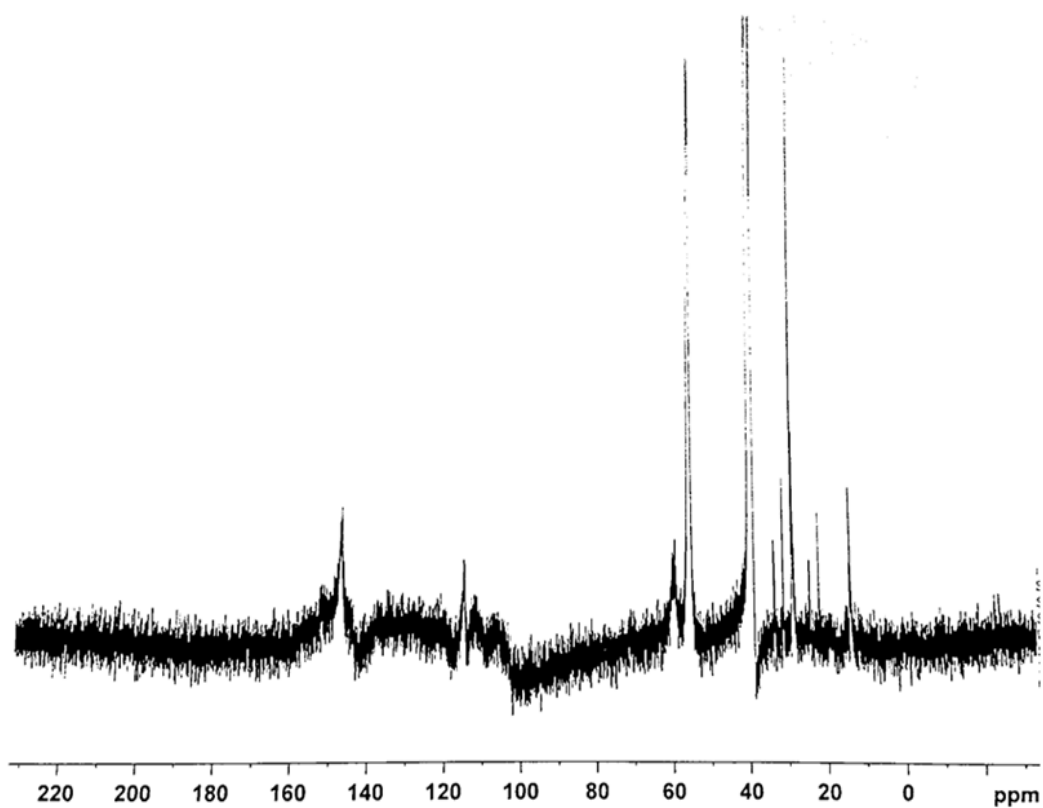


Figure D-9  $^{13}\text{C}$  NMR spectrums of Klason lignin from pretreated giant sensitive plant.

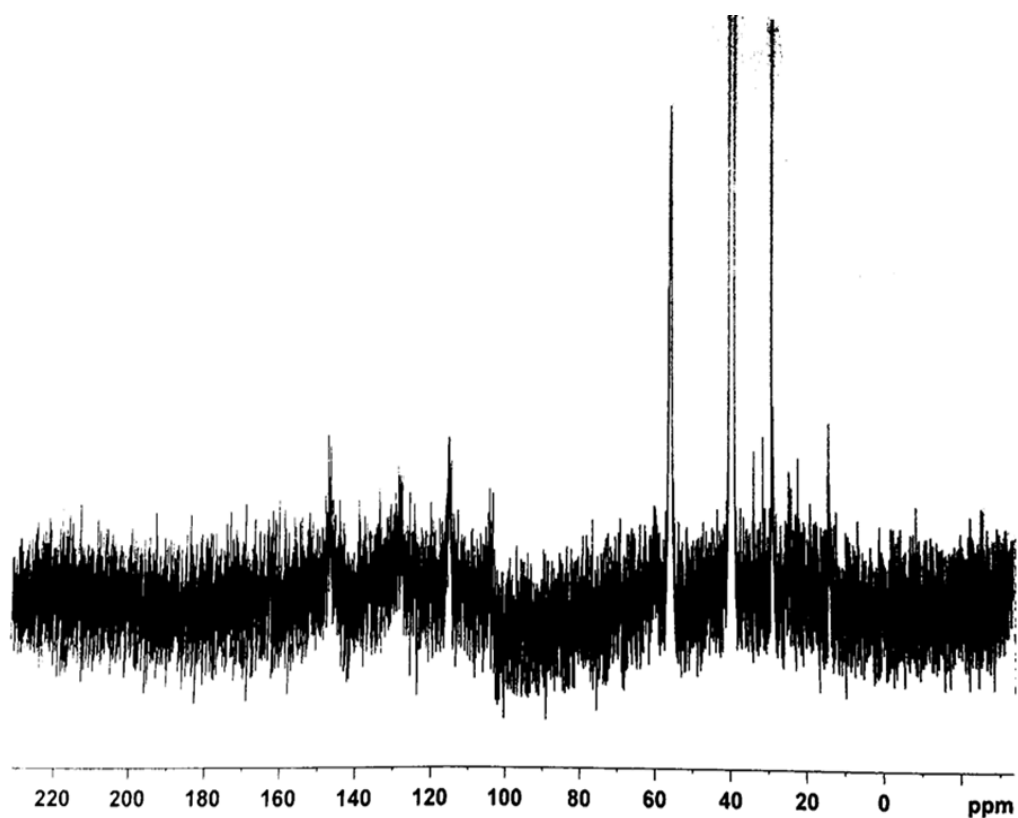


Figure D-10  $^{13}\text{C}$  NMR spectrums of Klason lignin from corncob.



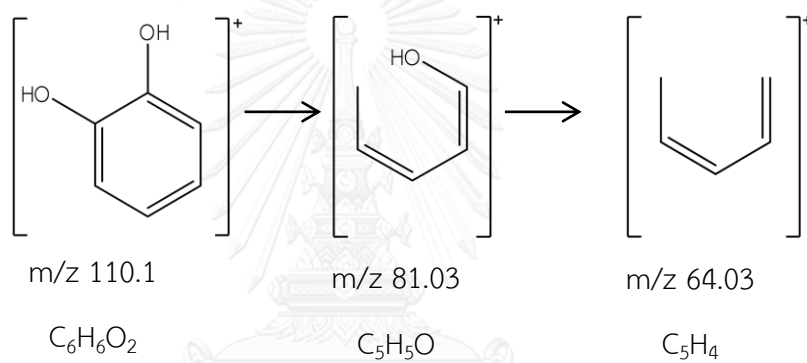
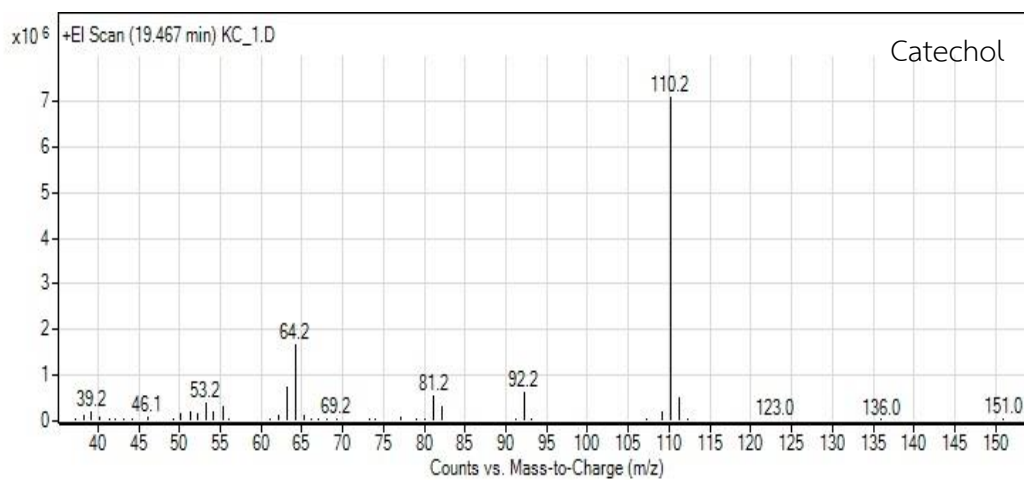


Figure E-1 Mass spectra of catechol.

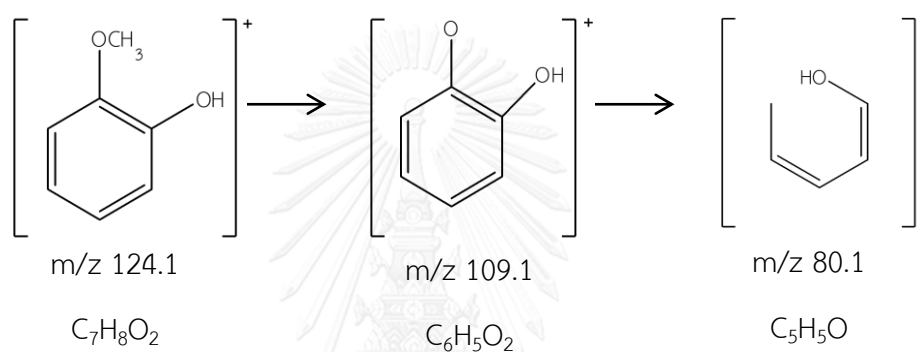
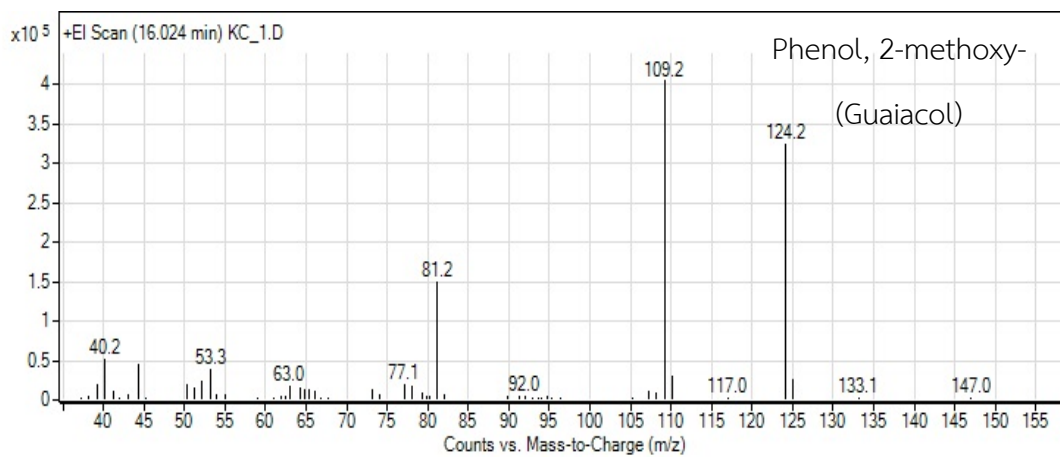


Figure E-2 Mass spectra of guaiacol.



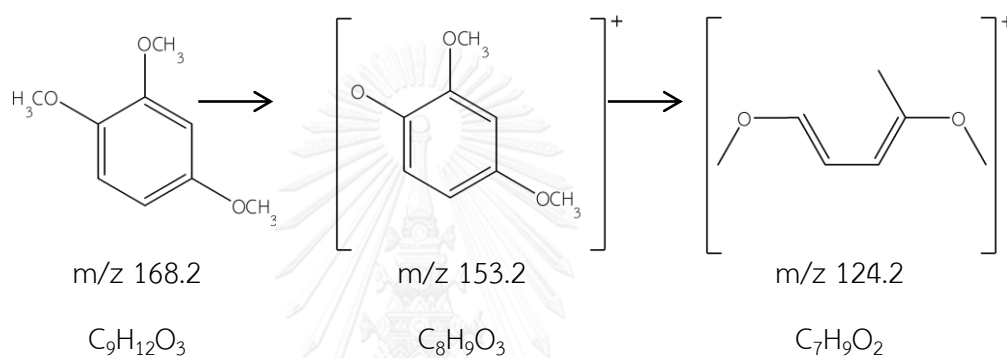
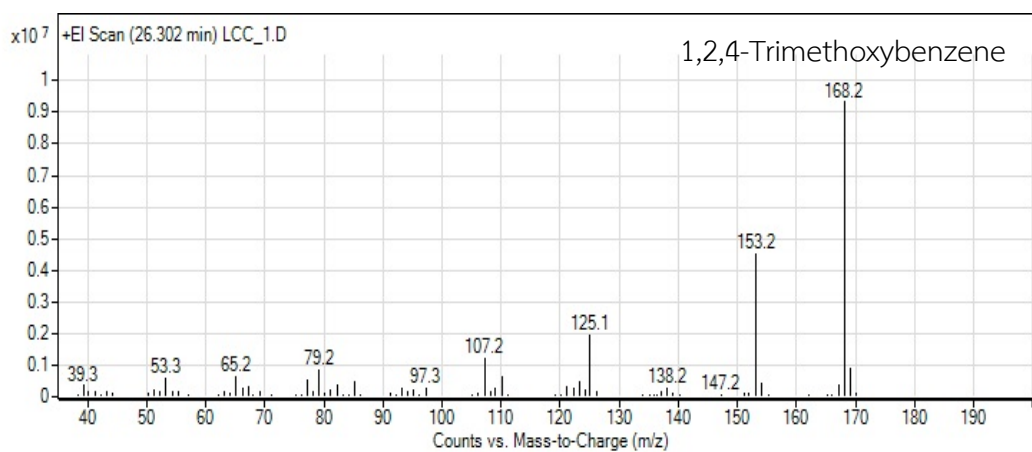


Figure E-3 Mass spectra of 1,2,4-trimethoxybenzene.

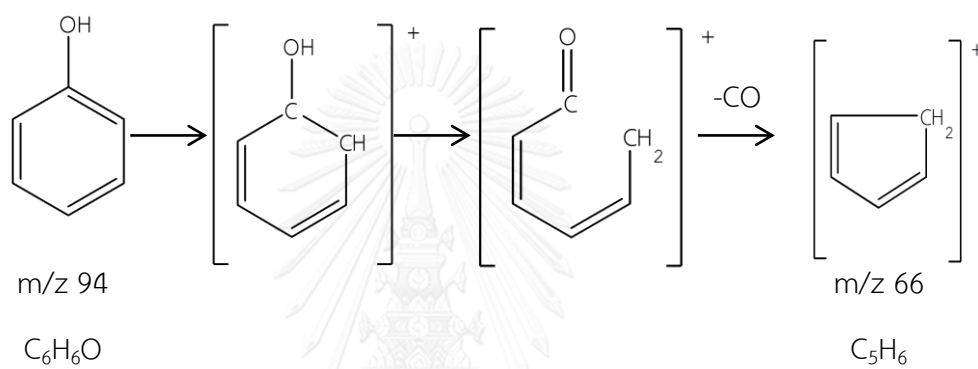
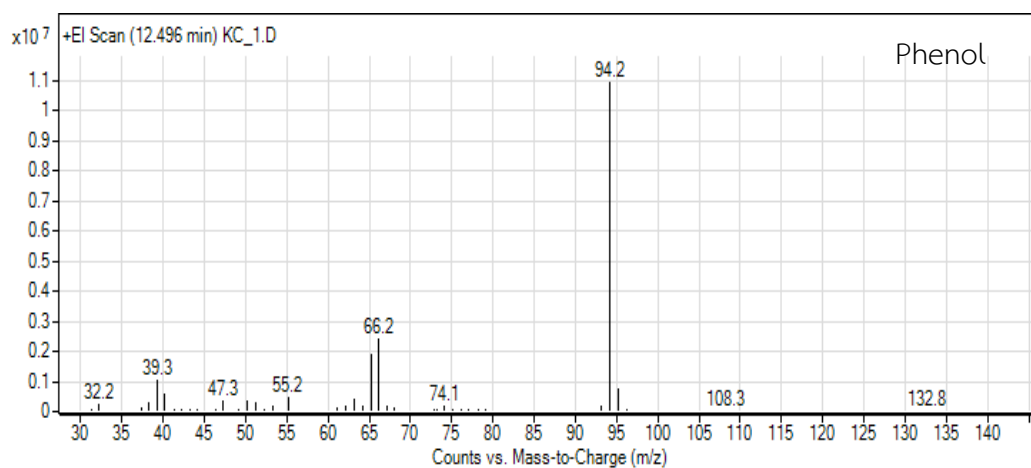


Figure E-4 Mass spectra of phenol.

**Table F-1** %Selectivity and conversion from lignin pyrolysis of pretreated giant sensitive plant.

Biomass	Lignin pyrolysis (g)	Pyrolysis product (%Selectivity)		Pyrolysis product (wt%)		%Conversion		Lignin separation (wt%)	Pyrolysis product (%wt)	
Pretreated giant sensitive plant	0.96 <sup>a</sup> , 0.94 <sup>b</sup>	1,2,4-Trimethoxybenzene		1,2,4-Trimethoxybenzene		1,2,4-Trimethoxybenzene		16.83 <sup>a</sup> and 16.12 <sup>b</sup>	1,2,4-Trimethoxybenzene	
		15.40 <sup>a</sup>	14.50 <sup>b</sup>	14.78 <sup>a</sup>	13.63 <sup>b</sup>	95.97 <sup>a</sup>	94.00 <sup>b</sup>		2.49 <sup>a</sup>	2.19 <sup>b</sup>
		Phenol		Phenol		Phenol			Phenol	
		9.40 <sup>a</sup>	9.80 <sup>b</sup>	9.02 <sup>a</sup>	9.21 <sup>b</sup>	95.96 <sup>a</sup>	93.98 <sup>b</sup>		1.52 <sup>a</sup>	1.49 <sup>b</sup>
		Catechol		Catechol		Catechol			Catechol	
		8.90 <sup>a</sup>	14.20 <sup>b</sup>	8.54 <sup>a</sup>	13.35 <sup>b</sup>	95.96 <sup>a</sup>	94.01 <sup>b</sup>		1.44 <sup>a</sup>	6.25 <sup>b</sup>
		Guaiacol		Guaiacol		Guaiacol			Guaiacol	
8.40 <sup>a</sup>	0.99 <sup>b</sup>	8.06 <sup>a</sup>	0.93 <sup>b</sup>	95.95 <sup>a</sup>	93.94 <sup>b</sup>	1.36 <sup>a</sup>	0.15 <sup>b</sup>			

a = Isolated crude lignin, b = Pure lignin with Klason method



**Table F-2** %Selectivity and conversion from lignin pyrolysis of corncob.

Biomass	Lignin pyrolysis (g)	Pyrolysis product (%Selectivity)		Pyrolysis product (wt%)		%Conversion		Lignin separation (wt%)	Pyrolysis product (%wt)	
Corncob	0.37 <sup>a</sup> , 0.32 <sup>b</sup>	Catechol		Catechol		Catechol		16.83 <sup>a</sup> and 16.12 <sup>b</sup>	Catechol	
		26.6 <sup>a</sup>	30.3 <sup>b</sup>	9.84 <sup>a</sup>	9.70 <sup>b</sup>	37.00 <sup>a</sup>	32.01 <sup>b</sup>		1.14 <sup>a</sup>	0.95 <sup>b</sup>
		Phenol		Phenol		Phenol			Phenol	
		19.3 <sup>a</sup>	26.8 <sup>b</sup>	7.14 <sup>a</sup>	8.58 <sup>b</sup>	37.00 <sup>a</sup>	32.02 <sup>b</sup>		0.82 <sup>a</sup>	0.84 <sup>b</sup>
		1,2,4-Trimethoxybenzene		1,2,4-Trimethoxybenzene		1,2,4-Trimethoxybenzene			1,2,4-Trimethoxybenzene	
		5.5 <sup>a</sup>	4.02 <sup>b</sup>	2.04 <sup>a</sup>	1.29 <sup>b</sup>	37.10 <sup>a</sup>	32.09 <sup>b</sup>		0.24 <sup>a</sup>	0.13 <sup>b</sup>
		Guaiacol		Guaiacol		Guaiacol			Guaiacol	
2.7 <sup>a</sup>	4.4 <sup>b</sup>	0.99 <sup>a</sup>	1.41 <sup>b</sup>	36.70 <sup>a</sup>	32.05 <sup>b</sup>	0.12 <sup>a</sup>	0.14 <sup>b</sup>			

a = Isolated crude lignin, b = Pure lignin with Klason method



## VITA

Miss Isara Mongkolpitchayarak was born November 24, 1990 in Saraburi, Thailand. She graduated with Bachelor of Chemistry from Faculty of Science, King Mongkut's University of Technology Thonburi in 2013. She continued her study in Petrochemistry and Polymer Science, Chulalongkorn University in 2013 and completed 2015. During her graduate study, she also received a research grant from the 90th anniversary of Chulalongkorn University (Ratchadaphiseksomphot Endowment Fund). She participated in the 41st Congress on Science and Technology of Thailand (STT41) on November 6-8, 2015 at Suranaree University of Technology, Nakhon Ratchasima, Thailand.

